NASA SP-5064

TECHNOLOGY UTILIZATION

NASA Contributions to METALS JOINING

NATIONAL AERONAUT N

NASA SP-5064

NASA Contributions to

METALS JOINING

By

W. J. Reichenecker and J. Heuschkel

Prepared under contract by
Westinghouse Electric Corp.

Technology Utilization Division
OFFICE OF TECHNOLOGY UTILIZATION 1967
NATIONAL AERONAUTICS AND SPACE ADMINISTRATION
Washington, D. C.

For Sale by the Superintendent of Documents
U.S. Government Printing Office, Washington, D.C. 20402
Price 60 cents
Library of Congress Catalog Card Number 66-62099

Foreword

Between 1962 and mid-1965, participants in the U.S. space program were challenged to join metals in new ways for highly reliable launch vehicles, ground-support structures, electronic control systems, etc. This survey of reports on such research and development in that period emphasizes information which the authors believe can be helpful in a broad spectrum of industries. It includes items about novel tooling, process development and application, base metal and filler metal relationships, and advances in understanding joining mechanisms.

The Technology Utilization Division of the National Aeronautics and Space Administration strives to make such information widely and appropriately available. Mr. Reichenecker and Mr. Heuschkel have specialized in metals-joining technology for many years and are widely known among persons especially likely to find nonaerospace uses for these contributions to the technology of joining metals.

GEORGE J. HOWICK, *Director,*
Technology Utilization Division,
National Aeronautics and Space Administration

PRECEDING PAGE BLANK NOT FILMED.

Contents

CHAPTER 1

Purpose of This Review

The usefulness of many metals has been limited by the lack of suitable joining techniques. Today the major problems are likely to be with the newer metals, such as the refractory metal alloys. Or one is concerned with the life and performance of a weld at perhaps 1000°, 1500°, or 2000° F, or at −50° F or even lower temperatures. New energy sources, such as electron beams, plasma guns, and lasers, now are of great interest to the metals-joining engineer and scientist. Our ability to produce hardware for industrial, consumer, military, and space applications is directly related to the state of our metals-joining technology.

To a large extent, the means of affixing one metal to another or to a nonmetal have been found by artisans. By and large, development of metals-joining techniques, filler metals, fluxes, and tooling has progressed empirically. Some compositions of filler metals for soldering, for example, are still the same as those used in early Roman work. Pliny refers to two solders, "argentarium" and "tertiarium," both of which are compositions in use today. Argentarium was described as containing equal portions of tin and lead, while tertiarium consisted of two parts lead to one of tin. That some of the early metals-joining craftsmen were very skilled in their art can be deduced from work which has reproduced Etruscan ornaments made by gluing tiny gold grains onto gold ornaments using a mixture of a copper salt and an organic gum. The assembly was then fired to a temperature in excess of 890° C. During the heating cycle the gum carbonized and reduced the copper salt to copper which then alloyed with the gold to braze the minute gold grains in place.

Welding, like soldering and brazing, is also an ancient art. Prehistoric bracelets made of precious metal have been found which show that the ends were forge welded together. In the latter half of the 19th century, discoveries were made that led to processes which replaced forge welding by modern welding practices. Moissan in 1881 used the carbon arc for melting metals and in 1887, in Russia, Bernandos applied this arc to welding. Shortly thereafter experiments with consumable metal electrodes were conducted by Slavianoff. Then in 1895 Le Chatelier invited the oxyacetylene blowpipe.

Resistance welding probably had its conception in the work by Joule in 1856 wherein he accomplished a weld by electrically heating two wires, then forged them together. Elihu Thompson, an American inventor, appears to have been the first engineer to employ contact resistance for welding (1877), and the resistance welding process has grown directly from his efforts. Since his early work, the changes in the process have been, for all practical purposes, engineering refinements.

We now have considerable empirical information pertaining to metals joining. Progress has been slow and publication of metals-joining knowledge often has been discouraged because of the skilled craftsman's feeling that his "trade secrets" constituted his job security. He guarded them jealously. Prior to World War I, welded construction was often regarded suspiciously as being something less than trustworthy and welding was avoided rather than required and encouraged. During and after World War I, welding gradually received greater acceptance and "modern industrial welding" probably can be said to have its roots in the 1930's. World War II and the heavy demands for tanks, ships, aircraft, and other items gave strong impetus to extensive applications of metals joining technology.

During and after World War II, the metals-joining field, along with other technologies, attracted greater interest on the part of engineers and scientists. In the last 15 or 20 years there has been a virtual cascade of technical and scientific knowledge and an increasing tendency toward specialization. Consequently, the technical man has greater and greater difficulty keeping abreast of his own and related fields. Reviews of literature can highlight ideas, equipment, and techniques so that one can maintain cognizance of technological or scientific change without reading the published literature in depth. This report will summarize documents from 1962 to about mid-1965 covering NASA-sponsored work in the metals-joining field.

Just as the material needs of World War II gave impetus to many technologies, the U.S. space program has fostered advances. The information presented herein has been largely the outcome of the efforts to solve day-to-day metals-joining problems which developed directly out of the efforts to produce space program hardware. Local shop conditions, availability of equipment, and presently applied methods will have a direct bearing on the usefulness of this information in industry.

Because the material reviewed for this report was related to a large degree to solving hardware problems, this report is certainly not a treatise on the latest state of the art of metals joining. Many areas will be conspicuous by their absence, or near absence; for example, there will be no references to magnesium alloy joining and very little information will be presented on titanium-alloy joining practices, soldering, and brazing. Some documents reviewed by the authors did not contain items of sufficient significance. Others were not sufficiently complete (as in the case of some progress reports) to permit intelligent conclusions as to the ultimate significance. In much of NASA's work, high reliability is a prime factor and some of the work to be described was aimed specifically at increasing reliability.

PRECEDING PAGE BLANK NOT FILMED.

CHAPTER 2

Nonwelding Processes

Soldering and brazing are not usually thought of as welding processes, but the American Welding Society uses the term "welding" in a generic sense, and therefore, classifies brazing as one of the many welding processes. Our classification of mechanical fasteners, soldering, and brazing as nonwelding processes is arbitrary, but such a grouping is an advantageous way of summarizing information in this instance.

MECHANICAL FASTENERS

Mechanical fastening is of considerable interest to the aerospace industry, and in 1964, Glackin and Gowen reported results of their evaluation of fasteners and fastener materials for aerospace applications (ref. 1). Various mechanical devices, including tension fasteners, point drive bolts and twist-off nuts, Jo bolts, solid rivets, and semiblind cherry rivets fabricated from specific alloy bases of iron, nickel, aluminum, or titanium were studied.

Fasteners were subjected to a range of tests from temperatures of −423° F to the "maximum utilization temperature" of the device/material combination. Tensile, shear, stress rupture, stress relaxation, nut reusability, and nut vibration tests were performed. Corrosion resistance was examined in seacoast atmosphere and accelerated salt-spray tests and the effects of thermal cycling were also studied. Application and design data were developed covering a considerable range of fastener device/fastener material combinations and a great deal of detailed information on mechanical properties is presented (ref. 1). Among the specific alloys evaluated were:

AISI H-11
AISI 4027
AISI 8740
AISI 4130
Waspaloy
A-286
Vasco Max. 300
Pyromet 718

U-212
Ti-7Al-12Zr
Ti-6Al-4V
Ti-1Al-8V-5Fe
Ti
Al-2024
Al-2017-T4

SOLDERING

Perhaps because soldering is an ancient art, and so many people make a soldered joint or two at sometime in their lives, there is a tendency to feel that "anyone can make a soldered joint." If carried into the industrial environment this type of thinking can lead to poor equipment performance and premature failures.

In the NASA programs the performance of soldered connections may determine a venture's success or failure (ref. 2). This is also true in the electrical industry wherein decisions must be based on the ultimate costs of poor performance accurately weighed against the cost of process control which minimizes failures. From the NASA concern for high-reliability soldered joints, especially in electrical equipment, a document was prepared covering procedures applicable to improving soldered-joint reliability (ref. 3). The items it sets forth are not necessarily novel or startling but represent a systematic elucidation of the principles and details which should make up a cognizant effort to produce reliable soldered electrical connections. Materials, equipment, tooling, inspection, and training are covered.

BRAZING

Brazing has been and still is used for joining assemblies for use at normal atmospheric or slightly elevated temperatures. Extension of the technique to parts used at higher temperatures has been limited because the usual brazing alloys are compositions that soften readily at relatively moderate temperatures. Brazed constructions that will withstand considerably higher temperatures are needed, and Sinclair and Gyorgak (ref. 4) state:

> Some of the most successful brazing materials developed for use up to 2000° F have been nickel alloys. The development of these alloys was needed to permit fabrication of objects to be used at high temperatures that could not be produced by forging, casting, or machining. Examples are: air-cooled turbine blades fabricated from formed, thin sheets brazed together to produce intricate air passageways; heat exchangers for nuclear reactors consisting of thin-walled stainless steel tubes brazed to headers; assemblies of extremely thin sections brazed to heavy ones; composite structures; and light weight assemblies for high temperature service in supersonic aircraft and space vehicles.

Some materials are damaged when subjected to a brazing cycle—the damage resulting from the thermal exposures involved or from interactions between the base metal and the brazing alloy. Sinclair and Gyorgak have reported the results of their investigation involving two nickel-base brazing alloys, Ni-Cr-Si-B and Ni-Cr-Si; and three sheet materials, L–605, A–286, and Inconel 700. The effect of the brazing variables, nickel plating, and heat treatment on the 1200° F stress-rupture life of the three sheet materials was investigated. (Figs. 1 to 7) (ref. 4)

Nickel plating is a prebrazing treatment employed on A-286 and Inconel 700 to facilitate wetting by the brazing alloy, since both of these alloys, because of their composition, form extremely stable surface oxides which are nearly impossible to reduce during the brazing cycle.

> When plating is required to enable brazing to be done, embrittlement of the resulting structure may occur, perhaps as a result of hydrogen pickup. This can be alleviated, at least in part, by thermal treatment during or following brazing. (ref. 4)

In the case of L-605 alloy, a 1-mil-thick coating of brazing alloy, Ni-Cr-Si-B, improves stress-rupture properties, the strengthening occurring as a result of diffusion of boron from the brazing alloy into

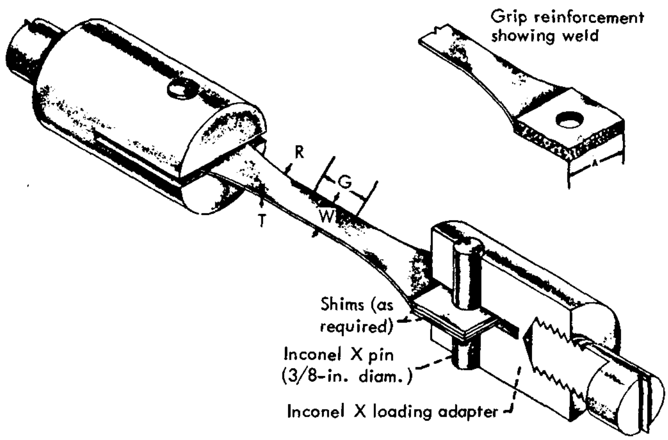

FIGURE 1.—Stress-rupture specimen and loading adapter (ref. 4).

Edges of test section parallel to ±0.002 inch

[Dimensions in inches]

Alloy	T	A	R	W	G
L-605	0. 021	1. 00	5. 00±0. 01	0. 500±0. 002	1. 000±0. 001
A-286	. 022	1. 00	5. 00±0. 01	. 500±0. 002	1. 000±0. 001
Inconel 700	. 030	1. 00	5. 00±0. 01	. 500±0. 002	1. 000±0. 001

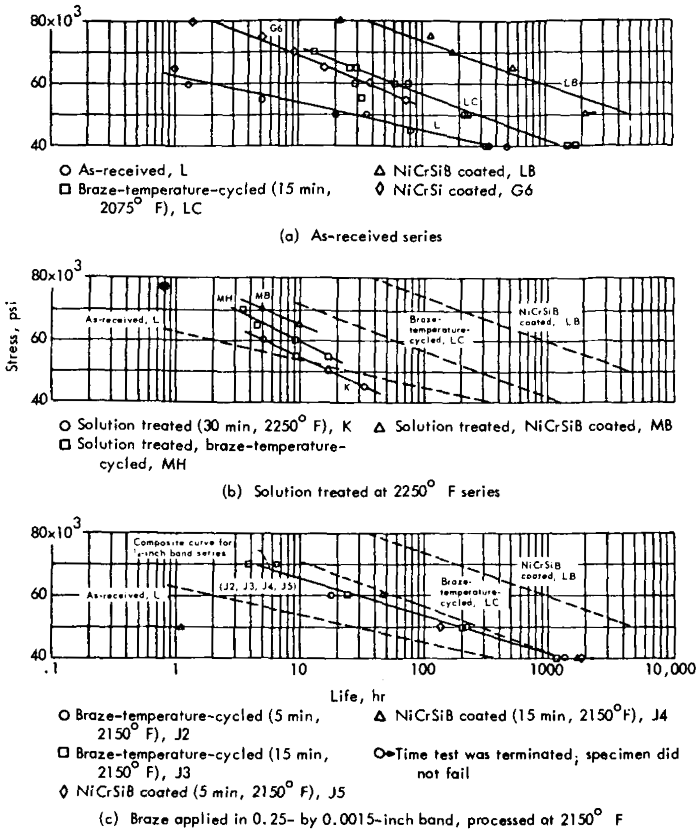

FIGURE 2.—Effects of brazing variables and heat treatment on 1200° F stress-rupture values of 0.020-inch-thick L–605 sheet (ref. 4).

the base metal during thermal processing. The Ni-Cr-Si brazing alloy also appears to strengthen the L–605 sheet material, but in this case the improvement is the result of thermal processing.

The Ni-Cr-Si brazing alloy apparently damaged the stress-rupture life of A–286 base metal and this damage could not be mitigated by heat treatment. The stress-rupture life of A–286 also was adversely affected by the Ni-Cr-Si brazing alloy, but the damage was less severe than that caused by Ni-Cr-Si-B brazing alloy. Again, post-braze heat treatments did not produce beneficial effects.

> When Inconel 700 was heat treated to produce optimum stress-rupture strength, the braze alloy [Ni-Cr-Si-B] had no effect; however, strengthening of Inconel 700 was obtained when it was not at its optimum strength. This strengthening of the Inconel was attributed to boron diffusion from the braze alloy during thermal processing.

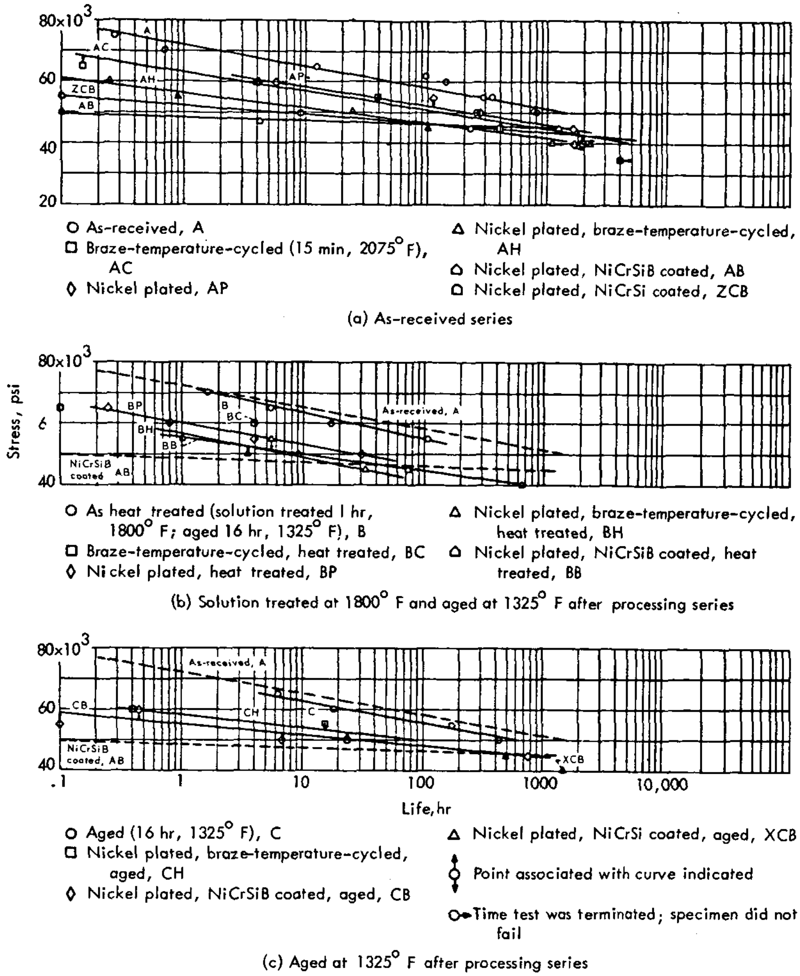

FIGURE 3.—Effects of brazing variables and heat treatment on 1200° F stress-rupture values of 0.020-inch-thick A–286 sheet (ref. 4).

Coating Inconel 700 with Ni-Cr-Si brazing alloy appears to have improved the stress-rupture strength. A quantitative determination of this improvement could not be made because the majority of failures occurred in the specimen grip areas after appreciable life at 80 000 psi to 90 000 psi. Strengthening is primarily attributed to a mechanical strengthening of the nickel-plated coating by the envelope of brazing alloy.

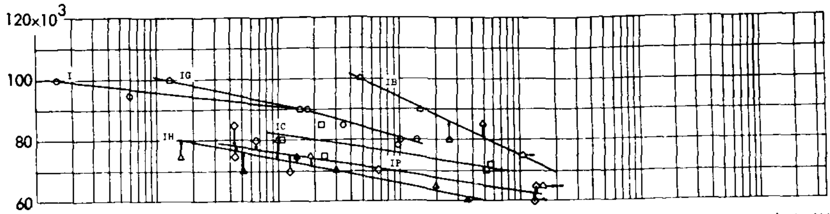

O As-received, I
□ Braze-temperature-cycled (15 min, 2075° F), IC
◊ Nickel plated, IP
Δ Nickel plated, braze-temperature-cycled, IH
⌂ Nickel plated, NiCrSiB coated, IB
⌂ Nickel plated, NiCrSi coated, IG

(a) As-received series

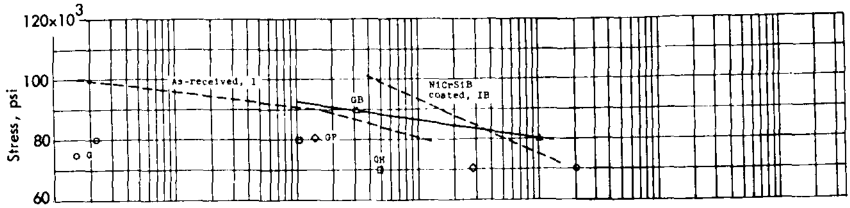

O As heat treated (solution treated 1 hr, 2275° F, aged 16 hr, 1600° F), G
◊ Solution treated, nickel plated, aged, GP
□ Solution treated, nickel plated, braze-temperature-cycled, aged, GH
Δ Solution treated, nickel plated, NiCrSiB coated, aged, GB

(b) Solution treated at 2275° F prior to processing and aged at 1600° F after processing series

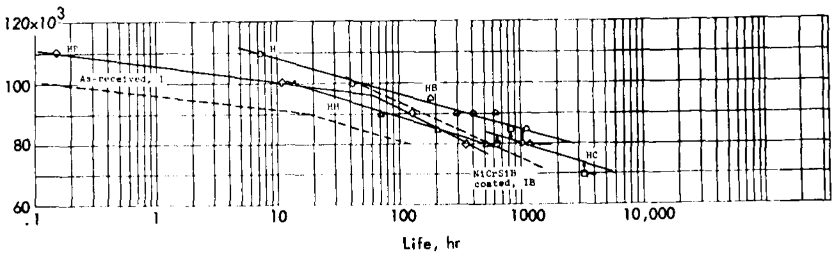

O As heat treated (solution treated 1 hr, 2150° F, aged 16 hr, 1600° F), H
□ Braze-temperature-cycled, heat treated, HC
◊ Nickel plated, heat treated, HP
Δ Nickel plated, braze-temperature-cycled, heat treated, HH
⌂ Nickel plated, NiCrSiB coated, heat treated, HB
Point associated with curve indicated
Time test was terminated; specimen did not fail

(c) Solution treated at 2150° F and aged at 1600° F after processing series

FIGURE 4.—Effects of brazing variable and heat treatment on 1200° F stress-rupture values of 0.030-inch-thick Inconel 700 sheet (ref. 4).

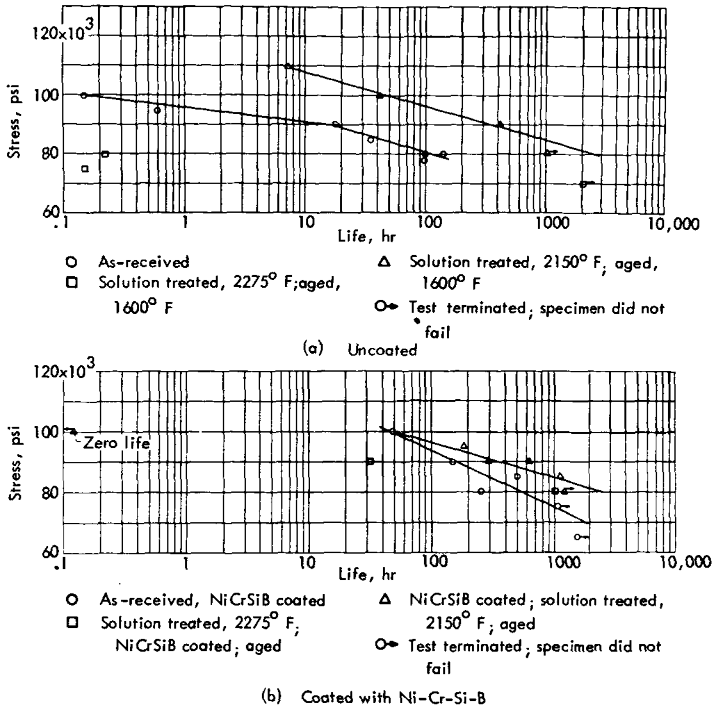

FIGURE 5.—1200° F stress-rupture values for Inconel 700 sheet, as received and solution treated (ref. 4).

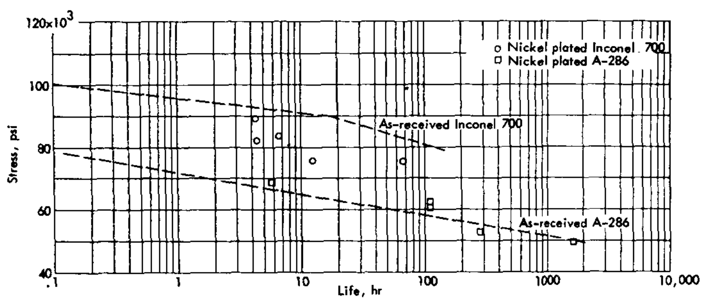

FIGURE 6.—1200° F stress-rupture values for Inconel 700 and A-286, bare and nickel plated (ref. 4).

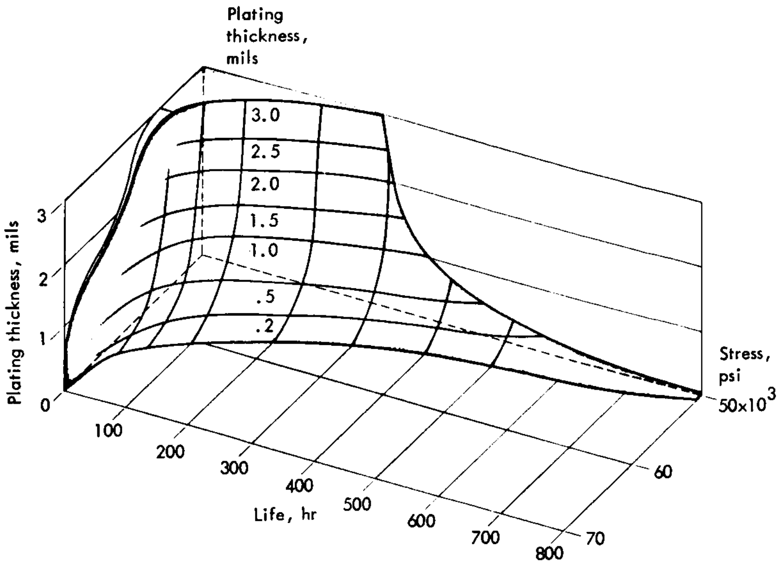

FIGURE 7.—Effect of nickel plating on stress and life of A-286 at 1200° F when loaded in tension under stress-rupture conditions (ref. 4).

Welding Processes

Welding procedures of one type or another are employed today to join almost every metal or alloy of industrial significance. The product spectrum ranges from tiny electronic gadgets to immense steam turbines, and from sling chains to supersonic aircraft. Our review of NASA-sponsored work showed interesting results in inert-gas shielded, nonconsumable electrode arc welding (TIG), inert-gas shielded, consumable electrode arc welding (MIG), and electron beam (EB) welding. A preliminary look at the potential of the laser as a welding tool also interested us.

INERT-GAS-SHIELDED, CONSUMABLE AND NONCONSUMABLE, ELECTRODE ARC WELDING

There is a well-established trend in the arc-welding industry to automate insofar as possible for economy of operation and to minimize variations in welding parameters on repetitive work, thus assuring a more uniform quality. When using the automated MIG process, the following parameters must be controlled:

(1) Maintain uniform electrode wire feed into the arc
(2) Maintain arc stability
(3) Maintain constant weld-bead shape
(4) Maintain constant motion of the work part with respect to the wire feed.

Freis describes the development of a system suited to maintaining integrated control of travel speed and wire feed without monitoring both variables independently (ref. 5). It is pointed out, however, that minor adjustments in power-source voltage were required to maintain satisfactory weld-bead generation.

At the Marshall Space Flight Center, automation of the welding process was examined as a means to reduce the number of special-purpose fixtures and amount of floorspace required on some programs.

> In essence, if one simple boom manipulator can be used in conjunction with simple holding fixtures to weld pieces of various contours and shapes, equipment utilization can be improved and the investment in plant and equipment greatly reduced (ref. 6).

The system developed consists of essentially a conventional boom manipulator and arc-welding system programed by means of function generators. The programs for voltage, current, wire feed, torch angle, and travel speed may be determined by an operator on a specific work piece. Changes between successive runs can be quickly made, since there is no intermediate step such as punching tape.

As the size of rocket booster engines has increased, heavier gages of aluminum plate have been necessary, and for the first stage of the Saturn V, thicknesses up to 1 inch are required. Conventional welding practice for 1-inch-thick aluminum requires that plate edges be prepared by machining to either a single- or double-V configuration. Then the joining process deposits filler metal at appropriate rates to fill up the V and the fitup space between adjoining plates.

> Recognizing the need for improving the conventional welding of 1-inch plate, NASA engineers developed a new method which allows 1-inch 2219–T87 aluminum alloy plates to be joined in a faster, less expensive manner (ref. 7).

A square butt joint is prepared by machining the plate edge smooth and square with the plate surface. Edges of plates to be joined are then fitted together with little or no gap and minimum misalinement. Welds are consummated with little or no external filler metal addition, making one pass along each side of the square butt joint (fig. 8), with a gas tungsten-arc welding torch (TIG welding). Precise control of welding parameters is required to assure a minimum of 1/8-inch tie-in between the roots of the two beads.

One pass on each side of a square butt joint gives better mechanical properties than conventional welds, but the problem of tie-in of two beads is critical because no nondestructive means of inspection exists.

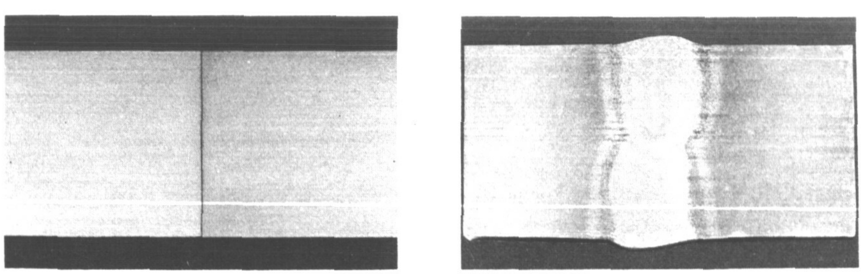

Full Size
(a) Preparation and fitup

Full Size
(b) Completed joint

FIGURE 8.—Square-butt joint used for 1-inch-thick welded aluminum alloy plates (ref. 7).

While the most economical welding position is the downhand, flat position, it is often necessary to make welds in the horizontal, vertical, and overhead positions—especially in large structures such as rocket motor or transformer cases and generator frames. Suitable automatic welding equipment for this purpose did not exist, and as the size of aluminum alloy rocket motor cases continued to increase, it became necessary to make welds out of position, i.e., vertically upward, and programs were initiated to develop suitable automatic equipment and prove its utility. Initially, the efforts were applied to the TIG process, but ultimately the work included MIG equipment (refs. 8, 9).

For vertical welding, expert welders develop wide-weave techniques. Studies of expert manual welders were therefore made and their torch movements observed and recorded. These movements or motions were then analyzed and reduced to the minimum requirements and components so that a machine could be designed to duplicate these manual techniques. A machine was developed capable of performing automatic, vertical-up, MIG welds in aluminum with a programed wave oscillation (ref. 10). Results of the out-of-position welding studies showed that "automatic out-of-position weave bead welding can be performed on 2014 and 5456 aluminum alloys in the overhead, vertical up and vertical down positions" (ref. 8). Also, "it is feasible to weld vertically up with the oscillating MIG process" (ref. 9). Much additional work needs to be done to explore various weave-bead patterns, "feedback" for improved control, and other parameters, some of which are not available to the manual welder. An example is controlling the torch oscillation pattern through feedback related to sensing the approach of the sidewall, since there is an influence of this approach on the arc power variable (ref. 10). While these approaches to developing automated out-of-position welding were primarily for aluminum rocket motor cases, there is no reason why the general nature of the equipment, the information gained, and the techniques employed should not be adaptable to other metals and other configurations.

For metallurgical reasons, many alloys require the use of inert gases to shield the welding arcs. Recognizing that the presence of contaminants such as oxygen, nitrogen, and hydrogen is detrimental to weld quality, it is helpful to know in advance, or during the welding operation, that such contaminants are not present. Techniques for spectrographic monitoring of atmospheric contaminants in inert-gas shields have been examined and may prove useful in the future for welding the gas-contaminant sensitive metals (ref. 11).

Continuous monitoring of the smoothness of the welding arc assures freedom from arc shorts and open-circuit outages, both of which contribute to rapid influx of those contaminating gases which cause weld porosity and other defects. Efforts have been made to provide closed-circuit television for remote visual control of a TIG welding arc. Fiber optics, a means of transmitting light through long, thin, flexible fibers of glass, plastic, or other material, also have been considered to obtain close visual observation of the arc (refs. 12, 13).

Special welding nozzle configurations have been tried to prevent accumulation of fumes and to provide better arc shielding (ref. 14).

Uniformity in welding wire cleanliness (both internal and external), straightness, size uniformity, level winding, and packaging are important considerations in consistent, economical production of high-quality welds. Marshall Space Flight Center evolved a specification, M–ME–MPROC 700.1, covering these various considerations for aluminum-alloy electrode wire and this specification is available as a model for those interested in the production of high-integrity aluminum-alloy welds (ref. 15). Lack of proper concern for weld-wire quality and packaging can lead to unacceptable X-ray quality welds, poor reproducibility, and a tendency for the wire to jam in the feed mechanism.

Welding aluminum, and the even more sensitive titanium, molybdenum, and columbium alloy systems, does not permit welded-on and cutoff assembly fixtures. Consequently, techniques and associated welding tooling had to be developed to permit precise fitup of large devices. From this need, a variety of useful techniques and auxiliary tooling have evolved. These have included combinations of special backup bars and fitup jigs; segmented, flexible backup bars; vacuum-type backup bars, fiber-glass tape backup bars; clamping devices; special guide tips for feeding filler wire in horizontal and vertical position welding; and improved methods of electrode arc spot welding utilizing the shielded inert-gas metal transferring arc method (figs. 9–12) (ref. 16). Also, various techniques were tried for upsetting plate edges to be welded (ref. 17).

ELECTRON BEAM WELDING

A long-recognized deficiency of the several electric-arc-welding processes, particularly when welding thick plates, is that a relatively large groove must be prepared to provide access to the weld root. The entire volume of the groove then must be slowly and expensively refilled to consummate the weld. Consequently, welding engineers are constantly seeking faster rates of metal deposition, improved heat sources, and minimum joint volume in terms of filler metal deposited in order to lower the cost of making welded joints. The advent of the electron beam process wherein heat is generated by a concentrated beam of electrons accelerated in a vacuum to about 10 percent of the speed of light, i.e., 18 600 mps, provided a new potential for expanding the capability to join metals.

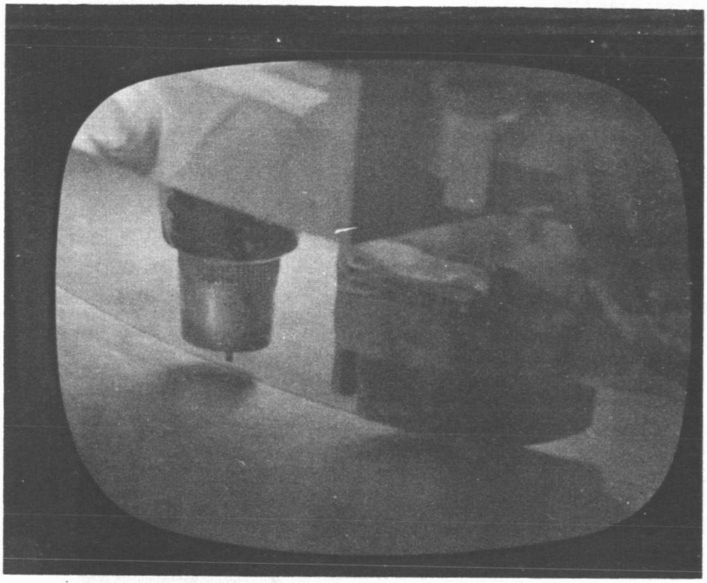

(a) Prior to initiating arc

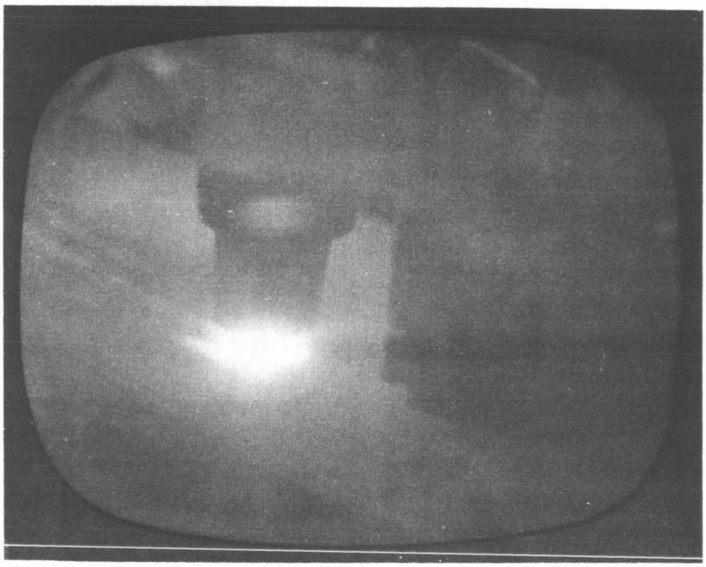

(b) Inert-gas shielded metal-arc weld in progress

FIGURE 9.—Closed-circuit television closeups while using a seam tracker and proximity transducer (ref. 16).

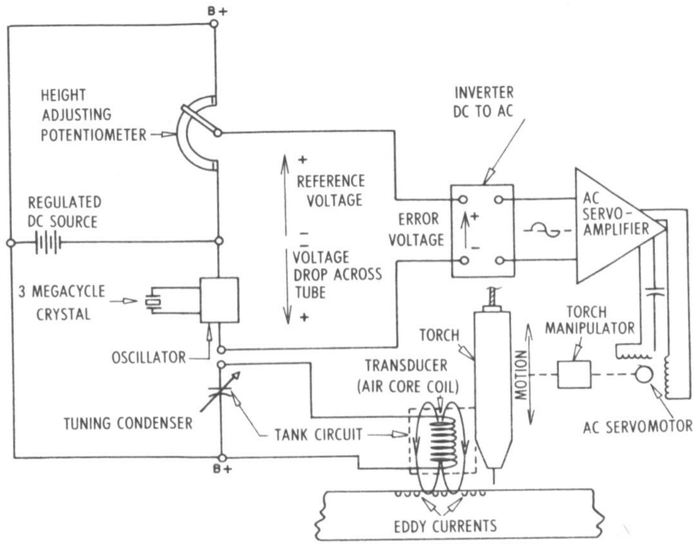

FIGURE 10.—Block diagram of proximity control unit (ref. 16).

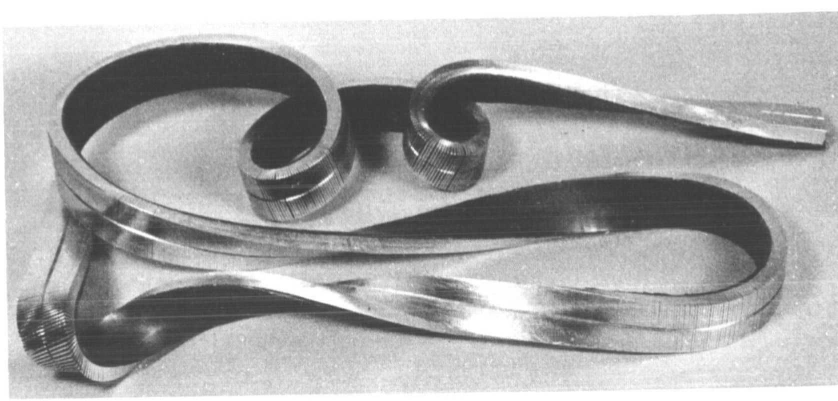

FIGURE 11.—Flexible 0.040-inch stainless-steel backup bar (ref. 16).

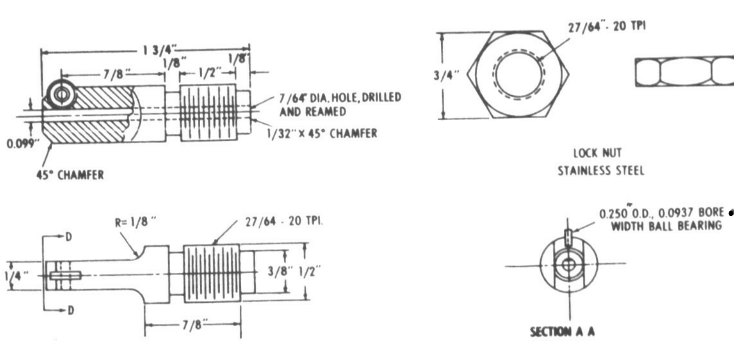

FIGURE 12.—Guide tip for feeding filler wire (ref. 16).

Tulisiak at the NASA Lewis Research Center reports a number of interesting joining problems relating to space engine components that were satisfactorily solved by using an electron beam welder (ref. 18). For example, the fabrication of porous tungsten emitters for ion engines for space propulsion could not be satisfactorily accomplished by gas-shielded, arc-welding techniques. Joints either had too wide a weld band, which led to cracking, or the joints became too contaminated for satisfactory performance. Satisfactory emitters were produced using electron beam (EB) techniques and appropriate weld sequencing to prevent distortion and cracking. Also mentioned is the brazing of a tungsten-to-tantalum joint using either columbium or titanium filler and the electron beam as a heat source. A tantalum tube, with the columbium or titanium filler ring fitted in place, was inserted in a hole in the tungsten part. The electron beam was focused on the filler ring. While the filler ring was melting, the adjacent tantalum and tungsten heated sufficiently so that a brazed joint was accomplished. Attempts to weld the tantalum tube to the tungsten plate were unsatisfactory because the weld alloy formed was brittle. Additional work relating to EB welding of tungsten showed that material as thin as 0.0015-inch was satisfactorily welded and butt welds of 0.002-inch tungsten sheet were accomplished. High welding speeds, up to 100 inches per minute, helped maintain crack-free welds.

With the electron beam process, in-vacuum welds of the highest known purity are obtained. Gaseous impurities total less than one part per million (1 ppm=0.0001 percent by weight). This contrasts sharply with 20 ppm or higher impurity levels for the best inert-gas-shielded welding methods (ref. 19). Also, the tremendous energy concentration available (1 million watts/sq. cm) and the fact that the electron beam can be focused to diameters of less than 0.010 inch permit the process to be used at very high depth-to-width ratios; e.g., over 20 to 1. Inasmuch as high vacuums are required in the beam chamber to permit generation and maintenance of the beam, the application of EB welding has generally been restricted to parts small enough to be enclosed conveniently within a vacuum cell. To enclose large structures such as the 33-foot-diameter aluminum alloy Y-ring for the Saturn C–5 first-stage booster in a vacuum chamber for welding is impractical—the pumping of such a large chamber to suitable vacuum levels would be a tedious, difficult, if not futile, task. Marshall Space Flight Center engineers in conjunction with NASA contractors evolved a technique wherein a suitable vacuum can be obtained in a relatively small chamber which surrounds only the immediate area of the Y-ring joint. The chamber is constructed in two pieces so that the Y-ring section to be welded can be inserted in the chamber, the chamber halves brought together, and vacuum obtained by pumping down this relatively small volume. Hermetic sealing is obtained by use of O-rings and flat rubber gaskets.

Electron beam welds in 2⅜-inch-thick aluminum-alloy Y-rings were consummated in a single pass at a speed of 30 inches per minute (fig. 13). This contrasts markedly with conventional inert-gas-shielded arc welding of a double-U-weld joint in 5-inch-thick aluminum, wherein a total of 50 passes per side (100 passes total) at a travel speed of 4 inches per minute were required to complete the weld. The equivalent travel speed for the complete weld in this latter instance is 0.04 inch per minute exclusive of interpass cooldown time.

The EB welding process has considerable versatility, being applicable to joining a wide variety of metals—including the refractory metals, dissimilar metal couples, metals of grossly dissimilar thicknesses, and metals covering a range of thicknesses from that of foil to over 2 inches thick. While the process is presently used primarily in vacuum, and this is too costly for some applications, there is currently intensive industrial effort to obtain the essential advantages of the EB energy source as a welding tool in open air.

LASER WELDING

> So far, the laser has evolved neither as a welding panacea, as claimed by many of the more spectacular early newspaper accounts, nor as the epitome of uselessness, as contended by some of its more vociferous detractors.

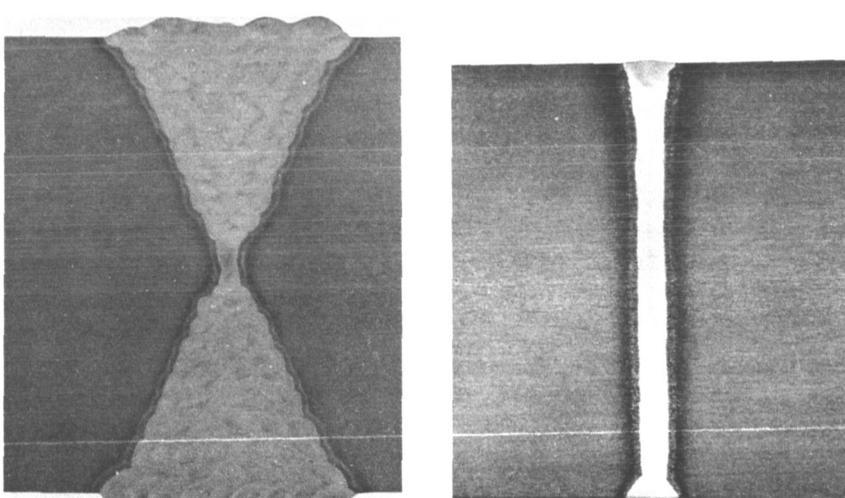

One-half size
(a) Double-U, 5-inches thick, 2219–T81, approximately 50 passes each side

Full size
(b) Single-pass electron beam, 2⅜-inches thick, 2219–T87

FIGURE 13.—Completed weld joints in aluminum-alloy plates (ref. 19).

Thus says Schwinghamer of the Marshall Space Flight Center in his "Laser Welding" published in 1965 (ref. 20). Six basic types of lasers are doped crystal, gas discharge, semiconductor junction, liquid, plastic, and glass. Wavelengths produced cover a wide range. Since the list of materials showing lasing properties is growing steadily, a listing of laser materials is soon out of date. Table 1 does list, however, a variety of laser materials and their operating wavelengths. The transition diagram for the pink-ruby laser system is shown in figure 14 and a number of high-power laser gun designs are presented in figure 15.

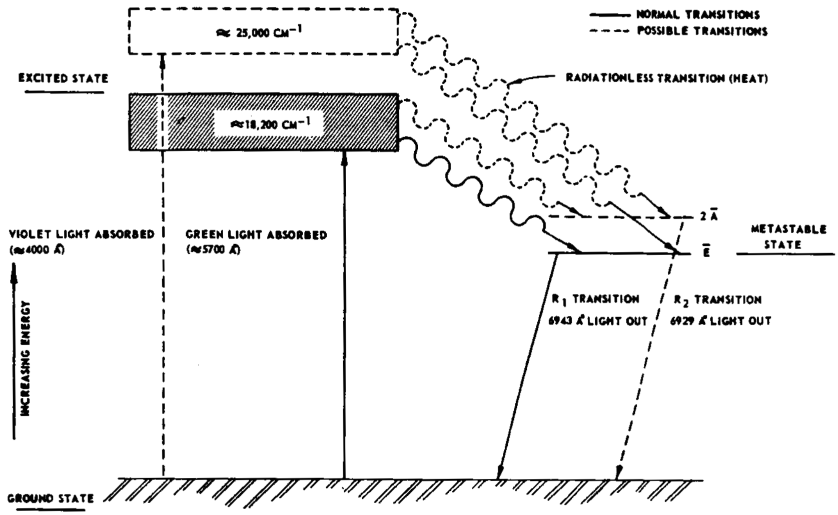

FIGURE 14.—Transition diagram, pink-ruby laser system (ref. 20).

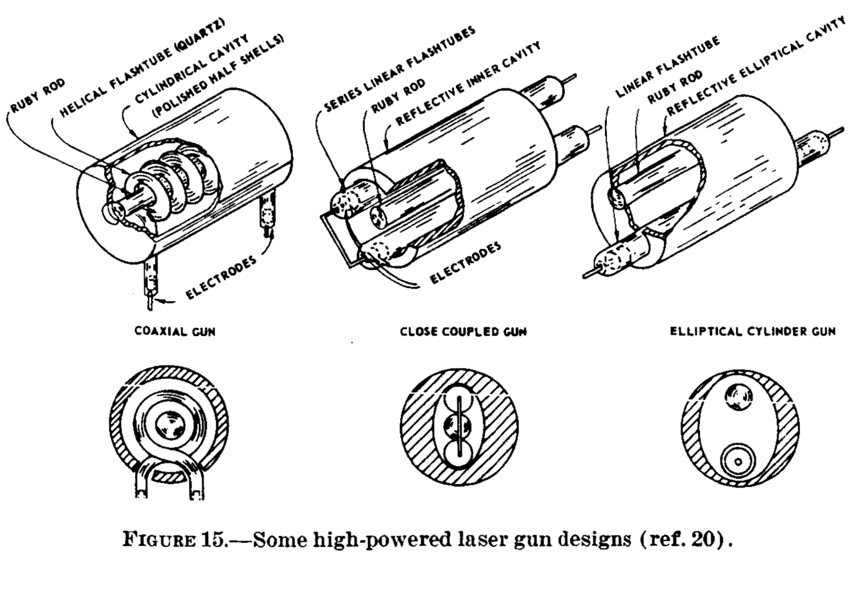

FIGURE 15.—Some high-powered laser gun designs (ref. 20).

TABLE 1.—*Materials and Output Wavelengths of Various Types of Lasers*
[Ref. 20]

State and material	Active element	Wavelength (λ ln Å or μ)	Excitation
Crystal:			
Pink ruby, Al_2OC	Cr^{3+} (R_2-R_1)	6929–6943 Å	Flashlamp, continuous lamp
Red ruby, Al_2O_3	Cr^{3+} (N_2-N_1)	7009, 7041 Å	Flashlamp, continuous lamp
Barium fluoride, BaF_2	U^{3+}	2. 556 μ	Flashlamp
	Nd^{3+}	1. 06 μ	Flashlamp
Calcium fluoride, CaF_2	Sm^{2+}	7083 Å	Flashlamp
	U^{3+}	2. 24–2. 61 μ	Flashlamp, continuous lamp
	Dy^{2+}	2. 36 μ	Flashlamp, continuous lamp
	Tm^{2+}	1. 116–1. 189 μ	Flashlamp
	Ho^{3+}	2. 05 μ	Flashlamp
	Nd^{3+}	1. 046 μ	Flashlamp
Calcium molybdate, $CaMoO_4$	Nd^{3+}	1. 06 μ	Flashlamp, continuous lamp
Calcium tungstate $CaWO_4$	Nd^{3+}	1. 063 μ	Flashlamp, continuous lamp
	Pr^{3+}	1. 047 μ	Flashlamp
	Ho^{3+}	2. 046 μ	Flashlamp
	Er^{3+}	1. 612 μ	Flashlamp
	Tm^{3+}	1. 911 μ	Flashlamp
Strontium tungstate, $SrWO_4$	Nd^{3+}	1. 06 μ	Flashlamp, continuous lamp
Lanthanum trifluoride, LaF_3	Nd^{3+}	1. 06 μ	Flashlamp, continuous lamp

	Pr^{3+}	5985 Å	Flashlamp
Strontium molybdate, $SrMoO_4$	Nd^{3+}	1. 064 μ	Flashlamp
	Pr^{3+}	1. 047 μ	Flashlamp
Strontium fluoride, SrF_2	U^{3+}	2. 407 μ	Flashlamp, continuous lamp
	Sm^{2+}	6967 Å	Flashlamp
	Tm^{3+}	1. 91 μ	Flashlamp, continuous lamp
	Nd^{3+}	1. 06 μ	Flashlamp, continuous lamp
$Na_{1/2}La_{1/2}MoO_4$	Nd^{3+}	1. 06 μ	Flashtube, continuous lamp
Lead molybdate $PbMoO_4$	Nd^{3+}	1. 06 μ	Flashlamp, continuous lamp
Gas:			
Helium-neon	Neon	0. 6328 to >3. 39 μ	dc and rf discharge
Cesium		3. 718 μ	Continuous lamp
Neon-oxygen	Oxygen	8446 Å	dc and rf discharge
Argon-oxygen	Oxygen	8446 Å	
Helium		2. 0603 μ	
Neon		1. 15–17. 8 μ	
Argon		1. 618–12. 14 μ	
Krypton		1. 69–7. 06 μ	
Xenon		2. 026, 5. 574, 35 μ	
Helium-xenon	Xenon	2. 026–12. 9 μ	
Nitrogen			Pulsed discharge
Semiconductor:			
Gallium arsenide	*p-n* junction	8400 Å	Pulsed or continuous dc
Gallium arsenide phosphide		6500–8400 Å	Pulsed
Indium phosphide		9100 Å	Pulsed or continuous dc
Indium arsenide		3.1 μ	Pulsed or continuous dc
Indium antimonide		5.2 μ	Pulsed.

TABLE 1.—*Materials and Output Wavelengths of Various Types of Lasers.*—Concluded

[Ref. 20]

State and material	Active element	Wavelength (λ In Å or μ)	Excitation
Liquid:			
Benzene	Stimulated Raman scattering	8819, 7455, 8052 Å	Ruby laser
Nitrobenzene	Stimulated Raman scattering	7568, 8539, 9632 Å	Giant pulse ruby laser
Toluene	Stimulated Raman scattering	7463 Å	Giant pulse ruby laser
1-bromonaphthalene	Stimulated Raman scattering	7672 Å	Giant pulse ruby laser
Pyridine	Stimulated Raman scattering	7457 Å, 8053 Å	Giant pulse ruby laser
Cyclohexane	Stimulated Raman scattering	8658 Å	Giant pulse ruby laser
Deuterated benzene, C_6D_6	Stimulated Raman scattering	7430, 7990 Å	Giant pulse ruby laser
Europium benzolyacetonate in alcohol	Eu^{3+}	6100 Å	Flashlamp
Plastic:			
Europium triflurothienylbutane-odione in polymethyl methacrylate	Eu^{3+}	6130 Å	Flashlamp
Glass:			
Borosilicate glass	Nd^{3+}	1.06 μ	Flashlamp, continuous lamp
Lanthanum-borosilicate glass	Nd^{3+}	1.06 μ	Flashlamp
Li-Mg-Al-Si	Yb^{3+}	1.02 μ	Flashlamp
Li-Mg-Al-Si	Gd^{3+}	3125 Å	Flashlamp
Li-Mg-Al-Si	Ho^{3+}	1.95 μ	Flashlamp

The laser does provide a new, high-intensity energy source for the joining of metallic assemblies. Unlike the electron beam which often requires vacuum, lasers can be operated in air. A laser beam can also be projected from an air environment into a vacuum chamber and acceptable welding accomplished. Care in application of laser energy is required, however, since large quantities of heat can be developed in the weld joint so rapidly that vaporization and subsequent drilling occur rather than welding. Use of the laser by NASA in meteoroid simulation studies involving momentum transfer, and cratering effects caused by giant pulses, shows that several component pulses occurring over a longer time interval cause more energy to be used for melting and results in less vaporization.

The laser has been well accepted for microwelding—the capability of joining dissimilar metals, metals of differing thicknesses, and the ability of the laser to operate in air have been attractive advantages. At the Marshall Space Flight Center, laser welding experiments were conducted using a 4000-joule commercial unit while a much higher power system—240 kJ—was being built to extend the studies. Because the laser releases high-energy density pulses, lens arrangements for focusing the light beam are somewhat of a problem, especially for the very high-power units. Satisfactory welds were obtained using the 4-kJ laser on 304 stainless steel with a pulse repetition rate of about 0.8 pulse/second. Attempts to weld either 5086 or 2219 aluminum alloy were unsuccessful, possibly because of oxide formation, since no shielding gas was used. Successful welds in aluminum alloys were made using a small evacuated box in which the materials were placed. The laser beam was projected through a piece of good-quality glass which made up one of the box walls.

There is evidence that laser welding may be enhanced as higher pulse repetition rates (PRR) and longer pulses are used. Logical extension of this thinking suggests the advantages of continuous wave (CW) lasers, which are not yet in the high-power range. Developments indicate that CW laser power output can be expected to increase.

Laser welding is an infant technology at present, but rapid, significant strides in the development and application of laser technology to metals joining can be expected. A word of warning regarding the laser is pertinent: Serious eye damage can occur to those working with lasers from direct or reflected beams and full eye protection is necessary. Certainly anyone planning to work with such equipment should carefully check all eye-protection measures for adequacy.

CHAPTER 4

Plasma Spray Bonding

The plasma torch and its adaptation to the spraying of various particulate materials on a variety of substrates is of considerable interest to industry. Metal spraying with conventional torch equipment, such as oxyacetylene, has been practiced for many years, but the temperature limitations in the heat source limit what can be accomplished. When plasma torches were developed, the extension and improvement of the capability to spray materials onto a substrate appeared likely. Studies of the bonding mechanism between tungsten on tungsten (ref. 21), tungsten on molybdenum (ref. 22), and plasma-sprayed tungsten on stainless steel (ref. 23), were conducted by Spitzig and Grisaffe at the NASA Lewis Research Center.

TUNGSTEN ON TUNGSTEN

The plasma-spray apparatus used by Grisaffe and Spitzig for studying bonding of sprayed tungsten on a tungsten substrate is shown in figure 16 (ref. 23). To obtain maximum information from these tests regarding the bonding mechanism, the number of particles sprayed on a surface was kept to a minimum. In a preliminary study the investigators noted that metallurgical bonding of plasma-sprayed tungsten did not occur to a nonpreheated, metallographically polished tungsten substrate. Consequently, preheated substrates were used.

Using commercial tungsten powder of 74- to 30-micron particle size and polished tungsten coupons $1 \times 1 \times 0.017$ inch, plasma-sprayed specimens were prepared as follows:

(1) Set coupon-to-torch distance
(2) Evacuate chamber to 20 microns and backfill to atmospheric pressure with high-purity dry nitrogen
(3) Start torch and bring to operating conditions
(4) Roll torch into position and permit plasma gas to preheat tungsten coupon
(5) When specimen temperature reaches equilibrium (2 to 3 seconds), activate powder spray for approximately 1 second
(6) Roll torch out of position and shut down
(7) Permit specimen to cool to room temperature and open tank.

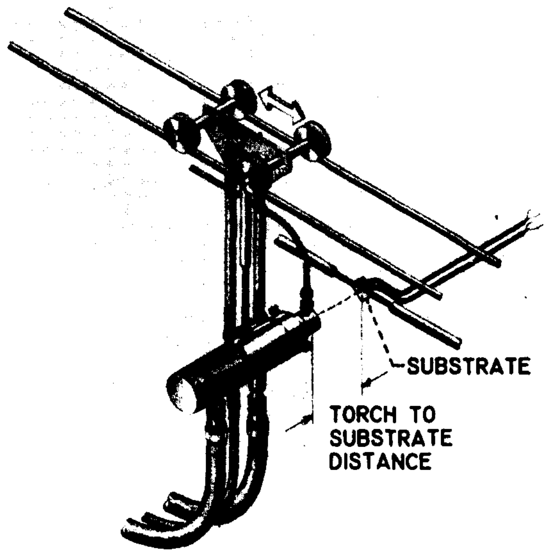

FIGURE 16.—Spraying apparatus within inert-gas-filled chamber (ref. 23).

Substrate temperatures were monitored during preheat, spray, and cooldown to about 400° C, all of which occurred in about 30 seconds. Substrate temperatures were also observed as a function of torch-to-substrate distance for the preheating and spraying cycles (fig. 17). Average particle velocity measurements were also made over a range of torch-to-substrate distances using a rotating disk velocimeter. These results, presented in figure 18, show interestingly that there is little difference in particle velocity between 4-inch torch-to-substrate distance (240 ft/sec) and 7-inch distance (215 ft/sec).

Metallurgical bonding of plasma-sprayed tungsten on polished tungsten substrates is achieved if the substrate is heated within the range of 2050° to 2700° F in an inert atmosphere. Further, it is possible to deposit such coatings while retaining the high strength properties of an as-worked surface, that is, the metallurgical bond can be obtained at a substrate temperature below the recrystallization temperature. From examination of sections through the coating-substrate specimens, it appears that the bond develops as a result of substrate surface grains growing into the coating. There is also strong evidence of extremely rapid short-range diffusion inasmuch as the coating-to-substrate interface is almost completely eliminated under very short time conditions.

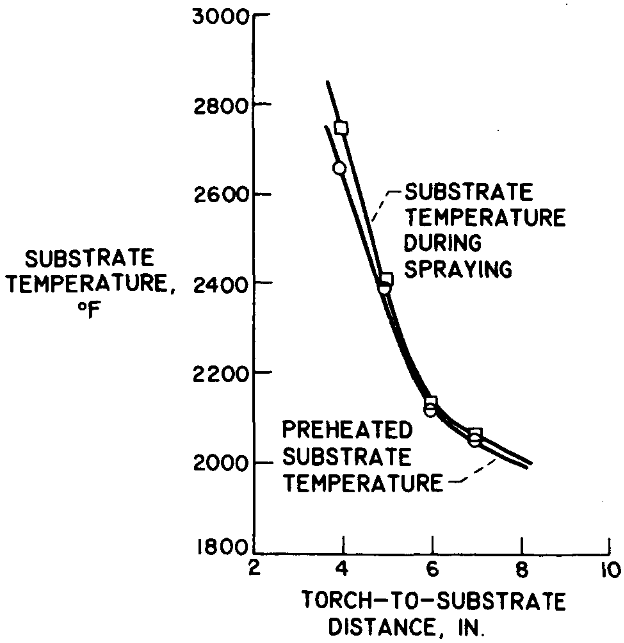

FIGURE 17.—Relation between torch-to-substrate distance and substrate temperature (ref. 23).

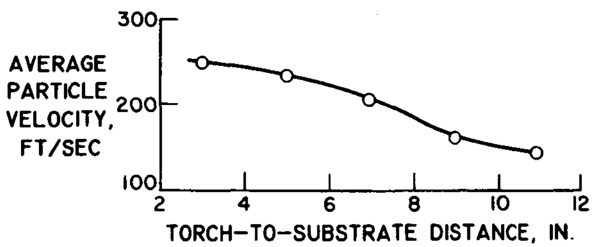

FIGURE 18.—Relation between torch-to-substrate distance and particle velocity (ref. 23).

TUNGSTEN ON HOT MOLYBDENUM

Metallurgical bonding of plasma-sprayed tungsten on hot molybdenum substrates was obtained (ref. 22). The substrates had been metallographically polished and were preheated to 1750° F or higher immediately before spraying. Substrate preheat temperatures ranging from 1750° to 2950° F were monitored by platinum/platinum-13 percent rhodium thermocouples which were read out on a millisecond-response recorder. Preheating and spraying were performed in a nitrogen atmosphere.

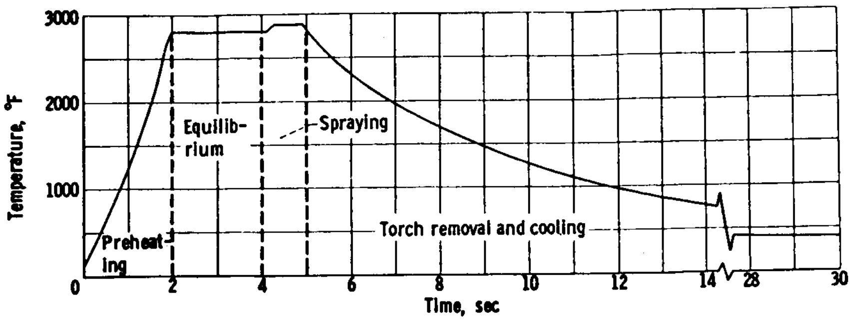

FIGURE 19.—Time-temperature history of substrate during spray treatment (ref. 22).

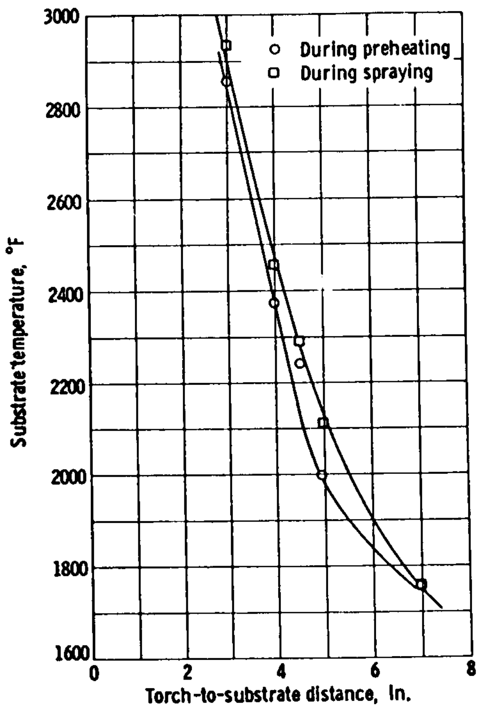

FIGURE 20.—Relation of substrate temperature and torch-to-substrate distance (ref. 22).

When substrate temperatures were between 2200° and 3700° F, metallurgical bonding between the sprayed tungsten and the preheated molybdenum occurred. At these temperatures the molybdenum substrate completely recrystallized even though the total time for preheating, spraying, and cooling to 400° C was only about 30 seconds (fig. 19). The substrate temperatures obtained as a result of preheating the specimens with the plasma gas varied with the torch-to-substrate distance, as shown in figure 20. This figure also shows the temperature of the substrate during actual spraying.

Torch-to-substrate distances ranged from 2 to 7 inches and the velocity of the tungsten particles was nearly constant over this range. Under these conditions the tungsten particles showed a considerable amount of plasticity. This was demonstrated by their deformation into shapes similar to flat, almost circular disks that had sufficient plasticity to flow over previously deposited particles.

Bonding between the sprayed tungsten and the preheated molybdenum substrate appears to result from growth of substrate grains into the coating, thus producing a coherent interface. Hardness values across a tungsten-molybdenum interface are shown in figure 21 for the as-sprayed and post-sprayed heat-treated condition.

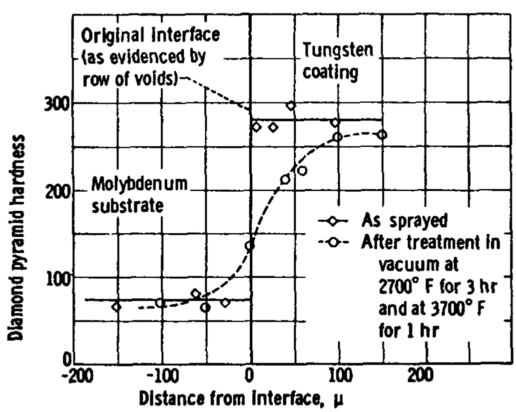

FIGURE 21.—Hardness variation across molybdenum to tungsten deposit for 3-inch torch-to-substrate distance (ref. 22).

TUNGSTEN ON STAINLESS STEEL

The bond strength of sprayed metal coatings is generally attributed to mechanical bonding of the sprayed particles to a preroughened substrate surface. However, Spitzig and Grisaffe had noted in earlier work that plasma-sprayed tungsten particles showed excellent adherence to a metallographically polished, 304 stainless-steel substrate which had not been preheated. Additional investigation of plasma-sprayed tungsten on 304 stainless steel showed that alloying and consequent bonding did occur (fig. 22) (ref. 23). The bonds appear to be achieved by rapid localized diffusion in the stainless steel directly

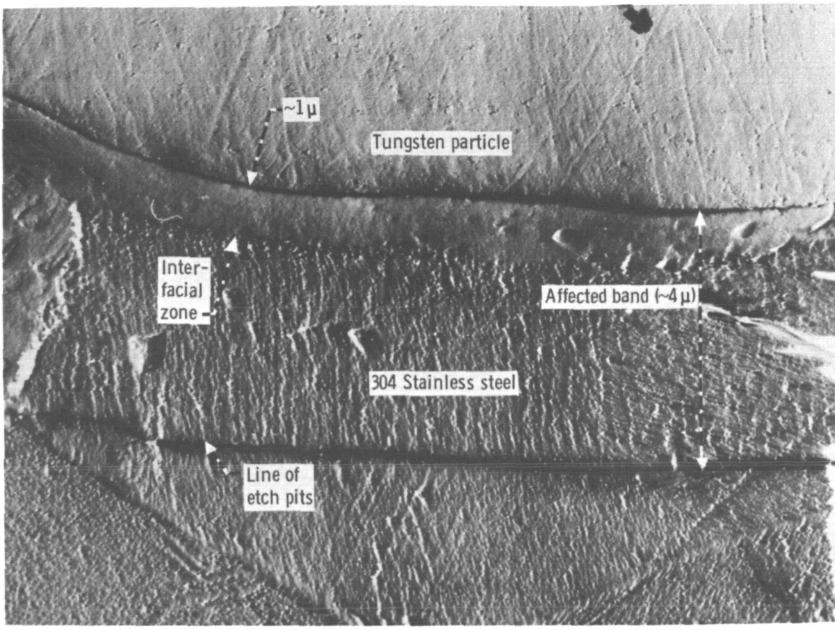

FIGURE 22.—Electron micrograph of cross section of tungsten coating on AISI 304 austenitic steel substrate for 3-inch torch-to-substrate distance. Oxalic acid etch (ref. 21).

beneath the impinging tungsten particle. Heat-transfer analysis demonstrated the possibility that the local temperature rise approaches the melting point of the stainless-steel substrate immediately under the tungsten particle, thus giving rise to rapid local diffusion. This temperature rise occurs when the tungsten particle gives up its energy, obtained as a result of heating and acceleration when traveling in the plasma stream, to a local area of the substrate. The substrate region is raised to temperatures near its melting point and cools to around 500° C in approximately 10^{-5} seconds.

Tungsten powder particle size ranged from 62 to 30 microns in this work and spraying was performed in air with the following plasma torch operating conditions:

Plasma Torch Operating Conditions

Spray nozzle inside diameter, in	7/32
Current, amp	450
Voltage, V	60
Plasma-nitrogen flow rate, cu ft/hr	80
Plasma-hydrogen flow rate, cu ft/hr	10
Carrier-nitrogen flow rate, cu ft/hr	10
Auger-type powder hopper setting	11.9

CHAPTER 5

Light Metals

Certainly one might expect great interest in light metals and their joining characteristics in a space program, and in fact, joining of aluminum alloys has received considerable attention, especially in attempts to develop higher strength, weldable alloys. (The Appendix gives the nominal composition of many aluminum alloys.) Studies of MIG welding of aluminum at various ambient pressures were made and the use of titanium alloy fasteners for mechanically joining aluminum was also examined. Some information is available regarding joining of beta titanium alloys and one study of ultrasonic welding of aluminum is reported.

ALUMINUM

Welding

Aluminum alloys have been employed extensively in the space program because of their good strength-to-weight ratio. Consequently, aluminum joining practices, joint properties, and joining processes have received attention. For example, considerable effort was expended under NASA sponsorship to develop an all-welded aluminum bulkhead for Saturn rocket motors. For such an application, high-quality, high-integrity welds are mandatory and the behavior of these welded joints under various conditions of stress and temperature must be predictable. Both inert-gas-shielded, nonconsumable electrode (TIG) and inert-gas-shielded consumable electrode (MIG) welding were employed and properties of joints were evaluated at temperatures as low as −423° F (tables 2 and 3) (refs. 24, 25).

> Welded joints in heavy gage wrought aluminum alloy material are generally considered to develop low joint efficiency in the as-welded condition. This conception is based on two facts. First, the heat of welding lowers the strength of wrought aluminum in all tempers other than annealed (−0). Second, the cast or weld metal generally develops lower strength than wrought metal. Welding heavy gage material usually requires multipass welds, the number of passes generally increasing with the gage, and thereby multiplying:

TABLE 2.—*Mechanical Property Summary of Tension Test Results From Vertical Position MIG and TIG Welds in 2014–T6 Aluminum Alloy*

[Ref. 25]

Test temperature and specimen type		MIG, integral chill			TIG, external chill			TIG, integral chill		
		Yield strength, Fty	Ultimate strength, Ftu	Elongation,[a] percent	Yield strength, Fty	Ultimate strength, Ftu	Elongation,[a] percent	Yield strength, Fty	Ultimate strength, Ftu	Elongation,[a] percent
Room temperature:										
Transverse	1	32.8	39.8	3.0	34.7	48.3	2.0	37.4	50.9	5.0
	2	32.0	38.6	3.0	31.9	48.0	2.0	38.3	45.7	3.0
	3	30.7	43.0	4.0	34.3	50.5	2.0	35.9	52.8	5.0
Average		31.8	40.5	3.3	33.6	48.9	2.0	37.2	49.8	4.3
All weld-metal longitudinal	1	22.8	40.6	10.0	23.4	43.2	16.0	24.5	43.8	12.0
	2	20.2	38.4	10.0	25.0	47.5	13.0	24.8	44.4	14.0
	3	19.6	38.0	10.0	25.9	44.5	12.0	26.2	45.1	9.0
Average		20.9	39.0	10.0	25.1	45.1	13.7	25.2	44.4	11.7
Joint longitudinal (1½ in. wide)	1	35.2	55.0	5.0	46.7	62.9	[b] 8.0	42.6	65.8	[b] 5.0
	2	31.9	50.8	12.0	44.0	61.4	7.0	[c] 48.6	[c] 62.1	[b] [c] 8.0
	3	37.2	57.1	11.0	43.7	61.2	[b] 7.0	44.1	63.5	10.0
Average		34.8	56.3	9.3	44.8	61.8	7.3	45.1	63.8	7.7
−321° F:										
Transverse	1	41.5	47.2	0	38.7	59.5	2.0	46.1	50.6	1.0
	2	37.0	50.1	1.0	40.7	56.6	1.0	54.8	54.9	0
	3	37.4	40.7	1.0	41.4	61.1	2.0	44.2	49.3	0
Average		38.6	46.0	0.7	40.3	59.1	1.7	48.4	51.6	0.3

All-weld-metal longitudinal	1	(d)	44.1	4.0	29.9	50.6	8.0	31.8	55.6	11.0
	2	22.5	44.1	4.0	34.2	52.1	5.0	30.2	55.9	10.0
	3	26.6	41.8	4.0	32.2	56.9	9.0	31.3	53.2	14.0
Average		24.5	42.3	4.0	32.1	53.2	7.3	31.1	56.6	11.7
Joint longitudinal (1½ in. wide)	1	48.4	64.6	6.0	51.4	71.2	6.0	58.9	77.9	8.0
	2	49.4	65.9	6.0	56.2	70.4	6.0	56.8	72.7	8.0
	3	49.2	63.5	7.0	56.9	69.7	[c] 4.0	56.8	74.6	8.0
Average		49.0	64.7	6.3	54.8	70.4	5.3	57.5	75.1	8.0
−423° F:										
Transverse	1	(d)	45.1	1.0	55.4	66.0	2.0	(d)	[e] 49.4	1.0
	2	45.7	48.8	1.0	49.8	63.2	2.0	62.2	63.0	1.0
	3	(d)	48.9	1.0	53.1	61.9	2.0	58.3	63.9	1.0
Average		45.7	47.6	1.0	52.8	63.7	2.0	60.2	63.4	1.0
All-weld-metal longitudinal	1	34.7	48.4	2.0	36.3	54.6	5.0	37.9	61.9	5.0
	2	33.2	46.5	3.0	37.3	57.8	5.0	39.7	58.5	3.0
	3	33.4	48.3	3.0	38.4	49.1	2.0	41.7	59.3	3.0
Average		33.8	48.3	2.7	37.3	53.8	4.0	39.8	59.9	3.7
Joint longitudinal (1½ in. wide)	1	55.8	70.2	4.0	65.4	75.6	3.0	56.8	73.8	5.0
	2	56.4	69.3	4.0	56.3	74.8	3.0	59.6	80.2	5.0
	3	55.9	67.8	3.0	63.8	75.4	3.0	65.3	80.6	5.0
Average		56.0	69.1	3.7	61.8	75.2	3.0	60.8	78.2	5.0

[a] Elongation measured over 2-in. gage length for transverse and longitudinal joint specimens; 1-in. gage used for all-weld-metal specimens.
[b] Specimen failed outside gage marks.
[c] Specimen failed in weld defect.
[d] Extensometer failed. No yield value obtained.
[e] Specimen failed in weld deposit. No defects noted.

TABLE 3.—*Comparison of Results of Vertical Position MIG and TIG Welds Tests* [Ref. 25]

Test No.	1	2	3	4A [a]	4B [b]	5	6
Joint/process	MIG external chill	MIG integral chill	TIG external chill	TIG integral chill	TIG integral chill	TIG backed	MIG backed
Weld energy input [b]	117	328	36	180	142	168	196
Mismatch tolerance	Not determined.	<0.015 in.	0.020	<0.015 in.	0.020 in.	<0.010 in.	0.010 in.
Gap tolerance	Not determined.	0.020 in.	0.030	<0.020 in.	0.030 in.	<0.010 in.	0.010 in.
Average weld deposit hardness—Rockwell 30T	39	43	48	50	50		
Average width of heat-affected zone	5/8 in.	3/4 in.	5/8 in.	11/16 in.	9/16 in.		
Average yield tensile Fty (ksi)	30.9	29.8	31.5	33.6	34.6	Not determined.	Not determined.
Average ultimate tensile Ftu (ksi)	42.6	40.4	44.6	49.9	47.4		
Average elongation percent E in 2-in.	2.0	1.4	1.4	3.0	1.0		
Temperature gradient, distance from weld centerline:							
700° F	1/2 in.	1/2 in.	3/8 in.	3/8 in.	5/16 in.		
600° F	1/2 in.	5/8 in.	7/16 in.	7/16 in.	3/8 in.	Not determined.	
500° F	3/4 in.	1 in.	9/16 in.	5/8 in.	1/2 in.		
400° F	1 in.	1 5/8 in.	7/8 in.	7/8 in.	11/16 in.		

[a] Joint 4A is square butt joint utilizing no additional filler metal. Joint 4B is a grooved joint, and includes the addition of filler material in the form of cold wire. Both joints are examples of the TIG process with integral chill.

[b] Weld energy input is determined as the product of arc current-x-arc voltage divided by weld speed, are power per unit speed. The values are meaningless in themselves, but provide a comparison of the relative rate at which welding heat is applied to the workpiece in the various combinations of process and joint.

1. The possibilities of encountering weld defects.
2. The time consumed in welding and inspection.
3. Control precautions to minimize distortion.

> Hence, any process that either provides increase in joint strength or requires fewer passes holds considerable advantage for welding heavy gage aluminum.

Brennecke thus introduces studies of electron beam welding of 2219 aluminum only (ref. 26).

Plate material ranging up to 2⅜ inches thick was used in this study, all joints being of the square-butt type in which the abutting edges were prepared by machining. Evaluation of EB weld quality was made by visual, radiographic, and metallographic techniques. Mechanical characteristics of welds were compared by means of tensile, bend, and hardness tests. Welds were made in both the flat and vertical positions employing various welding parameters.

Joint strength, penetration, and weld geometry are affected by welding speed and power input. Greater strengths were obtained at welding speeds of 90 inches per minute as compared with 44 inches per minute, but power inputs had to be increased at the higher welding speed to obtain satisfactory penetration. Joint strengths generally increased with plate thickness, but the strength of joints in the thinner material was less than optimum because welding parameters were controlled to produce equal width welds. Therefore, the depth-to-width ratio was not especially favorable in the thinner gages. Joint efficiency for EB welded aluminum alloy 2219–T87 plate is on the order of 70 to 80 percent (tensile), as compared to 60 to 65 percent for inert-gas-shielded tungsten-arc or metal-arc welds. Even higher joint efficiency is obtained when based on yield strength.

There is considerable experience and data regarding weld parameters and joint properties for conventional MIG and TIG welding of aluminum alloys at atmospheric pressure. There is little information, however, on welding aluminum at pressures above and below atmospheric. Under NASA sponsorship, Salter of the British Welding Research Association studied the effect of ambient pressures from 1 to 30 psia argon on weld parameters, arc characteristics, metal transfer, and other variables in both manual and automatic welding (ref. 27). Base metal employed was similar to 5456 and the filler metal approximated 5556. The need for information relating to effect of pressure on welding procedures and joint properties was related to the potential need for joining in space and undersea environments.

Salter's conclusions are essentially quoted in the following: The effect of ambient pressure on the characteristics of the gas, metal, and arc has an important bearing on the welding conditions required for any particular condition.

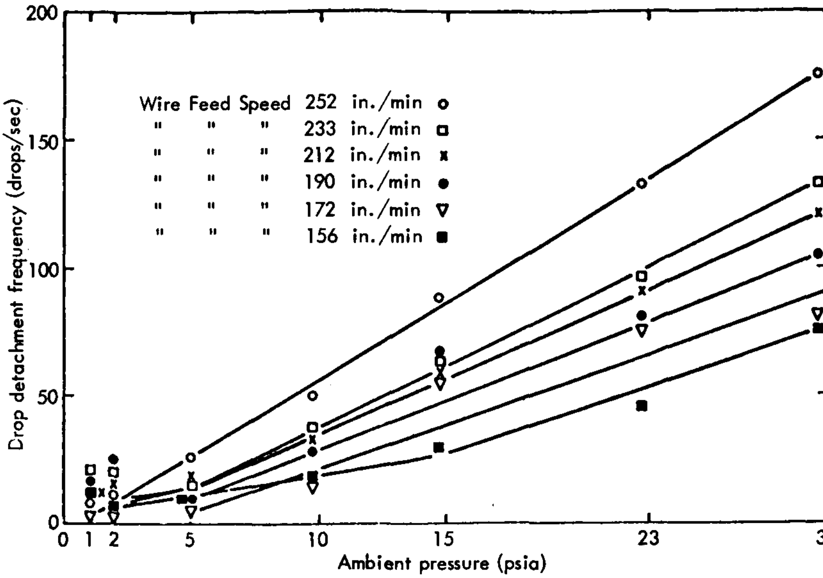

FIGURE 23.—Drop detachment frequency as influenced by pressure and wire feed speeds (ref. 27).

The most important effects of pressure are—

(1) The drop detachment frequency increases with ambient pressure over the whole pressure range (fig. 23).

(2) The current drawn for a fixed filler metal feed rate increases with increasing pressures (fig. 24).

(3) The arc voltage drawn for a fixed arc length increases with pressure (fig. 25).

The principal changes in welding conditions required at pressures other than atmospheric are—

(1) A higher filler metal feed rate is needed to draw sufficient current to produce adequate penetration at low pressures;

(2) A reduced feed rate must be used at high pressures to prevent burnthrough; and

(3) A reduced welding speed may be needed at low pressures to allow time for the formation of a molten pool bridging the two plates.

At pressures below 5 psi, the arc became diffuse and the energy input to the plate was dissipated, necessitating the use of a low welding speed. This was further aggravated by the increased contact tip-to-work distance needed to prevent arcing between the welding gun and the workpiece. At high ambient pressures, the welding process became more efficient. Penetration was increased and smaller edge preparations and higher welding speeds could be used.

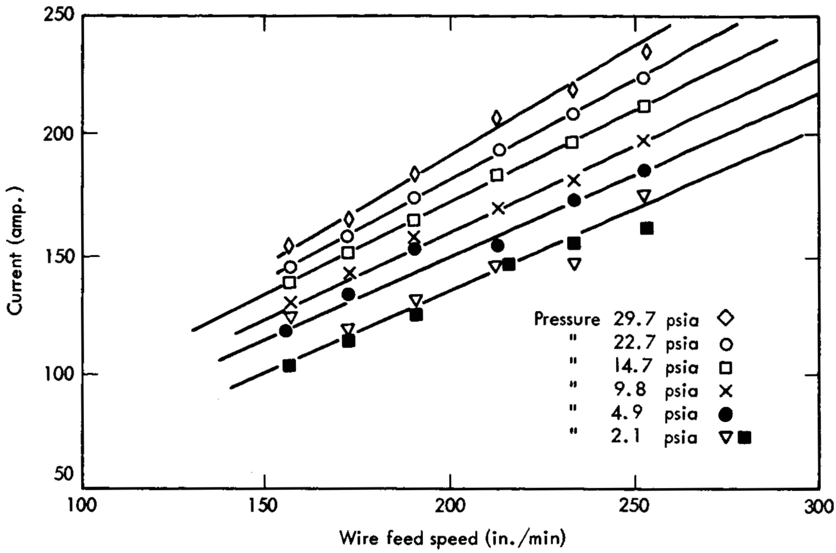

FIGURE 24.—Required arc current as influenced by pressure and wire feed speed (ref. 27).

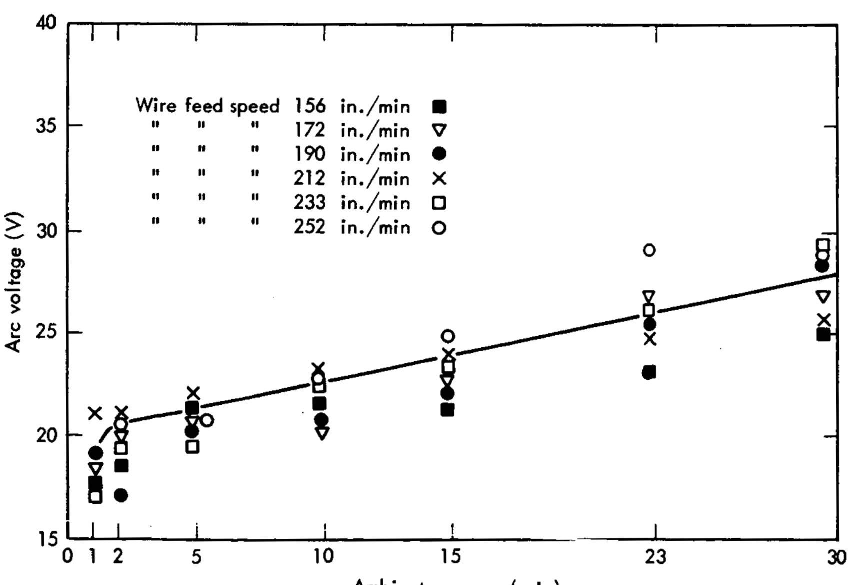

FIGURE 25.—Welding arc voltage as influenced by pressure (ref. 27).

Satisfactory transverse tensile properties and analyses were obtained at all pressures for a welding speed of 12 inches per minute. Radiographically clean welds were obtained with speeds of 25 and 12 inches per minute at all pressures above 5 psia. Welds made at pressures below 5 psia showed porosity at the lower welding speed and coarse porosity, together with some lack of side fusion at the higher speed.

Successful welds were made in the Al-Mg alloy (5456) at ambient pressures between 1 and 30 psia with the gas metal-arc process using argon gas. Photographs of typical arc character and weld microsections as a function of ambient gas pressure are given in figure 26.

Aluminum alloys, because of their high strength-to-weight ratio, have been extensively used in liquid fuel and oxidizer tanks and structural members of space vehicles. Al-Mg-Mn alloys of the 5000 series (nonheat treatable) having a yield strength of about 40 000 psi have been used, but in later designs the higher yield strength alloys 2014–T6 (60 000 psi) and 2219–T81 (50 000–55 000 psi) have been selected. Projected designs indicated that a still higher strength, weldable alloy was needed. Consequently, under NASA sponsorship a program was undertaken to develop such an alloy (refs. 28, 29). The objective was an aluminum alloy having 75 000 psi tensile strength, 65 000 psi yield strength, an elongation of 15 percent at room temperature, and no degradation of these properties at −423° F. Weldability similar to that of 5456 or 2219 aluminum alloys was desired with joint efficiencies of at least 80 percent at room temperature. Furthermore, the alloy should be relatively insensitive to notches and have high resistance to corrosion and stress corrosion cracking.

> In order to ascertain the merits and limitations of alloys presently available, those currently under development but still considered experimental, and alloys employed in various exploratory and survey research programs, the metallurgical publications and trade literature of the past 20 years pertaining to high strength alloys were reviewed. In addition, numerous reports based on both U.S. Government contract and industry-sponsored material evaluation programs were reviewed and the findings analyzed for possible leads or approaches that might be employed in the experimental program.
>
> This survey did not uncover any entirely new alloy systems capable of developing the high strengths required, and the most promising prospects for achieving the program objectives involve further development and refinement of existing alloy types.

Fricke, Haney, Anderson, and Hunsicker (ref. 28) have prepared an excellent presentation of the metallurgical aspects of a number of common aluminum alloy systems and excerpts are quoted herein.

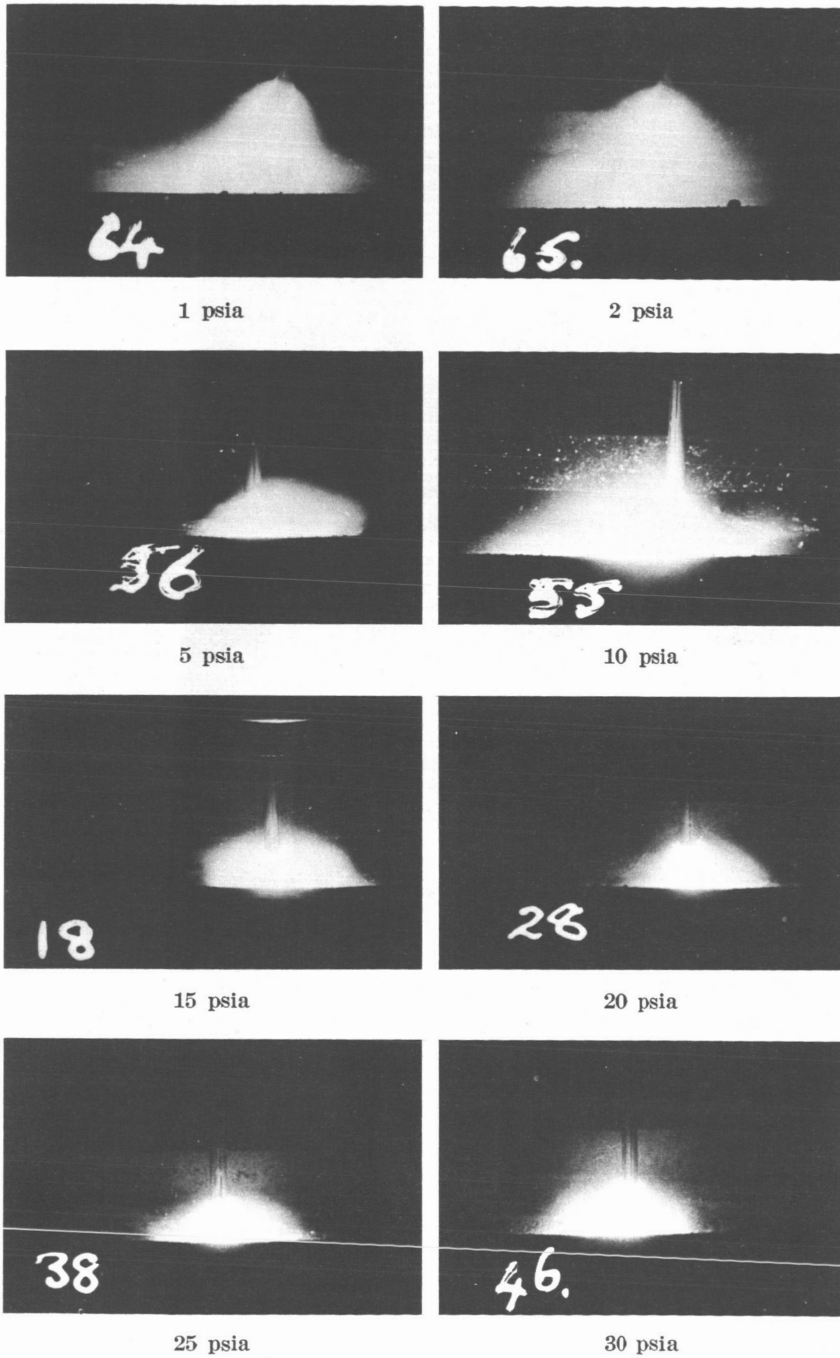

FIGURE 26.—Typical welding arcs and automatic weld microsections as influenced by enveloping pressures (ref. 27). (a) Welding arcs.

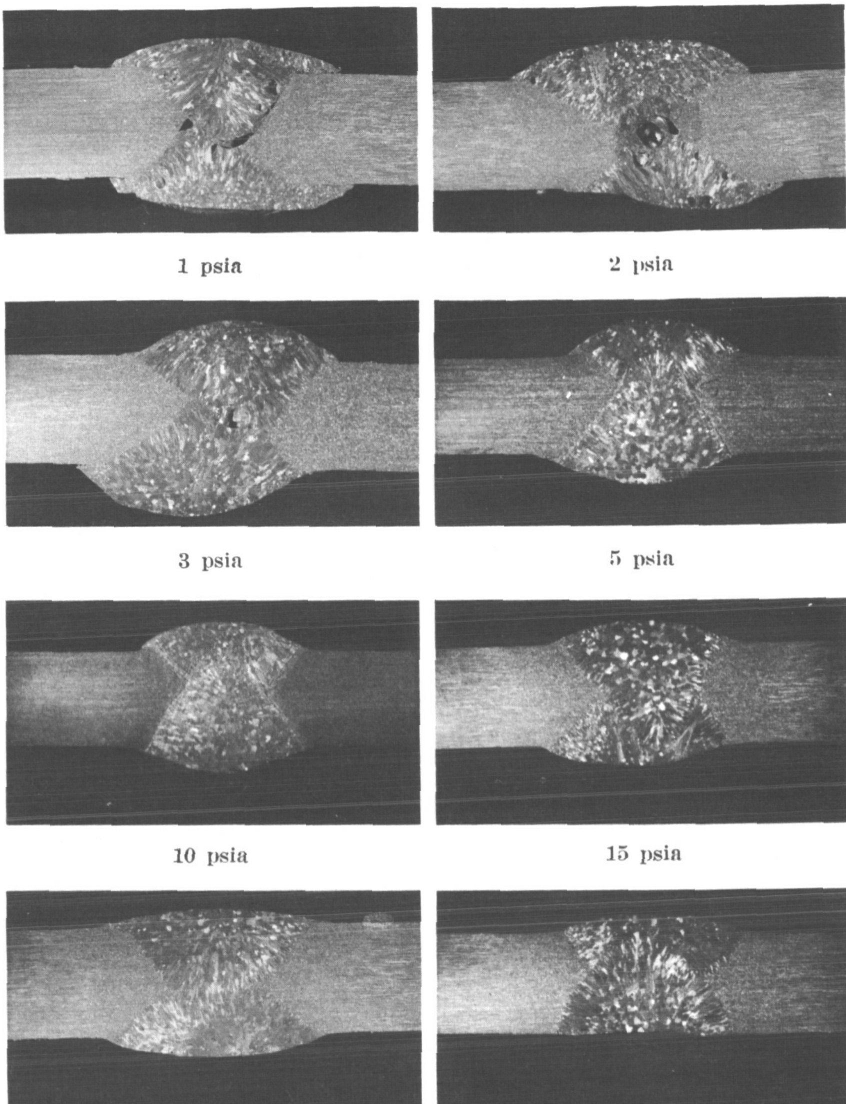

FIGURE 26.—Concluded. (b) Microsections.

The Al-Cu system is the basis for some of the oldest and most important structural alloys in use today. This is a precipitation-hardening system with a maximum solubility of 5.65 percent Cu at the eutectic temperature and less than 0.2 percent Cu at room temperature. The majority of the commercial alloys contain less than 5 percent Cu, although one alloy, 2219, which is outstanding among those that are available commercially because of its combination of weldability, strength, and insensitivity to stress concentrations at cryogenic temperatures, contains 6.3 percent Cu.

Numerous studies of the weldability of 2014 and 2024 have been carried out. Results show that satisfactory welds and good weld strengths can be obtained with the proper selection of welding conditions and filler alloy. The highest strengths and greatest efficiencies are obtained when preheat treatment of the weld is possible; however, considerable success has been obtained in increasing the strengths of as-welded structures through careful joint design, weld area reinforcement and rapid chilling.

In general, alloy 2024 has not been used much in welded structures because of greater difficulty in welding and lower weld properties than are obtained with 2014–T6. The preferred filler wire for use with 2024 is 4043, although 4543 and 2024 have also been employed.

Alloy 2014 was employed in welded missile applications. Both weldability and weld strengths are superior to those of 2024; however, the welding characteristics of 2014 are not as good as those of the 5000 series alloys and 6061.

Some weld properties for 2014–T6 at room and cryogenic temperatures are shown in table [4].* Results show an increase in the strength of the joint with decreasing temperatures. There is also a decrease in tensile elongation and some increase in notch sensitivity with decreasing temperatures.

The 2014 and 2219 alloys have the most attractive properties among commercial alloys of the 2000 group for applications in the aerospace field. Future research should explore the possibilities of improving the strengths of these alloys and the weldability of 2014 through modifications of the base composition and through additions of modulating elements such as Cd.

In the development of the more recently established alloys of this group, considerable emphasis was placed on their elevated temperature properties and very little, if any, attention was given to weldability or cryogenic temperature properties. It is anticipated that with improvement in these latter properties as primary objectives, research may disclose beneficial effects from some compositional or thermal treatment variations that were previously discarded as of no value at elevated temperatures.

Magnesium is the major alloying addition of the 5000 series of aluminum alloys. At 844° F the solid solubility of magnesium in aluminum is approximately 15 percent; however, this solubility decreases rapidly with decreasing temperature until at 392° F it is 4 percent and even less at room temperature. Decreasing solubility with decreasing temperature usually leads to substantial strengthening through precipitation; however, in the Al-Mg system the effect of

*Brackets indicate table number is not same as in original reports.

239–345 O—67——4

TABLE 4.—*Notch Sensitivity and Cryogenic Properties of Al-Cu Alloys*

[Ref. 28]

Alloy and temper	Temperature, °F	Properties of sheet					Properties of welded joints		
		Tensile strength, ksi	0.2 percent yield strength, ksi	Elongation in 2 in., percent	Notch tensile strength, ksi [a]	Notch tensile ratio	Tensile strength, ksi	Joint efficiency, percent	Elongation in 2 in., percent
2014–T6	78	71.1	65.7	11.0	74.5	1.02	57.1	73	2.0
	−100	71.4	69.3	12.0	79.2	1.04	56.7	74	2.0
	−320	87.1	74.4	14.0	85.5	.98	61.9	71	1.0
	−423	104.0	86.2	17.0	97.8	.94	75.6	73	1.2
2020–T6	75	81.0	75.4	7.1	35.0	.43			
2024–T3	78	67.9	47.4	16.0	60.2	.89			
	−100	70.2	48.9	21.0	61.2	.87			
	−320	87.0	60.9	22.0	76.2	.88			
	−423	110.0	73.1	17.0	83.8	.81			
2024–T4	78	67.1	42.8	19.0	59.0	.87			
	−100	69.8	43.7	22.0	60.7	.87			
	−320	84.9	51.1	27.0	71.9	.81			
	−423	107.0	73.3	16.0	88.3	.83			
2024–T86	75	75.8	71.3	5.2	51.3	.68			
	−320	91.2	83.5	8.0	47.0	.52			

2219–T62	70	60.9	44.1	12.0	56.5	.93	50.6	81	
	−110	66.5	50.2	11.2	56.8	.88	46.5	71	
	−320	77.9	54.3	14.5	67.1	.66	61.3	78	
	−423	92.3	59.1	18.0	72.8	.79	66.6	72	
2219–T81	70	64.6	51.5	10.7	62.4	.97	47.0	72	
	−110	69.7	55.9	9.5	64.9	.93			
	−320	81.8	63.2	12.7	73.4	.94	58.8	71	
	−423	96.9	68.5	15.3	79.9	.82	64.8	67	
2219–T87	78	70.7	58.2	9.0	59.7	.99	51.1	72	2
	−100	76.4	62.4	5.0	74.6	.98	49.5	65	4
	−320	88.4	76.4	11.0	85.0	.97	62.7	69	2
	−423	104.0	76.4	14.0	95.6	.92	73.0	70	1
2518–T6	70	58.2	52.1	8.7	59.7	1.03	49.2	84	
	−110	61.9	55.3	9.2	57.5	.93	52.8	84	
	−320	73.6	62.8	14.0	69.9	.95	58.6	81	
	−423	87.0	66.4	18.5	75.1	.86	65.7	76	
2618–T62	70	59.1	51.2	8.0	59.2	1.00	49.2	84	
	−110	61.1	50.9	8.0	60.7	.99	50.0	82	
	−320	73.4	57.6	11.6	65.4	.89	59.9	82	
	−423	85.6	63.1	17.8	70.9	.82	66.7	77	

[a] $K_t = 6.3$ for alloys referenced (62–8).
$K_t = 8.0$ for alloys referenced (61–36).
$K_t \geq 17$ for Alcoa data.

All specimens parallel to direction of rolling.

precipitation on strength is imperceptible below about 9–10 percent Mg.

> For this reason, the 5000 series alloys are generally classed as nonheat treatable, and magnesium is employed primarily as a solid solution strengthener. When the magnesium content retained in solid solution exceeds about 3.5 percent, a tendency for precipitation of the excess in the form of the Al-Mg intermetallic phase exists at atmospheric and slightly elevated temperatures. This precipitation, which normally occurs preferentially at grain boundaries and increases with the degree of supersaturation of the solid solution, tends to place a limitation on the Mg content of alloys for commercial application, since its presence may promote susceptibility to stress corrosion cracking.
>
> The commercial alloys generally contain manganese and chromium as supplementary strengtheners. These elements also serve to control grain size. The only other major alloying element occurring in the higher strength listed compositions of this group is zinc, which is employed in one experimental alloy.
>
> As a group, these alloys are outstanding in several respects in relation to the project requirements. The weldability of the alloys having the highest magnesium contents is excellent. The resistance to corrosion and stress corrosion cracking of the commercial alloys in approved tempers is high. Ductility as measured by elongation values at temperatures down to $-423°$ F remains at least equal to that observed at room temperature. The notch tensile strength generally increases with decreasing temperature although the rate of increase in this value is less than that of the unnotched tensile strength so that at $-423°$ F notch ratio values of 0.6–0.7 are observed with the highest strength alloy and temper. The most significant shortcoming in relation to the goals, however, occurs with respect to the tensile and yield strengths. Based on room temperature values, table [5], an increase of at least 20 ksi in both is required.
>
> The technology of welding with the Al-MG alloys has advanced to a high level of development. Because of the excellent welding characteristics of the high Mg alloys of the group, they may be welded by a variety of methods and are less sensitive to process variables than many other aluminum-base alloys.

There is extensive information from many sources which shows high joint efficiencies, good properties at cryogenic temperatures, and relatively low notch sensitivity of welded joints in the higher magnesium content commercial alloys. Representative weld property data are listed in table 6.

> Weld cracking tendency is highly dependent upon Mg content, the maximum sensitivity to this defect reportedly occurring at about 4 percent Mg in binary alloys of high purity and

TABLE 5.—*Mechanical Properties of 6000 and 5000 Series Wrought Aluminum Alloys Registered with the Aluminum Association*

[Ref. 28]

AA No.	Chemical composition limits,[a]—percent								Tensile properties [b]			
	Silicon	Iron	Copper	Manganese	Magnesium	Chromium	Zinc	Titanium	Product tested	Temper	Tensile strength, ksi	Yield strength, ksi
6151	0.6 -1.2	1.0	0.35	0.20	0.45-0.8	0.15-0.35	0.25	0.15	Forging	-T6	48	43
6061	0.40-0.8	.7	0.15-0.40	0.15	0.8 -1.2	0.15-0.35	.25	.15	Plate	-T6	45	40
6062	0.40-0.8	.7	0.15-0.40	0.15	0.8 -1.2	0.04-0.14	.25	.15	Plate	-T6	45	40
6066	0.3 -1.8	.50	0.7 -1.2	0.6 -1.1	0.8 -1.4	0.40	.25	.20	Extrusion.	-T6	57	52
6071	1.1 -1.9	.50	0.15-0.40	0.40-1.0	0.8 -1.4	0.10	.25	.15	Sheet	-T6	57	52
5154	0.45 Si + Fe		0.10	0.10	3.1 -3.9	0.15-0.35	.20	.20	Plate	-M34	42	33
5454	0.40 Si + Fe		0.10	0.50-1.0	2.4 -3.0	0.05-0.20	.25	.20	Plate	-M34	44	35
5456	0.40 Si + Fe		0.10	0.50-1.0	4.7 -5.5	0.05-0.20	.25	.20	Plate	-M343	56	43
5083	0.40	0.40	0.10	0.30-1.0	4.0 -4.9	0.05-0.25	.25	.15	Plate	-M343	52	41
5086	0.40	.50	0.10	0.20-0.7	3.5 -4.5	0.05-0.25	.25	.15	Plate	-M34	47	37

[a] Composition in percent maximum unless shown as a range or a nominal value.
[b] "Standards for Wrought Aluminum Mill Products," The Aluminum Association (unless indicated otherwise).

TABLE 6.—*Notch Sensitivity and Cryogenic Properties of Al-Mg Alloys*

[Ref. 28]

Alloy and temper	Temperature, centerline	Properties of plate: Tensile strength, ksi	0.2% yield strength, ksi	Elongation in 2 in., percent	Sharp notch tensile strength, ksi	Notch tensile ratio	Properties of welded joints: Tensile strength, ksi	Joint efficiency, percent	Elongation in 2 in., percent	Sharp notch tensile strength, ksi	Notch tensile ratio
5086–0	75	39.9	16.2	25	46.9	1.18					
	−320	56.8	16.2	43	55.9	.98					
	−423	80.5	20.7	40	60.0	.75					
5086–M34	75	50.3	38.8	10	63.2	1.26					
	−320	68.3	45.0	25	75.9	1.11					
	−423	93.5	48.9	27	73.1	.78					
5454–0	75	37.4	17.9	21	48.3	1.29					
	−320	56.4	21.6	38	58.2	1.03					
	−423	81.1	23.9	38	61.8	.76					
5454–M34	75	41.9	32.8	13	58.6	1.40					
	−320	61.7	40.0	31	70.5	1.14					
	−423	87.8	41.0	33	75.8	.86					
5083–0	75	46.8	20.2	20	48.8	1.04	43.2	92	14	43.7	1.01
	−320	63.0	22.5	36	57.0	.90	62.4	99	24	51.6	.83
	−423	85.2	25.2	32	59.3	.70	64.6	76	12	49.8	.77
5083–M113	75	48.6	34.9	16	61.2	1.26	43.7	90	15	44.5	1.02
	−320	65.4	40.8	31	70.2	1.07	62.4	95	20	52.8	.85
	−423	90.0	41.8	30	72.8	.81	64.2	71	11	51.5	.80

5456-0	75	50.4	23.2	17	50.4	1.00	46.7	93	15	44.6	.95
	−320	67.2	25.7	32	60.6	.90	60.3	90	15	50.9	.84
	−423	84.5	28.6	25	59.9	.71	62.4	74	9	47.5	.76
5454-M321	75	54.5	35.0	13	58.5	1.07	46.2	85	13	44.7	.97
	−320	73.4	38.3	24	68.1	.93	60.7	83	12	51.0	.84
	−423	96.2	43.9	22	71.2	.74	58.2	61	6	49.1	.84
5086-M34	78	47.8	35.7	9	48.7	1.02	39.0	82	4	------	------
	−100	48.9	36.6	15	50.3	1.03	39.5	81	5	------	------
	−320	65.4	40.8	24	61.9	.95	56.4	86	9	------	------
	−423	95.3	47.0	30	71.4	.75	75.3	79	11	------	------
5086-M38	78	64.2	58.2	7	64.6	1.01	------	------	------	------	------
	−100	66.2	58.4	10	67.5	1.02	------	------	------	------	------
	−320	76.8	60.9	18	75.3	.98	------	------	------	------	------
	−423	105.0	75.6	25	81.1	.77	------	------	------	------	------
5083-M38	78	62.7	56.7	5	62.1	.99	------	------	------	------	------
	−320	82.1	65.0	15	76.9	.94	------	------	------	------	------
	−423	101.0	71.5	13	87.1	.86	------	------	------	------	------
5154-M38	78	47.6	40.2	9	49.5	1.04	35.7	75	3	------	------
	−100	49.3	40.8	14	51.2	1.04	38.6	78	2	------	------
	−320	66.2	47.1	30	64.3	.97	55.5	84	7	------	------
	−423	93.5	54.0	35	77.6	.83	75.8	81	11	------	------
5456-M321	75	57.4	39.5	14.5	47.6	.83	51.9	91	13	54.4	1.05
	−320	76.6	46.7	26.8	52.7	.69	63.7	83	15.8	59.7	.93
	−423	96.4	52.6	21.7	56.7	.59	59.1	62	3.8	59.7	1.01
5456-M343	75	58.2	46.1	8.3	48.7	.84	51.9	90	7	53.2	1.03
	−320	77.1	51.4	18.5	53.3	.69	59.1	77	6.5	59.0	1.00
	−423	82.3	56.8	------	59.0	.72	58.8	72	3.0	59.9	1.02

All specimens parallel to direction of rolling.

at a lower level, 2 percent Mg, when Fe and Si are present in normal impurity concentrations. The cracking tendency decreases with increasing Mg beyond 4 percent so that at 6 percent the alloys are virtually crack-free. Titanium is customarily added to the fillers and is considered essential to provide greatest freedom from cracking.

Relatively little experimental work has been reported with alloys having Mg contents over 6 percent. Joint efficiencies generally decrease as the Mg increases. This is assumed to have resulted from dendritic segregation and intergranular deposition of the relatively brittle Al-Mg intermetallic phase in the weld deposit and possibly precipitation in the heat-affected zone, both of which would reduce the ductility and toughness of the joints. Possibly more modern welding methods would minimize this tendency. It has also been reported that weld unsoundness becomes more prevalent at higher Mg levels. To counteract this effect, chlorine additions to the shielding gas might have value.

Considerable work has been done to improve Al-Mg filler alloys to increase the strength of TIG welds in 5083 plate weldments. Strength was increased by raising Mg content or adding Zn. The Zn-free Al-Mg-Mn TIG weldments were not susceptible to stress corrosion or galvanic attack, but those containing Zn were highly susceptible, the degree of susceptibility increasing with Zn content. Furthermore, multipass MIG welds employing Zn-containing fillers developed grain boundary networks of brittle constituents with resulting embrittlement of the welds (ref. 28).

The prospects for meeting the strength and cryogenic notch toughness requirements with alloys of higher Mg content than those presently established as commercial in this country do not appear particularly encouraging; however, Fricke et al. suggest exploration of addition of Zn to the plate alloy as well as the filler metal to provide age hardening of the weld and heat-affected zones.

The 6000 series alloys are of the heat-treatable type, depending principally upon the controlled precipitation of the intermetallic phase magnesium silicide, Mg_2Si, for strengthening. This phase exhibits a maximum solid solubility in aluminum at the eutectic temperature, 1103° F. of 1.85 percent ($\sim$1.17 percent Mg plus 0.68 percent Si). The sharp decrease in solubility with decreasing temperature is the basis for the precipitation hardening of the 6000 group alloys and those that have the most desirable combinations of strength and resistance to corrosion contain Mg and Si in the Mg_2Si proportions. Alloy 6061, for example, with nominally 1.0 percent Mg and 0.6 percent Si will form approximately 1.6 percent Mg_2Si. Since the solubility of Mg in aluminum is rather high and this element is an effective solid solution strengthening addition, one might presume that alloys of increased strength and lower density could be developed by increasing the Mg content of the Mg_2Si type alloys. Actually, however, exceeding the Mg_2Si ratio results in a sharp decrease in solubility of the intermetallic phase so that alloys containing an excess of Mg over the favorable ratio develop inferior strengths.

The 6000 series alloys possess desirable weldability characteristics and are relatively insensitive to stress concentrations and the effects of cryogenic temperatures. Their modest strengths, which become even lower on welding, make the group unpromising as a basis for developing a high strength, weldable aluminum alloy.

Alloys of the 7000 series contain Zn and Mg as principal hardening agents and the properties of the alloys can be influenced by heat treatment. Copper may or may not be present in the alloys and the alloy characteristics are influenced by the presence or absence of this element.

Al-Zn-Mg alloys containing more than about 3 percent Zn and 0.5 percent Mg are capable of precipitation hardening, strengths increasing with increasing solute content. Optimum alloy compositions appear to be those associated with compositions in the area of the $Al_2Mg_3Zn_3$ and $MgZn_2$ phases. Alloys with high Zn and Mg contents develop strengths of the order desired and there is information indicating that higher strengths are possible provided more severe heat treating practices are employed.

A problem associated with Al-Mg-Zn alloys is their susceptibility to stress-corrosion cracking. This is related to composition, alloys containing less than 6 percent of Zn plus Mg being relatively free from stress-corrosion cracking and those with more than 6 percent of Zn plus Mg showing greater susceptibility. Because of this problem, commercial development of the ternary Al-Zn-Mg has been very slow. During World War II, the Germans made some use of these alloys, but their application was severely limited by the stress-corrosion problem. Another Al-Zn-Mg alloy has found application in Europe; however, the Zn and Mg contents are low and Cr is added to enhance resistance to stress-corrosion cracking. Because of the low alloying content, strengths are relatively low. In the United States, similar alloys are X7003 and X7005. Additional alloys of the Al-Zn-Mg type include X7006, X7038, and 7039.

Based on the European experiences, alloys X7006, X7038, and 7039 would be expected to show some susceptibility to stress-corrosion cracking. This is confirmed by tests on X7006, which indicate some susceptibility in the short transverse direction. No published data are available on the stress-corrosion characteristics of 7039 or X7038; however, it would be anticipated that 7039 would show moderate susceptibility to stress-corrosion cracking and X7038 an even higher susceptibility.

Evaluations of the new Al-Zn-Mg alloys indicate these materials have good weldability, although not as good as 5456 or 2219 alloys. Weldability appears to improve with increasing Mg contents up to 3 percent and small additions of Cr or Mn do not appear to have much effect. For MIG and TIG welding, Al-Mg and Al-Mg-Zn filler metals are recommended.

The Al-Zn-Mg alloys show weld efficiencies equal to or better than are obtained with 2000 series alloys, and better weld ductility. Since the Al-Zn-Mg alloys are relatively insensitive to the rate of quenching, welds in these alloys generally do not require post-weld heat treatment to develop good strengths. Natural aging of X7006 for several weeks will produce a stronger joint than can be obtained with non-heat-treatable alloys. Artificial aging usually provides even higher strengths and joint efficiencies.

Results of investigations show that the addition of Cu to the Al-Zn-Mg alloys increases strength, improves resistance to stress corrosion slightly, and reduces electrode potentials. Since the Al-Zn-Mg alloys are anodic to other structural alloys, the reduction in electrode potential tends to improve the compatibility of different alloy types and to minimize the possibility of galvanic corrosion.

Commercial Al-Zn-Mg-Cu alloys are listed in table [7]. Alloy 7075 is the best known member of this family and has been employed principally in military aircraft as sheet, plate, and structural members. Alloy 7277 is a rivet alloy but has been produced experimentally as sheet and plate. Alloy X7002 is a recently introduced composition for various structural applications, including service in the cryogenic field.

With the exception of 7277 rivets, Al-Zn-Mg-Cu alloy products are employed in the heat treated and artificially aged tempers. Typical room temperature properties for the alloys are shown in table [7]. Because of the high strengths obtainable with alloys such as 7075, 7079, and 7178, the possibilities of using these in cryogenic service have been investigated.

Results of tensile tests and notched tensile tests shown in Table 8 indicate these alloys are too notch sensitive for many cryogenic applications.

The weldability of the Al-Zn-Mg-Cu alloys is relatively poor in comparison with alloys such as 5456 and 2219, and inferior to the Cu-free Al-Zn-Mg alloys. Satisfactory welds can be made in alloys such as 7178 and 7075, however, with careful control of welding conditions and using 4043 or 5000 series alloy filler. Similar results are obtainable with alloy X7002. The weld properties of some of these alloys are shown in table [8].

The successful exploitation of these alloys in sensitive

TABLE 7.—*Mechanical Properties of 7000 Series Wrought Aluminum Alloys Registered With the Aluminum Association*

[Ref. 28]

AA No.	Chemical composition limits,[a] percent								Typical tensile properties [b]				
	Silicon	Iron	Copper	Manganese	Magnesium	Chromium	Zinc	Titanium	Product tested	Temperature	Tensile strength, ksi	Yield strength, ksi	Elongation, percent
					Al-Zn-Mg alloys								
X7003	0.35	0.35	0.10	0.10–0.50	0.9–1.6	0.05–0.20	4.3–5.3	0.20					
X7005	0.35 Si+ Fe		0.10	0.20–0.7	0.7–1.8	0.05–0.20	4.0–5.0	.15	Sheet	-T6	51	42	[c] 13
X7006	0.35 Si+ Fe		0.10	0.50	1.7–1.8	0.30	3.7–4.8	.15	Plate	-T6	61	55	[c] 13
X7038				*.50	*3.5		*4.5						
7039	.30	.40	0.25	0.10–0.40	2.3–3.3	0.15–0.25	3.5–4.5	.10	Plate	-T61	60	50	[d] 14
									Plate	-T6	65	55	[d] 13
					Al-Zn-Mg-Cu alloys								
7001	.35	.40	1.6–2.6	0.20	2.6–3.4	0.18–0.40	6.8–8.0	0.20	Rod	-T6	98	91	9
X7002	.20	.40	0.50–1.0	0.05–0.30	2.0–0.30	0.10–0.30	3.0–4.0	.15	Plate	-T6	67	57	[d] 12
7075	.30	.7	1.2–2.0	0.30	2.1–2.9	0.18–0.40	5.1–6.1	.20	Plate	-T6	83	73	11
7076	.40	.6	0.3–1.0	0.3–0.8	1.2–2.0		7.0–8.0	.20	Forging	-T6	70	60	[c] 14
7277	.50	.7	0.8–1.7		1.7–2.3	0.18–0.35	3.7–4.3	.10					
7176	.50	.7	1.6–2.4	0.30	2.4–3.1	0.18–0.40	6.3–7.3	.20	Plate	-T6	88	78	10
7079	.30	.40	0.4–0.8	0.10–0.30	2.9–3.7	0.10–0.25	3.8–4.8	.10	Plate	-T6	78	68	14

*Nominal composition.

[a] Compositions in percent maximum unless shown as a range or noted nominal.

[b] The Aluminum Association Standards for Wrought Aluminum Mill Products (Unless noted otherwise).

[c] Alcoa Data.

[d] 7039 Metal Working News, April 1963, Iron Age, July 18, 1963; 7002 Metal Progress, October 1962.

TABLE 8.—*Results of Cryogenic Temperatures on the Properties of High Strength Al-Zn-Mg-Cu Alloys and Weldments*

[Ref. 28]

Alloy and temper	Temperature, ° F	Longitudinal					Transverse				
		Tensile strength, ksi	0.2 percent yield strength, ksi	Elongation in 2 in., percent	Notch tensile strength, ksi [a]	Notch tensile ratio	Tensile strength, ksi	0.2 percent yield strength, ksi	Elongation in 2 in., percent	Notch tensile strength, ksi [a]	Notch tensile ratio
		Parent metal									
X7002–T6	75	69.8	61.8	11.5	66.8	0.96	69.3	59.6	10.8	65.1	0.94
	−112	-----	-----	-----	-----	-----	76.3	64.6	15.0	68.8	.90
	−320	-----	-----	-----	-----	-----	87.7	72.4	15.5	58.4	.67
7075–T6	75	82.1	74.4	11.2	68.4	.83	83.7	71.8	13.0	60.5	.72
	−320	100.2	91.0	14.3	42.5	.42	101.0	86.7	7.2	41.9	.42
	−423	113.2	105.2	6.3	40.4	.36	116.5	101.5	6.2	37.4	.32
7079–T6	75	77.5	72.3	11.5	70.8	.92	79.3	71.4	11.3	61.5	.78

	−320	94.8	85.6	14.3	60.5	.64	95.2	81.0	12.8	43.7	.46
	−423	114.9	95.5	15.8	59.6	.57	112.5	90.9	9.5	43.4	.39
7178–T6	75	90.0	83.6	12.2	51.8	.58	91.4	79.2	12.5	46.9	.52
	−320	107.7	99.6	9.5	35.5	.33	110.3	93.8	5.8	33.7	.31
	−423	123.1	111.6	8.2	31.5	.26	130.0	112.2	4.2	32.0	.25
					Welded metal						
7075–T6	75	46.5	45.0	1.0	43.6	0.94	47.2	47.0	3.0	---	---
	−320	52.3	51.6	1.0	42.2	.81	56.4	53.5	1.5	---	---
	−423	65.1	(b)	---	39.8	.61	69.1	65.3	1.0	---	---
7079–T6	75	50.7	42.3	1.5	52.9	1.04	49.9	42.1	1.3	55.3	1.10
	−320	57.2	54.3	1.2	59.2	1.03	57.0	54.8	1.4	57.0	1.00
	−423	57.2	---	.7	63.2	1.11	63.6	62.3	1.0	49.4	.78
7178–T6	75	54.1	51.0	1.3	53.0	.98	46.8	(b)	---	49.6	1.06
	−320	53.4	(b)	---	59.5	1.12	54.3	(b)	---	54.1	.99
	−423	55.6	(b)	---	49.8	.90	56.4	(b)	---	44.5	.79

[a] $K_t \gtreqless 17$.

[b] Fractured at less than 0.2 percent offset.

> aircraft applications can be attributed to improvements in resistance to stress corrosion achieved by composition control and the use of Cr to influence precipitation. As a result, these alloys have good resistance to stress corrosion in all but the short transverse directions of heavy sections.
>
> The high strength Al-Zn-Mg-Cu alloys such as 7075 fall short of the desired properties because of poor notch toughness and poor weldability. Lower strength Al-Zn-Mg-Cu alloys such as X7002 show much better notch toughness but lack the desired weldability. The Cu-free Al-Zn-Mg alloys such as X7006 and 7039 have good weldability and good notch toughness at room and cryogenic temperatures. At the present stage of development, however, these alloys do not meet [the desired] strength requirements. There is considerable hope for further improvement in strength through alloy development, and research to improve these alloys was recommended.

Following completion of the literature survey (ref. 28), experimental efforts were made to affect improvements (ref. 29). An attempt to improve the weld strengths of 2000 series alloys by varying the filler alloy was unsuccessful. Westerlund (ref. 29) points out that alloys of Al-Cu-Cd and Al-Cu-Cd-Sn (M825) welded as 0.125-inch sheet with 2319, M825, and Al-Cu fillers containing 0.23 Cd, 0.12 Mg, or 0.53 Mg showed little variation in weld strength.

> Tensile properties for the as-welded condition (naturally aged 25 days) and the post-weld aged condition (artificially aged 16 hours at 325° F) are shown in table [9].* No filler provided consistently higher tensile strengths than 2319, although there are isolated cases of improved properties. Specimens with the bead-on generally failed at the edge of the weld where no reinforcement occurred. Bead-off specimens usually failed through the weld and would be expected to show properties typical of the filler alloy. Therefore, it was surprising to see no effect of filler metal on bead-off tensile strengths. Post-weld aging raised strengths for both the bead-on and bead-off conditions, but was much more effective for the bead-off condition.

The weld properties of 0.525-inch-thick M791 and M793, 7000 series plate welded with M822 filler alloy are reported in table 10.

> All the reduced section specimens and many of the full section specimens failed adjacent to the weld in the heat-affected zone. The full section specimens that failed at the edge of the weld zone had tensile strengths approximately equal to the reduced section strengths, thus showing the two areas of the weld have similar strengths.

For the 7000 series welds, the increase in tensile strength with decreasing temperature was different for the as-welded and post-weld

TABLE 9.—*Weld Properties for 2000 Series Aluminum Alloys* [Ref. 29]

[Welded 0.125-Inch-thick sheet]

Alloy	Filler	Postweld age	Weld bead on				Weld bead off			
			Tensile strength, ksi	Yield strength, ksi	Percent elongation in 2 inches	Location [c] of failure	Tensile strength, ksi	Yield strength, ksi	Percent elongation in 2 inches	Location [c] of failure
Al+Cu+Cd (6.21 Cu; 0.17 Cd)	2319	No [a]	45.2	26.8	3.0	B	37.8	23.0	3.5	A
	2319	16 hr/325° F [b]	47.7	42.5	1.0	B	44.6	36.2	2.0	B
	Al-6 Cu-0.23 Cd	No	44.6	25.6	4.0	B	39.2	22.3	4.2	A
	Al-6 Cu-0.23 Cd	16 hr/325° F	48.6	40.8	1.8	B	44.8	34.7	3.0	A, B
	Al-6 Cu-0.12 Mg	No	43.5	27.7	3.5	B	38.8	23.8	4.2	A
	Al-6 Cu-0.12 Mg	16 hr/325° F	48.0	42.6	1.5	B	45.0	36.8	2.5	A
	Al-6 Cu-0.53 Mg	No	46.8	28.8	3.8	B	38.6	23.8	3.5	A
	Al-6 Cu-0.53 Mg	16 hr/325° F	51.8	41.3	1.8	B	44.3	34.9	2.5	A
	Al-6 Cu-0.14 Cd-0.05 Sn	No	41.8	27.3	3.0	B	34.7	23.2	3.0	A
	Al-6 Cu-0.14 Cd-0.05 Sn	16 hr/325° F	46.0	45.0	.8	B	44.2	37.4	2.2	A
Al+Cu+Cd+Sn (6.24 Cu; 0.14 Cd; 0.05 Sn)	2319	No	43.8	26.0	3.2	B	37.9	21.1	4.2	A
	2319	16 hr/325° F	51.0	43.3	1.5	B	44.8	36.6	2.2	A
	Al-6 Cu-0.23 Cd	No	44.6	26.2	4.0	B	37.7	22.2	4.2	A, B
	Al-6 Cu-0.23 Cd	16 hr/325° F	53.0	45.2	1.8	B	46.0	37.0	2.2	A
	Al-6 Cu-0.12 Mg	No	44.8	26.7	3.5	B	37.4	23.1	4.5	A
	Al-6 Cu-0.12 Mg	16 hr/325° F	47.4	40.7	1.5	B	43.9	34.2	2.8	A
	Al-6 Cu-0.53 Mg	No	44.0	27.8	3.5	B, C	37.8	25.0	3.2	A
	Al-6 Cu-0.53 Mg	16 hr/325° F	49.5	39.9	1.5	B	42.9	34.1	2.5	A
	Al-6 Cu-0.14 Cd-0.05 Sn	No	42.4	26.7	2.8	B	----------	21.3	2.0	A
	Al-6 Cu-0.14 Cd-0.05 Sn	16 hr/325° F	49.6	46.0	1.0	B, C	44.2	37.6	1.5	A, B

[a] Room temperature aged about 25 days.

[b] Postweld aged about 2 weeks after welding.

[c] Location of failure: A, through weld; B, through edge of weld; C, parent metal.

1. Thermal treatment of parent metal: both alloys solution heat treated 30 min. at 995° F and cold water quenched; 2219+Cd, preaged 1 hr at 325° F, stretched, and aged 16 hr at 325° F; 2219+Cd+Sn, stretched and aged 8 hr at 325° F.

2. Welded in the longitudinal direction; transverse specimens; yield strength is 0.2 percent offset (centered on weld).

TABLE 10.—*Weld Properties of 7000 Series Aluminum Alloys*

[Ref. 29]

[Full and reduced section]

Specimen No.	Alloy	Welding method	Condition [a] of weld	Full section properties		Reduced section properties [b]	
				Tensile strength, ksi	Location [c] of failure	Tensile strength, ksi	Location [c] of failure
292058–A1	M791	MIG	1	60. 8	B	59. 2	C
292058–A2	M791	MIG	2	60. 8	B	60. 6	C
292058–A3	M791	MIG	3	61. 2	B		
292058–B1	M791	TIG	1	55. 5	B	55. 8	C
292058–B2	M791	TIG	2	59. 0	C	[d] 54. 6	C
292058–B3	M791	TIG	3	60. 0	C		
292059–A1	M793	MIG	1	58. 0	B–C	[d] 54. 8	C
292059–A2	M793	MIG	2	57. 7	C	57. 7	C
292059–A3	M793	MIG	3	59. 2	C		
292059–B1	M793	TIG	1	52. 8	C	53. 0	C
292059–B2	M793	TIG	2	56. 8	C	[d] 51. 9	C
292059–B3	M793	TIG	3	56. 5	C		

[a] 1—As-welded, naturally aged over 2 months.
2—Postweld aged after 1 month at room temperature 8 hrs. at 225° F+16 hrs. at 300° F.
3—Postweld aged after 1 month at room temperature 48 hrs. at 250° F.

[b] Round reduced section specimens.

[c] B—At edge of the weld.
C—Adjacent to weld zone (in heat affected zone).

[d] No apparent reason for these strengths being lower than the full section strengths.

aged conditions. Comparing tensile strength at −320° F with that at room temperature gave ratios of 1 : 1 for the as-welded specimens and about 1 : 3 for the post-weld aged conditions.

Efforts to improve the aluminum alloy strength-weldability combination were further extended to cover the major interested producers and independent research agencies (refs. 30, 31). Baysinger reports on an extensive evaluation of the Al-Mg-Zn system, the results of which are herewith summarized (ref. 30). These alloys are heat treatable and, additionally, variation in thermal treatment practice can be applied to give certain desirable properties. The nominal chemical compositions of two of these alloys are:

Chemical Composition of 2 Al-Mg-Zn Alloys

Alloy designation	Composition, weight percent							
	Si	Fe	Cu	Mn	Mg	Cr	Zn	Ti
X7038	0. 10	0. 15	0. 05	0. 50	3. 5	0. 12	4. 5	0. 04
7039	. 30	. 40	. 10	0. 10–0. 40	2. 3–3. 3	0. 15–0. 25	3. 5–4. 5	. 10

Alloy 7039–T6 and alloy X7038–T7 were found to provide a desirable combination of strength, ductility, and notch toughness at room temperature and −320° F. This combination of properties, along with good formability and weldability, makes these materials attractive for fabrication of cryogenic vessels and many other structural applications. Although alloy X7038–T6 had higher parent metal strength, it did not provide any significant improvement in welded strength over 7039–T6 or X7038–T7. Moreover, X7038–T6 was found to be more susceptible to stress corrosion cracking than the other two materials, and X7038–T6 tungsten inert-gas (TIG) weldments were somewhat more crack sensitive than weldments in 7039–T6 or X7038–T7. Therefore, X7038–T6 is not considered to be as well suited as the other two materials for applications where high stress levels may be encountered.

> Alloy 7039–T6 has slightly higher tensile strength (60 000 to 68 000 psi) than does X7038–T7 (55 000 to 60 000 psi), and, additionally, does not show any tendency toward microfissuring in the weld fusion zone. Alloys 7039–T6 and X7038–T7 were readily weldable by tungsten inert-gas or metal inert-gas fusion processes. Weldments of these experimental alloys, when made with Al-Zn-Mg fillers, have the highest strength and ductility of any weldable aluminum alloy commercially

> available today. For example, flush machined weldments of 7039–T6 made with Al-Zn-Mg fillers attained tensile strengths of 50 000 to 56 000 psi; 30 000 to 34 000 psi apparent yield strength; and 8 to 13 percent elongation after 30 days or more natural aging at room temperature.

Of prime significance for heavy plate applications is the fact that these alloys can be welded under high restraint by the direct current, straight polarity, tungsten inert-gas (DCSP–TIG) process with a minimum of weld cracking. DCSP–TIG welds in highly restrained circular patch tests did not crack in either 7039 or X7038 alloy in ¾-inch thickness.

Three alloys (table 11) had excellent strength and ductility in both parent metal and weldments at −320° F.

> Alloy 7039–T6 increased in tensile strength from 65 000 psi at 75° F to 82 000 psi at −320° F. Ductility, as measured by elongation in a 2-inch gage length, likewise increased from 14 to 18 percent. For alloy 7039–T6 the notched-to-unnotched tensile strength ratio was greater than unity at 75° F and was 0.88 at −320° F. This ratio is based on a notch corresponding to a K_t factor of 6.3, which is commonly used as a measure of notch toughness for aluminum and other materials. Weldments of ¾-inch 7039–T6 plate made with X5039 (1A) filler increased in tensile strength after a minimum of 15 to 30 days natural aging to 51 000 psi at 75° F and 61 000 psi at −320° F. The ductility of such weldments remained adequate for cryogenic applications with 13 percent elongation (2-inch gage length) at 75° F and 8 percent elongation at −320° F. The formability of alloys X7038–T6 and –T7 and 7039–T6 and their weldments, as judged by bend tests and by hydraulic rupture tests, was excellent.

The chemical composition of the filler alloys is given in table 12. The major alloying elements of the four fillers are as follows:

Major Alloying Elements of 4 Aluminum Fillers

Filler designation	Composition; weight percent							
	Zn	Mg	Mn	Cr	Fe	Si	Cu	Ti
X5039	3.1	3.8	0.39	0.11	0.07	0.06	0.07	0.03
D1707	7.3	3.0	.01	.11	.09	.05	.07	.04
D1495	4.6	3.1	.39	.10	.08	.04	.07	.02
5183	.03	4.6	.60	.07	.16	.07	<.01	.02

TABLE 11.—*Transverse Tensile Properties and Chemical Composition of Aluminum Sheet and Plate Materials*

[Ref. 30]

Sheet and plate			Department of Metallurgical Research, chemical composition, weight percent											Trentwood Mill test data			DMR check tests		
Lot No.	Alloy	Gage, in.	Zn	Mg	Mn	Cr	Cu	Si	Fe	Ti	V	N	Be [a]	Tensile strength, ksi	Yield strength, ksi	Elongation in 2 in., percent	Tensile strength, ksi	Yield strength, ksi	Elongation in 2 in., percent
930755	5086-H112	1/8	0.10	3.8	0.45	0.12	0.08	0.21	0.19	0.05	----	----	0.006	([b])	----	----	47.5	33.4	12.0
12831	X7038-T6	1/8	4.52	3.04	.45	.12	.03	.09	.16	.01	0.01	0.004	.0001	([c])	----	----	71.8	63.7	12.3
12831	X7038-T6	1/4	4.52	3.04	.45	.12	.03	.09	.16	.01	.01	.004	.0001	72.9	64.8	11.5	73.2	64.6	15.3
12801	X7038-T6	1/2	4.40	3.35	.47	.13	.02	.08	.15	.01	.01	.004	.0001	74.6	66.5	12.3	74.5	65.6	17.0
5571	X7038-T6	3/4	4.57	3.25	.46	.12	.03	.10	.22	.02	.01	.004	.0001	76.1	69.2	12.2	75.8	70.0	10.6
12831	X7038-T7	1/8	4.52	3.04	.45	.12	.03	.09	.16	.01	.01	.004	.0001	([c])	----	----	61.7	48.1	14.6
12841	X7038-T7	1/4	4.58	3.13	.44	.13	.04	.08	.16	.01	.01	.004	.0001	57.7	43.5	14.0	56.9	43.0	18.0
12811	X7038-T7	1/2	4.46	3.56	.49	.12	.05	.08	.16	.03	----	----	----	61.8	48.3	13.2	60.7	46.3	19.6
5581	X7038-T7	3/4	4.61	3.24	.48	.11	.05	.11	.22	.02	.01	.004	.0001	60.6	46.6	13.0	60.3	46.5	12.6
253611	7039-T6	1/8	3.78	2.83	.22	.17	.03	.06	.18	.02	----	----	----	([c])	----	----	61.5	51.4	13.0
253581	7039-T6	3/8	3.85	2.83	.22	.18	Tr	.06	.16	.02	----	----	----	66.0	58.3	13.1	66.2	58.6	13.8
157851	7039-T6	3/4	3.81	2.93	.27	.19	0.02	.07	.17	.01	.01	.004	.0003	68.0	60.2	13.2	68.9	61.1	13.1

[a] B, Pb, and Sn, 0.000 each.
[b] Old DMR stock for which records are no longer available.
[c] 1/8 in. materials rerolled from ¼-in.-thickness mill plate.

TABLE 12.—*Chemical Composition of Aluminum Filler Metals*

[Ref. 30]

Filler	Spool	Diameter, in.	Composition, weight percent													
			Si	Fe	Cu	Mn	Mg	Cr	Zn	Ti	V	B	Pb	Sn	Ni	Be
5183	8455 1-3	3/32	0.09	0.12	<0.01	0.54	4.51	0.08	0.03	0.02	0.01	0.000	0.000	0.000	0.004	0.0001
5183	8468 2-49	1/16	.07	.16	.01	.59	4.64	.07	.03	.02	.01	.000	.000	.000	.004	.0001
X5039 [a]	2841-44	1/16	.07	.07	.07	.38	3.65	.11	3.13	.000	.000	.000	.000	.000	.004	.000
X5039 [a]	2841-45	1/16	.05	.07	.06	.39	3.87	.10	3.08	.000	.000	.000	.000	.000	.002	.000
D1495	2842-16	1/16	.05	.08	.06	.39	3.02	.10	4.60	.03	.000	.000	.000	.000	.002	.000
D1495	2842-17	1/16	.04	.07	.08	.39	3.12	.10	4.66	.02	.000	.000	.000	.000	.003	.000
D1707	2843-29	1/16	.04	.08	.07	.01	3.31	.10	7.41	.03	.000	.000	.000	.000	.002	.000
D1707	2843-32	1/16	.05	.10	.07	.01	2.88	.11	7.21	.05	.000	.000	.000	.000	.002	.000

[a] Originally designated "1A."

TABLE 13.—*Average Results of Notched and Unnotched Tensile Tests of Nonwelded and DCSP-TIG Welded X7038-T6, X7038-T7, and 7039-T6 at 75° and −320° F*

[Ref. 30] [K_t=6.3]

Base material: Alloy and temper	Base material: Lot No.	Base material: Gage, in.	Filler alloy	Postweld natural aging time, days	Number of samples, 75° F: Notched	Number of samples, 75° F: Unnotched	Number of samples, −320° F: Notched	Number of samples, −320° F: Unnotched	Tested at 70°-75° F: Notched TS, ksi		Tested at 70°-75° F: TS, ksi	Tested at 70°-75° F: YS, ksi	Tested at 70°-75° F: Elongation in 2 in., percent	Tested at 70°-75° F: Ratio, NTS/UTS	Tested at −320° F: Notched TS, ksi	Tested at −320° F: TS, ksi	Tested at −320° F: YS, ksi	Tested at −320° F: Elongation in 2 in., percent	Tested at −320° F: Ratio, NTS/UTS	Typical hardness, Rockwell B: Weld, min.	Typical hardness, Rockwell B: Heat affected zone, min.	Typical hardness, Rockwell B: Parent metal, max.	Typical hardness, Rockwell B: Aging time, days
X7038-T6	12831	⅛ (rerolled from ¼ in.)	Not welded		3	4	3	4	Av	77.0	71.2	62.5	12.4	1.08	78.2	88.6	74.1	12.1	0.88				
									Min	76.9	71.0	62.5	12.0	1.08	75.9	88.4	73.0	11.0	.85				
									Max	77.1	71.5	62.6	12.5	1.09	81.7	88.9	75.0	15.0	.92				
			X5039	131	4	4	4	4	Av	47.9	49.5	34.0	4.2	.97	53.0	65.2	43.3	3.8	.81	48	57		105
									Min	47.2	48.7	33.6	3.0	.93	49.8	64.2	33.6	3.0	.75				
									Max	48.6	50.5	34.8	5.0	1.00	56.9	66.6	34.8	4.0	.89				
			D1495	130	4	4	3	2	Av	49.9	51.0	34.6	4.8	.96	55.4	67.2	45.6	4.5	.82	52	46		104
									Min	46.0	50.4	32.2	4.5	.89	53.7	65.5	45.3	4.0	.78				
									Max	50.2	51.7	35.4	5.0	1.00	57.7	68.9	46.0	5.0	.88				
			D1707	122	4	4	4	4	Av	48.0	53.5	36.0	4.6	.90	60.2	66.4	46.9	3.6	.91	51	52	82	96
									Min	45.4	52.6	34.5	4.0	.84	51.8	62.8	45.4	3.0	.71				
									Max	51.1	54.3	37.4	5.0	.97	69.9	72.6	48.7	5.5	1.11				
			5183	92	4	4	4	4	Av	46.1	49.7	33.3	4.5	.93	51.5	64.2	40.2	5.2	.80	46	44		146
									Min	44.8	48.1	32.0	4.0	.89	48.0	55.5	36.6	4.5	.71				
									Max	46.7	50.4	34.4	5.0	.97	57.9	67.9	43.0	5.5	1.04				
			Fusion only	168	4	3	4	3	Av	48.7	54.5	36,4	4.0	.95	54.5	67.5	47.4	3.7	.81	43	56		145
									Min	48.0	53.2	38.7	4.0	.89	53.3	65.8	44.6	3.0	.78				
									Max	49.0	54.1	39.0	4.5	.92	56.5	68.7	49.7	5.0	.86				

TS=tensile strength; YS=yield strength; NTS=notched tensile strength; UTS=unnotched tensile strength.

TABLE 13.—*Average Results of Notched and Unnotched Tensile Tests of Nonwelded and DCSP–TIG Welded X7038–T6, X7038–T7, and 7039–T6 at 75° and −320° F*—Continued

[Ref. 30] [K_t=6.3]

Base material: Alloy and temper	Base material: Lot No.	Base material: Gage, in.	Filler alloy	Postweld natural aging time, days	Number of samples, 75° F: Notched	Number of samples, 75° F: Unnotched	Number of samples, −320° F: Notched	Number of samples, −320° F: Unnotched		Tested at 70°–75° F: Notched TS, ksi	Tested at 70°–75° F: TS, ksi	Tested at 70°–75° F: YS, ksi	Tested at 70°–75° F: Elongation in 2 in., percent	Tested at 70°–75° F: Ratio, NTS/UTS	Tested at −320° F: Notched TS, ksi	Tested at −320° F: TS, ksi	Tested at −320° F: YS, ksi	Tested at −320° F: Elongation in 2 in., percent	Tested at −320° F: Ratio, NTS/UTS	Typical hardness, Rockwell B: Weld, min.	Typical hardness, Rockwell B: Heat affected zone, min.	Typical hardness, Rockwell B: Parent metal, max.	Typical hardness, Rockwell B: Aging time, days
X7038–T6	12831	¼	Not welded		4	4	4	4	Av	79.8	72.5	67.2	14.0	1.10	84.4	88.9	79.6	10.0	0.95				
									Min	79.6	72.3	67.0	13.5	1.10	83.9	88.4	79.3	8.0	.94				
									Max	80.1	72.6	67.3	14.5	1.11	85.4	89.6	80.0	11.0	.97				
			X5039	166	4	4	1	2	Av	51.1	51.5	35.4	6.0	.99	55.4	67.5	44.9	5.7	.82	52	64	84	65
									Min	49.8	48.7	34.7	5.0	.93	55.4	64.9	43.5	4.5	.79				
									Max	52.2	54.2	36.0	7.0	1.07	55.4	70.2	46.2	7.0	.85				
			D1495	141	4	4	3	3	Av	47.6	53.2	35.4	7.0	.90	55.7	66.5	45.4	6.1	.84	52	51		35
									Min	45.7	51.2	34.8	6.5	.84	52.1	64.3	44.3	6.0	.76				
									Max	49.6	54.5	35.8	7.5	.97	59.0	68.5	46.3	6.5	1.25				
			D1707	141	4	4	4	4	Av	49.0	53.0	35.1	6.8	.92	54.0	58.3	45.3	3.8	.92	52	42		35
									Min	46.3	52.5	34.6	6.0	.87	51.3	48.5	44.8	2.0	.77				
									Max	52.8	53.4	35.7	7.0	1.00	56.0	62.7	46.3	7.0	1.27				
			5183	46	2	2	3	2	Av	50.1	52.7	34.3	7.5	.95	54.9	68.2	42.2	8.7	.80	57	58		166
									Min	47.5	52.6	34.3	7.5	.90	53.1	66.6	41.3	8.0	.76				
									Max	53.7	52.8	34.3	7.5	1.02	57.0	69.9	43.1	9.5	.86				
			Fusion only	102	4	4	4	4	Av	50.7	54.0	38.1	5.5	.94	51.0	57.8	47.2	2.8	.88	61	67		159
									Min	50.2	52.4	37.4	5.0	.92	50.5	51.4	46.6	1.0	.76				
									Max	51.1	55.2	38.5	6.0	.98	51.9	66.0	48.2	5.0	1.03				

			Not welded		3	4	4	4	Av	82.1	74.4	69.5	10.6	1.10	85.9	92.1	82.8	12.0	0.93				
									Min	81.0	73.9	69.0	10.0	1.08	83.0	91.2	82.4	11.0	.90				
									Max	83.1	75.1	70.3	11.0	1.13	89.1	92.7	83.1	13.0	.98				
			X5039	179	4	2	4	3	Av	50.3	53.1	33.4	10.5	.96	49.4	59.8	40.8	5.5	.82	56	51		53
									Min	49.8	53.0	33.4	10.0	.94	46.3	58.4	40.7	4.5	.76				
									Max	50.5	53.2	33.5	11.0	1.03	51.4	60.9	40.9	6.0	.99				
			D1495	174	4	3	4	4	Av	51.1	53.2	33.3	10.0	.92	49.0	59.2	40.0	5.3	.82	55	47		53
									Min	50.2	51.7	32.2	10.0	.92	47.5	56.5	38.7	4.0	.73				
									Max	52.6	54.7	34.5	10.0	.93	52.0	64.7	41.3	8.0	.92				
X7038-T6	5571	¾	D1707	173	4	4	4	3	Av	51.8	53.5	33.8	10.0	.96	50.3	60.2	40.5	5.6	.83	62	50	85	54
									Min	50.5	53.0	33.6	9.0	.94	48.3	56.7	40.6	4.0	.74				
									Max	52.4	53.8	34.1	11.0	.99	51.8	65.5	41.1	8.0	1.00				
			5183	175	4	4	4	4	Av	47.8	53.8	32.5	12.0	.88	47.6	62.7	39.8	6.7	.76	52	50		52
									Min	46.6	53.2	32.2	11.0	.87	46.8	58.2	39.5	5.0	.72				
									Max	49.4	54.3	32.6	13.0	.93	49.7	65.1	40.8	8.0	.85				
			Fusion only	181	4	4	4	4	Av	50.7	55.5	35.7	12.1	.91	51.3	63.9	43.0	6.8	.80	60	54		60
									Min	48.3	55.2	35.1	10.0	.86	46.4	62.6	42.3	6.0	.70				
									Max	53.6	56.1	36.4	12.5	.97	54.0	66.1	43.7	8.5	.86				
			Not welded		4	4	4	4	Av	64.2	60.1	47.9	13.4	1.07	70.6	79.8	56.8	16.3	0.88				
									Min	64.1	59.8	47.8	13.0	1.06	70.2	79.5	56.4	16.0	.88				
									Max	64.4	60.4	48.2	13.5	1.08	70.8	80.1	57.2	17.0	.89				
			X5039	141	4	4	4	4	Av	47.2	49.6	35.1	4.9	.95	55.2	64.8	44.4	4.5	.85	46	47	68	92
									Min	45.6	48.2	35.0	4.0	.90	51.4	63.4	43.9	4.0	.76				
									Max	48.7	51.5	35.3	5.0	1.01	58.9	67.3	45.3	5.0	.93				
			D1495	173	4	4	4	4	Av	50.8	52.8	37.1	5.8	.96	55.7	68.2	46.0	6.1	.81	47	44	68	69
									Min	50.5	50.9	36.5	5.0	.92	53.1	66.7	44.9	5.5	.76				
X7038-T7	12831	⅛ (rerolled from ¼ in.).							Max	51.1	54.8	37.7	7.0	1.00	59.6	70.0	46.7	7.0	.89				
			D1707	81	4	4	4	4	Av	46.4	52.1	35.4	6.1	.88	50.5	64.2	41.6	6.0	.78				(a)
									Min	43.8	49.6	34.8	5.0	.83	46.0	60.9	40.5	5.0	.70				
									Max	47.9	53.7	35.8	7.0	.97	55.4	66.0	42.7	6.5	.91				
			5183	91	4	4	4	4	Av	44.0	48.6	33.7	3.9	.91	52.8	63.9	41.3	4.9	.83	50	43	68	145
									Min	38.2	44.3	31.0	2.5	.75	45.8	56.8	39.1	3.0	.67				
									Max	47.6	51.2	35.3	4.5	1.07	61.6	68.5	43.9	6.0	1.08				
			Fusion only	165	4	4	4	4	Av	49.2	52.0	37.2	5.1	.95	54.3	66.4	47.1	5.2	.82	46	53	68	142
									Min	48.8	51.2	35.8	4.0	.91	52.3	64.7	44.7	4.0	.76				
									Max	50.2	53.2	38.1	6.0	.98	55.6	67.8	49.6	7.0	.86				

TS=tensile strength; YS=yield strength; NTS=notched tensile strength; UTS=unnotched tensile strength.

TABLE 13.—*Average Results of Notched and Unnotched Tensile Tests of Nonwelded and DCSP-TIG Welded X7038-T6, X7038-T7, and 7039-T6 at 75° and —320° F*—Continued

[Ref. 30] [K_t=6.3]

Base material			Filler alloy	Postweld natural aging time, days	Number of samples				Tested at 70°-75° F						Tested at −320° F					Typical hardness, Rockwell B			
					75° F		−320° F																
Alloy and temper	Lot No.	Gage, in.			Notched	Unnotched	Notched	Unnotched	Notched TS, ksi		TS, ksi	YS, ksi	Elongation in 2 in., percent	Ratio, NTS/UTS	Notched TS, ksi	TS, ksi	YS, ksi	Elongation in 2 in., percent	Ratio, NTS/UTS	Weld, min.	Heat affected zone, min.	Parent metal, max.	Aging time, days
X7038-T7	12841	¼	Not welded		4	4	4	4	Av	60.8	56.0	43.0	15.9	1.09	65.6	74.3	50.6	18.8	0.88				
									Min	60.4	55.8	42.7	15.5	1.07	65.2	74.2	50.4	18.5	.88				
									Max	61.2	56.3	43.3	16.0	1.09	65.9	74.9	51.0	19.0	.89				
			X5039	170	4	4	4	4	Av	49.4	53.9	35.6	7.5	.92	52.3	65.7	44.7	6.4	.80	56	57	74	64
									Min	48.8	53.1	35.1	7.0	.89	50.4	60.5	43.8	4.0	.73				
									Max	50.6	54.8	36.1	8.0	.95	55.1	68.7	45.5	8.5	.91				
			D1495	135	4	4	4	4	Av	51.9	53.2	34.6	10.8	.98	58.6	65.7	44.2	7.0	.89	49	53	74	67
									Min	50.9	52.6	34.4	8.5	.95	57.0	61.8	43.5	4.0	.80				
									Max	52.4	53.8	34.8	13.0	1.00	60.2	67.9	45.2	11.0	.97				
			D1707	135	4	4	4	4	Av	51.2	53.0	33.7	12.4	.97	56.5	66.3	42.6	8.4	.85	51	51	74	34
									Min	50.5	51.5	32.9	9.5	.93	51.5	64.8	41.3	7.0	.74				
									Max	52.7	54.5	34.4	14.0	1.02	60.2	69.4	43.4	10.0	.93				
			5183	42	2	2	3	3	Av	46.6	49.9	32.8	7.0	.93	51.8	67.0	40.5	7.8	.77	56	62	74	162
									Min	45.3	49.9	32.6	7.0	.91	49.5	65.2	40.3	7.5	.71				
									Max	47.9	50.0	33.1	7.0	.96	55.3	69.4	40.7	8.0	.85				
			Fusion only	165	4	4	4	4	Av	49.3	54.8	36.3	10.8	.90	52.7	55.4	44.5	4.0	.90	58	62	74	52
									Min	48.0	54.1	35.9	7.5	.87	51.2	53.3	43.6	3.0	.84				
									Max	51.2	55.1	36.7	12.0	.95	54.1	61.2	46.3	5.0	1.01				

X7058-T7	5581	¾	Not welded		3	4	4	4	Av	60.5	58.2	44.9	13.5	1.04	67.1	77.0	53.2	16.0	0.87				[a]
									Min	60.3	58.1	44.8	13.0	1.03	66.9	76.8	52.9	15.5	.87				
									Max	60.6	58.3	45.0	14.0	1.04	67.5	77.2	53.4	17.0	.88				
			X5039	179	4	4	4	3	Av	50.9	52.3	33.2	11.3	.97	50.9	58.4	39.7	5.3	.87	55	50	70	53
									Min	48.6	51.8	32.8	11.0	.92	49.3	53.1	39.2	3.5	-----				
									Max	53.1	53.0	33.7	11.5	1.02	52.5	62.3	40.2	7.0	-----				
			D1495	162	4	4	4	4	Av	51.3	52.2	32.9	10.2	.98	47.2	60.7	39.3	6.3	.77	54	50	70	53
									Min	48.6	52.1	32.6	10.0	.93	40.1	56.0	38.6	4.0	.79				
									Max	51.9	52.5	33.1	11.0	1.00	50.8	64.7	39.7	8.5	1.07				
			D1707	180	4	4	4	2	Av	51.0	52.2	32.8	9.5	.97	52.3	61.4	39.8	6.2	.88	60	50	70	51
									Min	48.2	52.0	32.5	9.0	.91	50.8	58.5	38.8	5.0	.75				
									Max	51.9	52.7	33.2	10.0	1.00	52.5	64.4	40.0	7.5	.91				
			5183	179	4	4	4	4	Av	48.7	52.6	31.7	11.0	.92	46.7	63.6	38.1	8.3	.70	50	47	70	52
									Min	48.1	51.8	31.2	9.0	.90	45.3	61.7	36.8	7.0	.68				
									Max	49.2	53.3	32.0	12.0	.92	47.7	66.3	39.7	9.5	.72				
			Fusion only	49	2	3	3	2	Av	51.8	50.5	32.0	8.0	1.02	55.2	66.5	39.9	9.5	.83	65	52	70	169
									Min	51.0	47.0	31.5	5.5	.96	52.4	65.1	39.9	8.5	.77				
									Max	52.7	53.0	32.7	10.0	1.12	57.2	68.0	39.9	10.5	.81				
7039-T6	253611	⅛	Not welded		4	4	4	4	Av	66.3	63.3	56.6	14.0	1.01	78.0	79.8	67.4	19.5	0.98				
									Min	66.1	63.2	56.3	14.0	1.04	77.9	79.6	67.2	19.0	.98				
									Max	66.5	63.6	56.8	14.0	1.05	78.1	79.9	67.7	20.0	.98				
			X5039	66	4	4	4	4	Av	43.3	46.0	30.0	5.0	.94	48.9	63.0	36.5	7.0	.78	39	33	75	27
									Min	39.8	43.4	28.5	4.5	.83	45.5	60.0	34.8	6.0	.74				
									Max	45.4	48.1	31.2	5.5	1.04	51.5	66.1	38.4	8.0	.86				
			D1495	66	4	4	3	4	Av	44.5	47.0	30.5	5.0	.94	48.8	57.7	37.4	4.8	.85	38	40	75	27
									Min	42.7	44.5	29.0	4.0	.85	47.0	54.7	35.4	4.5	.76				
									Max	46.3	50.5	32.5	6.0	1.04	49.8	61.7	39.9	5.5	.95				
			D1707	66	4	3	4	3	Av	43.2	49.2	31.7	5.5	.88	47.5	57.6	35.7	6.5	.82	40	33	75	27
									Min	41.3	44.1	29.3	4.5	0.80	46.5	45.2	29.6	4.5	.71				
									Max	46.7	51.9	33.1	6.0	1.17	49.2	63.4	39.2	8.0	1.09				
			5183	66	4	3	4	3	Av	41.4	45.2	29.0	4.8	.92	47.4	61.4	35.5	7.3	.77	23	32	75	27
									Min	38.6	44.6	28.2	4.5	.84	46.3	60.2	34.5	6.0	.74				
									Max	43.8	45.8	29.7	5.0	.98	49.9	62.9	36.2	8.0	.83				
			Fusion only	66	4	2	4	4	Av	44.5	48.0	32.8	4.5	.94	50.8	63.0	38.8	5.9	.81	24	48	75	27
									Min	44.4	47.7	32.8	4.5	.92	50.1	60.5	38.1	5.0	.77				
									Max	45.8	48.2	32.9	4.5	.96	51.4	65.0	39.6	6.5	.85				

[a] No sample obtained.

TABLE 13.—*Average Results of Notched and Unnotched Tensile Tests of Nonwelded and DCSP–TIG Welded X7038–T6, X7038–T7, and 7039–T6 at 75° and −320° F*—Concluded

[Ref. 30] [K_t=6.3]

Base material: Alloy and temper	Base material: Lot No.	Base material: Gage, in.	Filler alloy	Postweld natural aging time, days	Number of samples, 75° F: Notched	Number of samples, 75° F: Unnotched	Number of samples, −320° F: Notched	Number of samples, −320° F: Unnotched		Tested at 70°-75° F: Notched TS, ksi	Tested at 70°-75° F: TS, ksi	Tested at 70°-75° F: YS, ksi	Tested at 70°-75° F: Elongation in 2 in., percent	Tested at 70°-75° F: Ratio, NTS/UTS	Tested at −320° F: Notched TS, ksi	Tested at −320° F: TS, ksi	Tested at −320° F: YS, ksi	Tested at −320° F: Elongation in 2 in., percent	Tested at −320° F: Ratio, NTS/UTS	Typical hardness, Rockwell B: Weld, min.	Typical hardness, Rockwell B: Heat affected zone, min.	Typical hardness, Rockwell B: Parent metal, max.	Typical hardness, Rockwell B: Aging time, days
7039–T6	253581	3/8	Not welded	----	4	4	4	4	Av	69.8	63.4	56.9	15.8	1.08	80.1	80.2	67.0	19.0	1.00	----	----	----	----
									Min	69.6	63.2	56.8	15.5	1.06	79.9	80.0	65.1	19.0	.99				
									Max	70.1	63.5	57.0	16.0	1.10	80.3	80.4	67.8	19.0	1.00				
			X5039	69	4	4	4	3	Av	51.0	51.6	31.8	9.5	.99	50.6	60.8	38.1	6.8	.84	41	52	80	26
									Min	50.4	50.6	31.1	7.5	.96	50.2	60.3	38.1	6.5	.81				
									Max	51.4	52.5	32.2	11.0	1.01	50.9	61.1	38.2	7.5	.97				
			D1495	69	4	4	4	4	Av	50.5	54.3	32.8	11.0	.93	51.1	52.5	39.5	4.0	.97	43	44	80	26
									Min	50.1	52.3	32.5	9.0	.91	50.6	47.9	39.2	2.5	.87				
									Max	50.9	55.1	32.9	12.0	.97	51.4	57.9	39.8	6.0	1.07				
			D1707	69	4	4	4	2	Av	50.4	54.2	33.0	11.1	.93	51.3	61.3	39.8	8.0	.84	62	63	80	26
									Min	47.5	52.4	32.2	9.5	.85	49.1	54.9	39.8	3.0	.73				
									Max	53.0	56.0	33.6	13.0	1.01	53.7	67.7	39.9	11.0	.98				
			5183	69	4	4	4	4	Av	49.6	50.5	31.0	9.3	.97	49.6	57.6	37.7	6.0	.86	36	46	80	26
									Min	48.6	47.9	30.8	8.0	.93	47.9	50.1	37.4	3.5	.80				
									Max	51.7	52.1	31.6	10.0	1.08	52.1	62.6	38.0	7.5	1.04				
			Fusion only	69	4	4	4	3	Av	51.5	53.4	32.6	9.5	.96	51.4	60.9	38.9	7.5	.84	43	44	80	26
									Min	51.3	52.1	31.8	9.0	.93	50.7	58.2	38.5	6.5	.79				
									Max	51.7	55.4	33.3	10.5	.99	52.1	64.4	39.2	9.5	.90				

7039-T6	157841	¾	Not welded		4	4	4	4	Av	72.2	67.4	60.7	12.1	1.07	83.2	85.2	72.4	16.8	0.98				
									Min	71.8	67.0	60.3	12.0	1.06	82.8	85.1	72.2	16.0	.97				
									Max	72.5	67.7	61.0	12.5	1.08	83.8	85.5	72.6	17.0	.98				
			X5039	196	4	4	4	4	Av	48.4	51.0	30.8	13.0	.94	48.9	61.0	38.2	9.3	.80	47	48	80	84
									Min	48.1	49.8	29.8	13.0	.92	47.3	57.5	37.6	7.0	.71				
									Max	49.3	51.8	31.8	13.0	.99	50.0	66.6	38.6	14.0	.87				
			D1495	179	4	4	4	3	Av	48.5	50.8	31.8	12.2	.95	48.5	62.7	38.2	9.6	.77	50	45	80	52
									Min	47.2	50.3	31.1	12.0	.93	45.3	58.1	37.7	6.0	.68				
									Max	49.7	51.3	32.6	12.5	.99	52.3	66.6	38.7	14.0	.92				
			D1707	180	4	4	4	3	Av	48.9	49.8	31.2	10.0	.98	46.6	56.3	38.4	4.0	.71	57	45	80	53
									Min	47.6	49.0	30.8	9.0	.94	42.6	51.2	38.2	4.0	.65				
									Max	49.8	50.4	31.9	11.0	1.02	50.1	65.3	38.9	4.0	.96				
			5183	179	2	2	2	2	Av	46.1	49.6	29.0	12.0	.92	47.6	63.9	36.2	12.0	.74	38	45	80	52
									Min	46.1	48.6	28.5	12.0	.91	46.8	60.7	36.2	10.0	.70				
									Max	46.2	50.7	29.6	12.0	.95	48.5	67.2	36.3	14.0	.80				
			Fusion only	208	4	4	4	4	Av	52.0	53.7	34.4	11.2	.95	52.9	64.2	42.1	9.1	.82	55	58	80	140
									Min	50.4	52.9	33.9	10.0	.93	51.5	56.0	41.7	4.0	.73				
									Max	53.2	54.3	34.9	11.5	.97	53.7	70.2	42.5	16.0	.93				

TS = tensile strength; YS = yield strength; NTS = notched tensile strength; UTS = unnotched tensile strength.

TABLE 14.—*Average Results of Notched and Unnotched Tensile Tests in ¼-inch X7038–T6 Metal and DCSP–TIG Welds (As welded vs Postweld Thermal Treatment)*

[Ref. 30] [K_t=6.3]

Filler alloy	Test condition	Time interval, days at room temperature: Weld to thermal treatment	Time interval, days at room temperature: Weld or artificially aged to test	Number of samples, 75° F: Notched	Number of samples, 75° F: Unnotched	Number of samples, −320° F: Notched	Number of samples, −320° F: Unnotched	Tested at 70°–75° F: Notched TS, ksi		Tested at 70°–75° F: TS, ksi	Tested at 70°–75° F: YS, ksi	Tested at 70°–75° F: Elongation in 2 in., percent	Tested at 70°–75° F: Ratio, NTS/UTS	Tested at −320° F: Notched TS, ksi	Tested at −320° F: TS, ksi	Tested at −320° F: YS, ksi	Tested at −320° F: Elongation in 2 in., percent	Tested at −320° F: Ratio, NTS/UTS	Typical hardness, Rockwell B: Weld, min.	Typical hardness, Rockwell B: Heat-affected zone, min.	Typical hardness, Rockwell B: Parent metal, max.	Typical hardness, Rockwell B: Aging time, days
Not welded	Parent T-6	...	...	4	4	4	4	Av	79.8	72.5	67.2	14.0	1.10	84.4	88.9	79.6	10.0	0.95	...	...	...	...
								Min	79.6	72.3	67,0	13.5		83.9	88.4	79.3	8.0					
								Max	80.1	72 7	67.3	14.5		85.4	89.6	80.0	11.0					
X5039	As-welded	...	166	4	4	1	2	Av	51.1	51.5	35.4	6.0	0.99	55.4	67.5	44.9	5.7	0.82	52	58	84	65
								Min	49.8	48.7	34.7	5.0		55.4	64.9	43.5	4.5					
								Max	52.2	54.2	36.0	7.0		55.4	70.2	46.2	7.0					
D1495	As-welded	...	141	4	4	3	3	Av	47.6	53.2	35.4	7.0	.90	55.7	66.5	45.4	6.1	.84	52	51	84	35
								Min	45.7	51.2	34.8	6.5		52.1	64.3	44.3	6.0					
								Max	49.6	54.5	35.8	7.5		59.0	68.5	46.3	6.5					
D1707	As-welded	...	141	4	4	4	4	Av	49.0	53.0	35.1	6.8	.92	54.0	58.3	45.3	3.8	.92	52	42	87	35
								Min	46.3	52.5	34.6	6.0		51.3	48.5	44.8	2.0					
								Max	52.8	53.4	35.7	7.0		56.0	66.5	46.3	7.0					
5183	As-welded	...	46	2	2	3	2	Av	50.1	52.7	34.3	7.5	.95	54.9	68.2	42.2	8.7	.80	57	59	84	166
								Min	47.5	52.6	34.3	7.5		53.1	66.6	41.3	8.0					
								Max	53.7	52.8	34.3	7.5		57.0	69.9	43.1	9.5					
Fusion only	As-welded	...	102	4	4	4	4	Av	50.7	54.0	38.1	5.5	.94	51.0	57.8	47.2	2.8	.88	61	67	83	159
								Min	50.2	52.4	37.4	5.0		50.5	51.4	46.6	1.0					
								Max	51.1	55.2	38.5	6.0		51.9	66.0	48.2	5.0					

X5039	Artifically aged 48 hr. at 250° F	53	123	4	4	4	4	Av	61.8	56.3	49.2	2.8	1.10	71.0	72.2	59.1	3.2	0.98	64	66	85	45
								Min	59.2	54.6	47.5	2.5		67.8	67.5	57.1	2.5					
								Max	64 0	58.0	50.9	3.0		75.3	75.3	61.0	4.0					
D1495		23	124	4	4	4	4	Av	58.9	57.6	49.8	3.8	1.02	68.4	70.8	59.9	2.7	.95	65	67	35	45
								Min	57.1	57.0	48.8	3.0		61.8	68.5	56.4	2.0					
								Max	60.2	58.9	51.4	5.0		75.0	73.6	61.2	3.0					
D1707		22	126	4	4	4	4	Av	60.6	59.7	52.1	3.4	1.02	68.6	72.3	62.8	2.1	.95	68	71	35	45
								Min	59.9	58.9	51.8	3.0		65.6	71.3	62.5	2.0					
								Max	61.4	60.1	52.4	3.5		75.6	74.2	62.9	2.5					
5183		154	124	4	4	4	4	Av	58.0	56.2	48.2	3.0	1.03	67.8	72.5	58.0	3.2	.95	63	62	85	45
								Min	57.0	52.7	43.8	2.5		58.5	71.0	54.0	3.0					
								Max	58.8	59.0	51.0	4.0		75.9	74.2	61.1	4.0					
Fusion only		143	124	4	4	4	4	Av	63.7	61.8	55.1	3.3	1.03	64.5	71.9	66.1	2.1	.90	71	75	84	45
								Min	60.6	59.9	54.2	3.0		59.5	66.9	64.5	2.0					
								Max	65.5	63.1	55.6	4.0		68.0	74.6	68.2	2.5					
X5039	High temperature and artificially aged	17	126	4	4	3	4	Av	70.1	66.7	60.6	6.0	1.05	76.5	79.2	72.5	3.8	0.97	79	80	83	45
								Min	66.7	65.6	59.3	5.0		70.7	78.1	71.5	2.0					
								Max	73.5	68.7	62.9	8.0		85.6	82.2	73.1	4.0					
D1495		23	126	4	4	4	4	Av	68.2	67.2	60.8	5.2	1.01	71.1	77.5	72.2	2.6	.92	80	81	83	45
								Min	65.7	64.3	59.3	4.5		65.7	73.8	71.0	1.5					
								Max	69.7	68.6	62.5	6.0		75.5	82.1	73.1	4.5					
D1707		22	126	4	4	4	4	Av	71.3	68.6	61.8	6.2	1.04	72.8	78.6	72.8	2.0	.93	79	80	83	45
								Min	68.8	68.4	61.3	6.0		65.3	76.3	71.8	2.0					
								Max	74.2	69.0	62.2	7.0		79.2	80.2	73.5	2.0					
5183		154	129	4	4	4	4	Av	66.8	64.2	58.2	4.2	1.04	70.4	74.9	69.5	2.0	.94	77	79	83	45
								Min	64.3	62.8	57.8	4.0		62.4	73.9	68.7	2.0					
								Max	68.0	64.9	59.2	5.0		75.6	75.8	70.0	2.0					
Fusion only		143	129	4	3	4	4	Av	71.0	69.2	61.9	6.9	1.03	59.7	77.5	74.4	1.7	.77	80	81	83	45
								Min	69.9	68.3	61.1	6.5		56.7	76.4	73.0	1.5					
								Max	72.8	70.4	62.8	8.0		62.6	78.8	77.0	2.0					

TS = tensile strength; YS = yield strength; NTS = notched tensile strength; UTS = unnotched tensile strength.

Baysinger indicates that the best overall performance with weldments of these alloys was obtained with filler X5039 containing approximately 4 percent Mg and 3 percent Zn. Weldments of 7039–T6 made with filler X5039 gave high tensile strength and excellent ductility and were readily made under restraint with a minimum of weld cracking. For those interested in greater detail, tables 13 to 19 contain test data gathered in this investigation (ref. 30).

Lenamond, McDonald, and Speirs employed hydraulic bulge testing to evaluate the deformability of aluminum alloy weldments (ref. 31). Hydraulic bulge specimen tests were made on ¾-inch-thick TIG-welded 2219 alloys to demonstrate the capability of weldments to withstand extensive deformation under biaxial stress. TIG welds were made, using the square-butt design, two-pass technique, with one

TABLE 15.—*Summary of Cracking Results in Circular Patch Tests of DCSP–TIG Welds in 18-Inch-Square Plates*

[Ref. 30]

[Crater cracks disregarded]

Base alloy	Patch diameter, in.	Rating [a]				
		Fusion only	X5039	D1495	D1707	5183
½ in. X7038–T6	4	0	4	5	3	0
	8	0	2	4	3	5
	12	0	4	0	5	0
Subtotal		0	10	9	11	5
½ in. X7038–T7	4	0	3	5	4	0
	8	0	0	4	0	5
	12	0	0	0	5	0
Subtotal		0	3	9	9	5
⅜ in. 7039–T6	4	0	4	5	3	0
	8	0	0	4	0	5
	12	0	0	0	0	0
Subtotal		0	4	9	3	5
Total		0	17	27	23	15

[a] Points given as follows: 5—most cracking; 4 through 1—descending order of cracking; 0—no cracking.

TABLE 16.—*Rupture Disk Tests in DCSP–TIG Weldments of ⅛-Inch Aluminum Alloy Sheets*

[Ref. 30]

Filler alloy	Test time, days	Failure pressure, psi	Elongation in 8 in. of bulge, percent	Bulge height, in.	Location of failure	Filler alloy	Test time, days	Failure pressure, psi	Elongation in 8 in. of bulge, percent	Bulge height, in.	Location of failure
7039–T6						X7038–T7					
Not welded	------	6200	6.5	1.1		Not welded.	------	4700	6.5	1.4	
		6100	5.9	1.3				4600	6.5	1.3	
X5039	90	1825	.7	.7	Fusion line.	X5039	124	1600	2.1	.7	Fusion line.
		1600	1.3	.5			127	1350	1.3	.5	
D1495	90	2090	.7	.8		D1495	124	2650	4.9	.9	Base metal.
		1700	1.3	.7				2200	4.3	.7	
D1707	3	1600	1.3	.7	Weld.	D1707		1790	2.6	1.0	Fusion line (both sides).
								2600	2.9	.9	Base metal.
5183	90	1900	2.1	.7	Fusion line.	5183		2100	3.3	1.0	Fusion line (both sides).
		1700	.7	.7				2000	2.1	.6	
(a)	------	1525	.7	.6	FL and weld.	(a)	113	600	.7	.3	Weld.
(a)	------	1300	2.0	.5		(a)	------	500	.8	.3	

[a] Fusion pass, no filler.

TABLE 16.—*Rupture Disk Tests in DCSP–TIG Weldments of 1/8-Inch Aluminum Alloy Sheets*—Concluded

[Ref. 30]

5086–H112

Filler alloy	Test time, days	Failure pressure, psi	Elongation in 8 in. of bulge, percent	Bulge height, in.	Location of failure
Not welded	------	3500	4.4	1.3	
		3100	4.5	1.1	
X5039	------	------	------	------	
5183	4	1850	3.3	.9	(Fusion line and base metal.)
		1600	3.3	.8	Fusion line.
(a)	------	1900	2.7	.9	
(a)	------	1590	2.6	.8	

X7038–T6

Filler alloy	Test time, days	Failure pressure, psi	Elongation in 8 in. of bulge, percent	Bulge height, in.	Location or failure
Not welded	------	5900	8.4	1.5	
		5600	9.7	1.6	
X5039	122	2200	.7	.7	Fusion line.
		1775	2.0	.7	Fusion line.
D1495	122	1250	1.3	.5	Fusion line.
		1200	1.3	.5	Fusion line.
D1707	122	1400	2.1	.6	Fusion line.
		1400	2.0	.8	Fusion line.
5183	122	1100	2.0	.8	Fusion line.
		350	.7	.4	Weld.
(a)	------	600	.6	.4	Weld.
(a)	118	50	.7	.1	Weld.

[a] Fusion pass, no filler.

TABLE 17.—*Stress Corrosion Resistance of X7038–T6 and –I7 and 7039–T6 Plate Exposed 2 Months to 6 Percent NaCl Solution by Continuous Immersion*

[Ref. 30]

Alloy and temper	Original properties (3 specs.)						Stressed 50 percent of yield strength (4 specs. exposed)					Stressed 85 percent of yield strength (4 specs. exp.)				
	Tensile strength, ksi		Yield strength, ksi		Elongation in 2 in., percent		Applied stress, ksi [a]	Failure time	Properties after exposure			Applied stress, ksi [a]	Failure time	Properties after exposure		
	Min.	Max.	Min.	Max.	Min.	Max.			Tensile strength, ksi	Yield strength, ksi	Elongation in 2 in., percent			Tensile strength, ksi	Yield strength, ksi	Elongation in 2 in., percent
X7038–T6	73.8	74.2	67.3	68.1	8.0	9.0	34.0	3F/4 11 da 26 41 1 OK 60 da	73.5	68.2	8.0	57.8	4/4 24 hr.	----------	----------	----------
X7038–T7	57.8	60.2	45.5	47.1	11.5	12.0	23.0	0/4	59.3–60.7	45.5–46.3	11.0	39.1	0/4 60 da (NF)	59.0–59.5	45.1–46.4	10.5–11.0
7039–T6	66.3	66.8	59.4	59.9	10.0	11.0	30.0	0/4	66.2–66.8	59.0–59.3	9.5–10.0	51.0	1/4 30 da 3 OK 60 da	66.1–66.6	59.0–59.3	10.0–10.5

[a] All samples stressed longitudinally transverse to rolling direction.

239-345 O—67——6

TABLE 18.—*Stress Corrosion Resistance and Corrosion Resistance of DCSP–TIG Welded X7038–T6 and –T7 and 7039–T6 Plate Exposed 2 Months to 6 Percent NaCl Solution by Continuous Immersion*

[Ref. 30]

Plate filler	Aging or treatment prior to exposure	Original properties (3 specifications tested)			Unstressed (3 specifications exposed)			Stressed 30 percent of TS					Stressed 50 percent of TS				
								Applied stress ksi [a]	Failure time [b]	4 specifications exposed			Applied stress, ksi [a]	Failure time [b]	4 specifications exposed		
		TS, ksi	YS, ksi	Elongation in 2 in., percent	TS, ksi	YS, ksi	Elongation in 2 in., percent			TS, ksi	YS, ksi	Elongation in 2 in., percent			TS, ksi	YS, ksi	Elongation in 2 in., percent
7039–T6																	
D1495	4 mo RT	49.9	31.4	9.7	49.0	31.4	8.7	15.0	NF	48.2	30.6	9.5	25.0	NF	48.0	31.1	9.3
	2 mo RT, 12 hr 350° F	45.5	32.3	7.0	45.9	33.0	8.0	13.7	NF	46.4	32.8	7.1	22.8	NF	46.5	32.6	7.4
X7038–T7																	
D1495	4 mo RT	51.2	33.3	11.0	51.5	33.1	7.0	15.4	NF	51.6	33.7	7.5	25.6	NF	51.1	32.9	8.0
	2 mo RT, 12 hr 350° F	49.4	34.0	7.0	49.0	35.0	7.0	14.8	NF	49.4	33.9	6.4	24.7	NF	49.0	33.1	7.4

X7038–T6

D1495	4 mo RT	50.3	32.9	8.3	49.9	32.7	6.0	15.1	NF	49.8	34.2	7.0	25.2	NF	50.2	32.8	6.3
	2 mo RT 12 hr 350° F	49.0	34.9	6.5	48.4	33.9	6.8	14.7	NF	48.1	34.3	4.5	24.5	NF	47.9	32.8	6.3
D1707	4 mo RT	51.9	34.4	8.8	51.4	34.4	8.0	15.6	NF	51.1	34.1	7.5	26.0	NF	51.4	34.8	7.1
	2 mo RT 12 hr 350° F	51.0	37.8	7.2	48.1	34.2	6.0	15.3	NF	50.2	36.7	6.5	25.5	NF	49.2	36.0	6.3
Zn coating	4 mo RT	50.1	33.3	5.2	51.5	35.5	8.0	15.0	NF	50.0	34.2	4.0	25.1	NF	51.5	35.0	7.5
Al coating [c]		51.3	33.8	6.8	[c] 51.7	34.5	7.0	15.5	NF	52.8	35.8	9.0	25.9	NF	51.6	35.7	7.3
X5039	4 mo RT	52.4	34.7	9.5	51.8	34.4	6.0	15.4	NF	52.0	34.4	7.0	25.7	NF	52.4	34.9	6.5
	2 mo RT 12 hr 350° F	51.7	37.1	7.5	50.1	36.6	6.3	15.7	NF	50.9	36.5	5.6	26.2	NF	51.4	37.2	7.0
5183	4 mo RT	50.2	32.7	6.7	47.0	29.9	8.5	15.1	NF	51.7	32.6	7.0	25.1	NF	51.0	31.9	9.8
	2 mo RT 12 hr 350° F	45.4	30.8	8.8	45.5	30.4	9.0	13.6	NF	45.5	30.0	8.0	22.7	NF	46.1	30.9	7.5

All weldments tensile fractured in parent metal, away from weld.

Selective attack of HAZ of "as-welded" corrosion test specifications had no effect on properties or location of tensile failures.

[a] All samples stressed longitudinally transverse to weld and to rolling direction.

[b] NF = no failures.

[c] Al spray coating partially broke away from surface of 2 of specifications tested unstressed, 2 of 4 specifications stressed to 30 percent of TS, 2 of 4 specifications stressed to 50 percent of TS.

TS = tensile strength; YS = yield strength; RT = room temperature.

TABLE 19.—*Average Results of Tensile and Bend Tests of MIG-Welded X7038-T6 and -T7 and 7039-T6 Plate, As-Welded*

[Ref. 30] [Average of 4 specimens each]

Base material			Filler alloy	Postweld Natural aging time, days	TS, ksi		YS, ksi	Elongation in 2 in., percent	Joint efficiency, percent	Free bend		Typical hardness, Rockwell B			
Alloy and temper	Lot No.	Gage, in.								Radius, T	Angle, deg.[a]	Weld, min.	Heat-affected zone, min.	Parent metal, max.	Aging time, days
										Face and root					
X7038-T6	12831 (TS 73.0 ksi)	¼	X5039	57	Av.	45.3	34.0	5.0	62	4	180	58	59	83	60
					Min.	41.0	32.9	3.0							
					Max.	51.6	34.9	8.0							
			D1495	57	Av.	49.0	34.9	8.5	66	5	180	61	60	83	60
					Min.	45.4	34.4	5.0							
					Max.	54.5	35.3	11.0							
			D1707	57	Av.	49.9	35.1	9.0	67	2.5	115	65	64	83	60
					Min.	42.4	34.3	3.5							
					Max.	56.0	36.1	14.0							
			5183	26	Av.	45.1	28.2	7.0	62	4	180	37	43	83	143
					Min.	44.1	27.3	6.5							
					Max.	45.9	28.9	7.0							
X7038-T7	12841 (TS 57.7 ksi)	¼	X5039	56	Av.	52.4	34.5	10.0	91	5	180	52	51	74	79
					Min.	48.9	34.4	6.5							
					Max.	54.6	34.8	14.0							
			D1495	56	Av.	50.3	34.7	10.7	87	3.5	180	57	57	75	79
					Min.	45.4	34.3	5.0							
					Max.	54.9	35.0	18.0							
			D1707	56	Av.	52.2	35.9	8.6	89	3.5	180	67	57	75	79
					Min.	46.0	35.4	4.5							
					Max.	55.3	36.5	12.0							
			5183	26	Av.	46.8	28.4	8.1	80	4	180	40	42	75	148
					Min.	46.1	26.0	7.5							
					Max.	47.3	30.7	9.0							

7039–T6	253581 (TS 65.0 ksi)	⅜	X5039	33	Av.	50.1	29.9	11.0	77	2	95	42	47	77	22[a]
					Min.	49.4	28.7	10.0							
					Max.	50.7	30.7	12.5							
			D1495	22	Av.	52.3	30.4	14.8	80	1.75	125				
					Min.	52.0	30.0	13.0							
					Max.	52.5	30.7	17.5							
			D1707	33	Av.	54.8	32.4	15.0	84	2	110	62	52	80	22
					Min.	54.5	32.1	14.0							
					Max.	55.2	32.8	16.0							
			5183	33	Av.	44.2	26.6	9.6	68	1	100	20	51	76	22
					Min.	42.1	26.1	9.0							
					Max.	44.9	27.4	10.5							
										Side bend					
X7038–T6	5571 (TS 76.0 ksi)	¾	X5039	46	Av.	56.7	35.9	11.0	75	3⅛	60	41	57	85	77
					Min.	54.7	35.6	10.0							
					Max.	58.3	36.3	12.0							
			D1495	46	Av.	58.3	37.8	5.8	77	4	50	49	60	85	77
					Min.	56.2	37.2	4.0							
					Max.	59.4	38.1	9.5							
			D1707	46	Av.	53.7	38.8	6.7	71	5	30	67	67	85	77
					Min.	50.5	38.3								
					Max.	56.2	39.7								
			5183	45	Av.	47.3	30.7	7.0	62	5	40	30	62	85	182
					Min.	45.0	30.4	5.5							
					Max.	48.5	31.3	8.0							
X7038–T7	5581 (TS 60.6 ksi)	¾	X5039	66–70	Av.	55.8	34.9	14.5	92	2.5	180	58	53	70	72
					Min.	55.7	34.9	14.0							
					Max.	56.0	35.0	15.0							
			D1495	65	Av.	55.9	36.0	14.8	92	3	180	51	52	69	72
					Min.	55.3	35.6	13.5							
					Max.	56.3	36.2	16.0							
			D1707	65	Av.	54.6	38.4	8.5	90	6	90	71	52	70	72
					Min.	49.0	38.0	3.5							
					Max.	57.0	38.7	12.5							
			5183	97	Av.	50.3	33.1	8.7	83	3⅛	50	32	53	69	129
					Min.	49.7	32.6	8.0							
					Max.	51.1	33.7	9.5							

[a] Bending was stopped when ⅛ in. crack occoured on tension surface. TS = tensile strength; YS = yield strength.

TABLE 19.—*Average Results of Tensile and Bend Tests of MIG-Welded X7038–T6 and –T7 and 7039–T6 Plate, As-Welded*—Continued

[Average of 4 specimens each]

Base material: Alloy and temper	Base material: Lot No.	Base material: Gage, in.	Filler alloy	Postweld Natural aging time, days	TS, ksi		YS, ksi	Elongation in 2 in., percent	Joint efficiency, percent	Free bend: Radius, T	Free bend: Angle, deg.[a]	Typical hardness, Rockwell B: Weld, min.	Typical hardness, Rockwell B: Heat-affected zone, min.	Typical hardness, Rockwell B: Parent metal, max.	Typical hardness, Rockwell B: Aging time, days
7039–T6	157851	¾	X5039	65	Av.	54.1	32.1	12.5	79	2	90	42	52	80	71
					Min.	53.7	31.8	11.0							
					Max.	54.7	33.3	13.5							
			D1495	65	Av.	55.6	33.1	13.9	81	2	110	52	48	79	71
					Min.	55.3	32.7	13.5							
					Max.	55.9	33.5	14.5							
			D1707	65	Av.	49.2	34.4	7.4	72	5	50	56	57	78	71
					Min.	39.7	33.8								
					Max.	55.0	34.9								
			5183	63	Av.	46.1	27.2	9.5	68	1.5	80	23	52	78	60
					Min.	41.2	26.6	7.0							
					Max.	48.7	27.6	11.5							

[a] Bending was stopped when ⅛ in. crack occurred on tension surface.

TS=tensile strength; YS=yield strength.

bead made from each side to secure full-depth welds. The bulge tests were similar to the explosion bulge specimens used to evaluate high-strength welded steels, except the strain rates were relatively very slow. Strains up to 20 percent were measured in the weld metal and up to 10 percent in the heat-affected zone of those low-strength metals. In these tests, crack propagation followed the path of intermetallic constituents.

Although development of improved base metals and better filler metals is constantly sought, the benefits of such improved materials can be mitigated by imperfections in welded structures. In mid-1963, a serious problem with defective welds in 2219 aluminum alloy arose in connection with the RIFT program. Steen (ref. 32) reports that subsequent investigation showed that the inadequate weld quality could be attributed to imperfections in the 2219 welding wire. The weld filler wire flaws were of two types: (1) surface pits, and (2) foreign particulate matter which adhered to the wire. Most of the weld defects seemed associated with the foreign surface material.

Although 2219 aluminum alloy provides ease of welding and excellent cryogenic characteristics, experience at Marshall Space Flight Center indicated that arc stability, using 2319 aluminum-alloy filler electrodes, is not as good as desired. Consequently, the advantages of the MIG process have not been fully exploited. An investigation was made, therefore, to improve the arc stability and melting characteristics of 2319 electrodes by one of the following approaches:

(1) Heat treatment of the electrode
(2) Surface coating with a stabilizing element
(3) Modification of chemical composition.

Dudas indicates that—

> arc stability and melting characteristics were evaluated while depositing weld beads on ½- x 6- x 24-inch 2219 plate, using the electrodes of table [20] (ref. 33). Plate surface was prepared by etching in 5 percent caustic and 10 percent nitric solutions. Welds were made either in the flat or horizontal positions with completely automatic procedures, using the following welding conditions, unless modified to study the effect of a particular variable:
>
> 1. 60 cu ft/hr argon shielding gas (⅝-inch-diameter nozzle orifice).
> 2. 25 in./min travel speed.
> 3. ½-inch gas cup-to-work distance.
> 4. ⅝-inch contact tip-to-work distance.
> 5. 5° torch lead angle.
> 6. Zero slope and inductor settings.
>
> Welding current was varied within the range of 200–350 amps by adjusting the electrode feed rate. Arc voltage, controlled by turning a crank on the power unit, was measured

TABLE 20.—*Compositions and Tensile Properties of 1/16-Inch-Diameter Aluminum-Alloy Electrodes*

[Ref. 33]

Filler alloy	Lot No.	Composition, percent														Electrode tensile data [a]		
		Cu	Mg	Fe	Si	Mn	Zn	Ni	Cr	Ti	V	Zr	Cd	Be	Ca	Tensile strength	Yield strength	Elongation in 10 in., percent
2319	098081	6.24	0.01	0.20	0.11	0.24	0.11	0.01	0.00	0.11	0.08	0.13				40,770	32,800	1.2
5556	000451	.02	5.17	.19	.09	.77	.01	.00	.09	.09						50,830	25,700	16.1
2014	624544	4.40	.38	.39	.86	.78	.10	.01	.01	.04						27,400	16,200	10.0
4043	467211	.00	.00	.27	5.44	.00	.00	.00	.01	.00						27,270	21,400	1.5
4145	21482051	4.17	.02	.36	10.0	.02	.00	.00	.01	.01						36,430	30,700	1.8
A	204094	5.33	.00	.14	.11	.28	.04	.02	.00	.13	.11	.14				27,970	16,600	11.0
B	204095	3.45	.00	.14	.10	.26	.04	.01	.00	.11	.08	.13				26,200	18,000	10.0
C	204098	5.17	.00	.16	1.16	.26	.04	.02	.00	.12	.09	.14				26,900	17,500	10.9
D	204043	4.45	.00	.13	.12	.29	.01	.00	.00	.12	.09	.16				24,530	11,100	13.9
E	204096	4.47	.00	.15	1.98	.30	.03	.02	.00	.14	.09	.14				28,500	17,200	11.0
F	204097	2.43	.00	.18	3.95	.30	.03	.02	.00	.14	.10	.14				26,830	19,500	8.8
G	226039	6.30	.00	.18	.11	.28	.02	.00	.00	.13	.09	.11	0.00	0.0004		28,300	20,500	8.4
H [b]	285312	Zinc-coated 2319 (Lot 098081)																
I [b]	285313	Cadmium-coated 2310 (Lot 098081)																
J (M788)	226036	6.36	0.00	0.18	0.11	0.29	0.27	0.01	0.00	0.13	0.10	0.11	0.00	0.0000		26,740	16,300	11.0
K (M789)	226037	6.40	.00	.18	.11	.29	1.00	.01	.00	.13	.10	.11	.01	.0000		26,440	17,800	9.9
L	226038	6.32	.00	.18	.11	.30	.02	.01	.00	.14	.10	.11	.23	.0000		27,420	20,800	9.0
M	285399	6.16	.12	.19	.09	.29	.00	.00	.00	.13	.09	.16			0.00			
N	285400	6.16	.53	.18	.09	.29	.00	.00	.00	.14	.09	.15			.00			
O	285401	6.15	.00	.19	.08	.29	.00	.00	.00	.13	.10	.15			.20			
P	285402	6.24	.00	.19	.08	.29	.00	.00	.00	.10	.01	.10			.00			
Q	285403	6.46	.00	.24	.08	.29	.00	.00	.00	.09	.00	.00			.00			
1100	039881	0.13	.00	.50	0.09	.01	.00	.00	.00	.00								
Base metal: 2219		6.23	.00	.23	.10	.27	.01	.00	.00	.06	.09	.16						

[a] Experimental electrodes were annealed to facilitate chemical cleaning and spooling.

[b] Cleaned in caustic soda and nitric acid, zincate treated, flashed with copper plating, electroplated with zinc or cadmium.

between the welding torch contact tube and ground connection terminal. Because no slope or inductance was added, the machine functioned as a nearly constant potential unit.

Equipment for gas metal-arc welding consisted of:

1. Linde SVI 500 constant potential DC power supply (variable slope and inductance).
2. Aircomatic filler wire feeder, Model AHF–C, and Model AHF–B control.
3. Aircomatic pull gun Model AH–35A.
4. Airco No. 20 radiograph.
5. 36-inch welding table with grooved copper backup.

Welding current and voltage were recorded on Esterline Angus Model AW instruments. Shielding gases were Linde high-purity, dry (99.995 percent) argon and Airco Grade A helium.

Melt-off rates for magnesium electrodes are more than twice those for aluminum. When alloyed with aluminum, magnesium increases the melt-off rate of the resultant alloy in proportion to the amount of magnesium added. For example, Al-Mg alloys 5052 and 5554 contain less magnesium than 5556 and consequently have melt-off rates between 5556 and Mg-free aluminum alloys.

Despite the different melt-off rate exhibited by 5556 electrodes, the mode of metal transfer across the arc during welding was similar to other aluminum electrodes. All electrodes had similar melting characteristics at any given current, although the mode of metal transfer differed substantially at various current levels in the range of 200 to 350 amperes.

At 200 to 260 amps the molten metal was transferred across the arc as a mixture of large globular drops and finer droplet spray. This current range is approximately 75 amps above the transition current of 125–130 amps for $\frac{1}{16}$-inch-diameter aluminum electrodes. The transition current is the critical level of welding current where metal transfer suddenly changes from very large globular drops (larger than the electrode diameter) detached at a very slow rate to a mixture of small drops and fine spray transferred at a higher rate of frequency from the electrode. Welds can be deposited at a current just above the transition range, but it is not until approximately 200 amps are reached that sufficient melting rate and arc stability are achieved for normal welding. In the range of 200–260 amps the electrode assumes a blunt-nosed tip. Gravity, electromagnetic pinch effect, and other forces within the arc cause the drops to be released from the electrode and accelerated toward the workpiece at high speed. The arc is fairly stable with moderate force; the weld bead is narrow but generally uniform. This range is desirable for flat position welds with low heat input and shallow penetration.

With increasing current, the molten drops become smaller and are transferred at greater frequency. At approximately 260 amps, the droplets become so small they are no longer visually detectable and the mode of metal transfer changes to a fine spray.

Spray transfer is characterized by a pointed electrode tip, a narrow axial arc column, and strong arc force. Weld penetration is deep and the bead contour is smooth and uniform. Axial-spray arcs are preferred for most welding applications because of deeper penetration and greater arc stability than globular-spray arcs. They are especially useful for out-of-position welding because the narrow arc column can be easily directed into horizontal or vertical fillets without affecting arc behavior.

Above 325 amps the arc force is so strong that the arc becomes quite erratic. The arc length varies without change in voltage or current, and beads are not uniform. With increasing current noticeable plunging of the arc occurs. The wire tip is alternately extended below the plate surface and burned back to expose the arc. The bead becomes very irregular—being composed of a series of blackened oxide folds. This is the very unstable condition termed "puckering" by the British.

The range of 260 to 325 amps provided best arc stability and deep weld penetration for all six aluminum electrode compositions. This range, however, is applicable only for 1/16-inch-diameter aluminum electrodes. Other wire diameters experience the same general melting behavior, but the current ranges are higher for larger wire, lower for smaller wire.

Shielding gas composition has a profound effect on arc behavior during welding. For 5000 series Al-Mg alloys, an inert shielding gas containing 50–65 percent helium, with the balance argon, provides a more stable arc than pure argon or other argon-helium mixtures. Weld spatter and porosity were reduced, permitting the use of wider ranges of arc voltage, current, and travel speed.

Bead-on-plate tests comparing arc stability for 100 percent argon versus a 65 percent helium-35 percent argon shielding gas were conducted for 1/16-inch 2319 and 5556 electrodes. The benefit of argon-helium for welding Al-Mg alloys was confirmed. The 65 percent helium-35 percent argon mixture permitted arcs with 5556 electrode to stabilize at a shorter length and over a wider range of arc length and arc voltage than pure argon. Although a higher arc voltage was required to achieve the same arc length as in pure argon, weld spatter was noticeably reduced.

With 2319 filler, argon-helium mixtures also required a higher arc voltage, but arc stability was not improved. 2319 exhibited an even narrower range of stable arc length and voltage than with pure argon, requiring very precise weld machine settings to maintain a stable arc. Because of the erratic behavior of 2319 with argon-helium mixtures, further comparison weld tests with experimental electrodes were made using only 100 percent argon shielding.

One reason advanced for the inherently poor arc stability obtained for 2319 is its microstructural difference from other electrodes. Metallographic studies of 2319 electrode have revealed, in many instances, the presence of undissolved particles (mostly $CuAl_2$) throughout the microstructure. These particles, if large enough, could conceivably interfere with metal transfer characteristics during welding and reduce arc stability.

For gas metal-arc welding (electrode positive) the work plate is the cathode and the consumable electrode the anode. A large cathodic area is available to maintain the supply of electrons, but the positive charges must come from either or both of two sources: (1) ionized gas atoms from the inert-gas stream, or (2) ionized metal vapors from the melted electrode. Welding arcs that develop fine metal spray provide more metal vapor than globular spray arcs and thus exhibit better arc stability.

Table 21 lists the ionization potential, boiling point, and thermionic work function for selected chemical elements. The metals are generally more easily ionized than argon or helium gases used for shielding. If vapors from these metals are present in substantial quantities, they provide an abundant source of ions for stabilizing the welding arc.

Although aluminum and copper are easily ionized, they vaporize at a relatively high temperature. As a result few ionized metal vapors are provided during gas metal-arc welding with 1100 (Al) or 2319 (Al-Cu) electrodes. The arc

TABLE 21.—*Selected Physical Properties That Influence Welding Characteristics*

[Ref. 33]

Element	Ionization potential, eV	Boiling point, °F	Thermionic work function, eV
Aluminum	5. 96	4 440	4. 00
Copper	7. 68	4 700	4. 50
Magnesium	7. 61	2 030	3. 70
Cadmium	8. 96	2 625	4. 00
Zinc	9. 36	1 663	3. 60
Calcium	6. 09	1 440	2. 70
Silicon	8. 12	4 200	4. 50
Beryllium	9. 28	5 020	3. 90
Tungsten	8. 1	10 700	4. 52
Argon	15. 68	−302	
Helium	24. 46	−452	

> column must therefore rely on the shielding gas to supply positive ions. At arc lengths above 1/4 inch, however, even this source apparently does not provide sufficient ions and the arc becomes unstable. Helium is more difficult to ionize than argon and explains why argon-helium mixtures produce a less stable arc than pure argon during welding with 2319.
>
> Magnesium has the desirable characteristic of: (1) a low ionization potential, and (2) a low vaporization temperature. When present as an alloying element in aluminum electrodes (5556 and 2014, for example), magnesium provides an abundant source of easily ionized metal vapors that stabilize the welding arc.' This is borne out by weld bead photographs, which show the smoothest beads and largest amounts of welding dust were exhibited by Mg-containing electrodes.
>
> One notable factor affecting arc characteristics that has not been considered is thermionic work function. The lower the work function of the cathode, the more easily electrons are emitted for sustaining the welding arc. Refractory materials like tungsten make excellent electrodes because they have both an inherently low work function and a high boiling temperature. Tungsten emits sufficient electrons below its boiling temperature to easily sustain a straight polarity (electrode negative) arc.
>
> Most structural metals have a lower work function than tungsten, but because of their lower boiling temperature, fewer electrons are emitted for welding. If the cathode area is small, as in gas metal arc welding (electrode negative), insufficient electrons are produced to maintain a stable arc. This is why gas metal-arc welding of aluminum enjoys success only with reverse polarity current, electrode positive). The cathode area is large and ample electrons are available to maintain a stable welding arc. Unstable arcs appear to be caused by a shortage of positive ions to balance the supply of electrons rather than insufficient electrons. For gas metal-arc welding (electrode positive) then, the ionization potential and boiling temperature of the electrode are of more significance to arc stability than thermionic work function.

Attempts to improve the arc stability of 2319 electrode wire by solution heat treating to dissolve $CuAl_2$ particles were unsuccessful. Although the heat treatment did reduce the amount and size of the $CuAl_2$ particles observed in the microstructure, no significant improvement in arc stability was observed.

Electrodes of the 2319 type modified by lowering the copper content or by adding silicon or beryllium were also tested. None of these changes enhanced arc stability but they did adversely affect the strength and ductility of resultant welds.

Fifty-foot sections of 2319 welding wire were flash copper coated and then electroplated with various thicknesses of either cadmium or zinc. Arc stability tests conducted by Dudas in the 260–300-ampere current range showed definite improvement in arc stability using these plated wires. Metal transfer characteristics differed markedly from the standard 2319 filler wire. Below about 300 amperes, metal transfer was of the globular spray type, using the plated wires. With the other electrode wires, transition to axial spray occurred at a lower current—about 260 amperes. It was also noted that surface resistance of the plated wires seemed to vary sufficiently to cause a variation in arc length of about $\pm 1/16$ inch.

Investigation of the effect of alloying additions on arc stability resulted in two experimental 2319-type electrodes, 2319+0.25 percent Zn and 2319+1.0 percent Zn, both of which provided a wider range of stable arc length and arc voltage than standard 2319 alloy wire for MIG welding of 2219 alloy plate. They permitted a stable arc to be maintained with less precise control of weld conditions and a more favorable bead shape and size during out-of-position welding. Welds with these fillers were equal to or better than 2319 welds in tensile strength, freedom from cracking, and electrochemical potential in the weld zone. Among other elements investigated for their effort were cadmium, magnesium, calcium, zirconium, and vanadium.

> No slope or inductance were added to the constant potential source machine used in this investigation in order to permit a more valid comparison to be made among the changing electrode compositions. Normally, however, some adjustments in power characteristics are desirable to minimize the effect of current variation on arc length, to reduce weld spatter, and to improve puddle fluidity. For the more finalized zinc-containing compositions, added slope and inductance appear desirable to achieve optimum arc characteristics.

The conclusions Dudas reached from this study were (ref. 33):

1. 2319 welding electrode alloy exhibited a narrower range of arc stability than aluminum alloy electrodes 5556, 2014, 4043, and 4145 for gas metal-arc (MIG) welding 2219 alloy plate.

2. Additions of volatile, easily ionized elements such as zinc, cadmium, or magnesium to 2319 provided excellent arc stability similar to the aluminum-magnesium alloy 5556. Zinc was preferred to cadmium, magnesium, or calcium as a stabilizing addition because cadmium generated toxic fumes during welding and magnesium and cadmium significantly increased weld cracking.
3. M788 (2319+0.25 Zn) and M789 (2319+1.0 Zn) electrodes combined desirable arc stability for gas metal-arc welding 2219 plate with low sensitivity to cracking, high weld strength, and favorable weld zone electrochemical potentials.
4. Electroplated zinc and cadmium on 2319 wire markedly

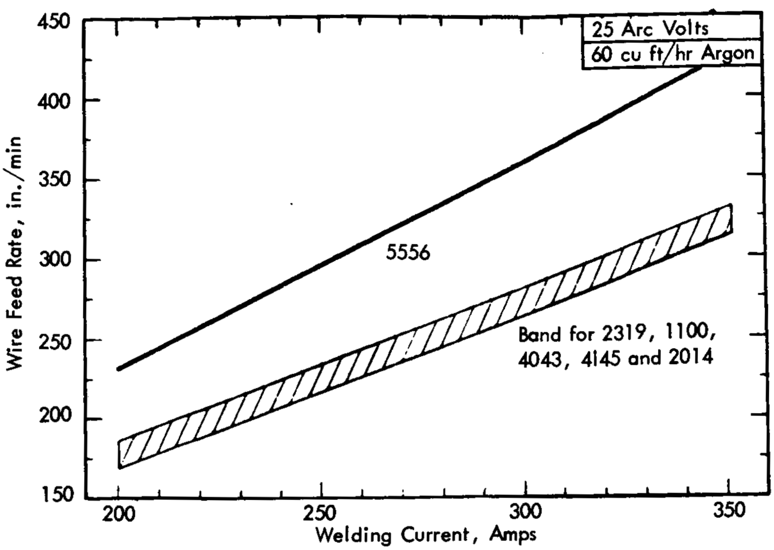

FIGURE 27.—Melt-off rates for 1/16-inch-diameter standard aluminum alloy electrodes (ref. 33).

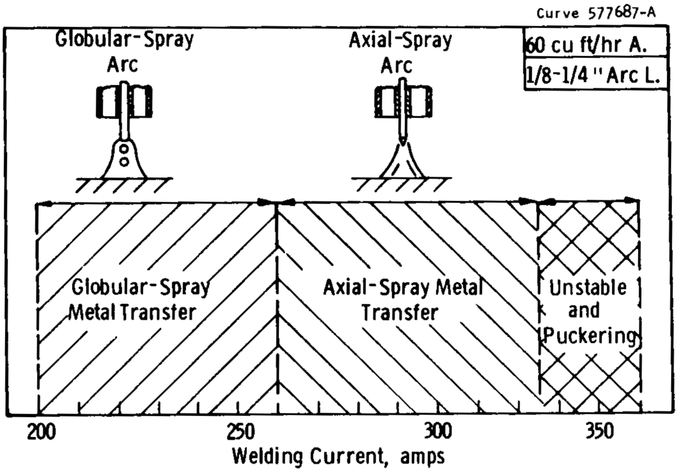

FIGURE 28.—Metal transfer characteristics for 1/16-inch-diameter 2319, 1100, 5556, 2014, 4043, and 4145 standard aluminum alloy electrodes (ref. 33).

improved arc stability but interfered with current flow from the contact tube to the electrode.

5. Additions of silicon (1.2 percent) or beryllium (0.0004 percent) to 2319-type electrodes to reduce surface tension of molten aluminum did not substantially improve arc stability. Strength and ductility of welds in 2219 plate were decreased by silicon additions to the electrode.

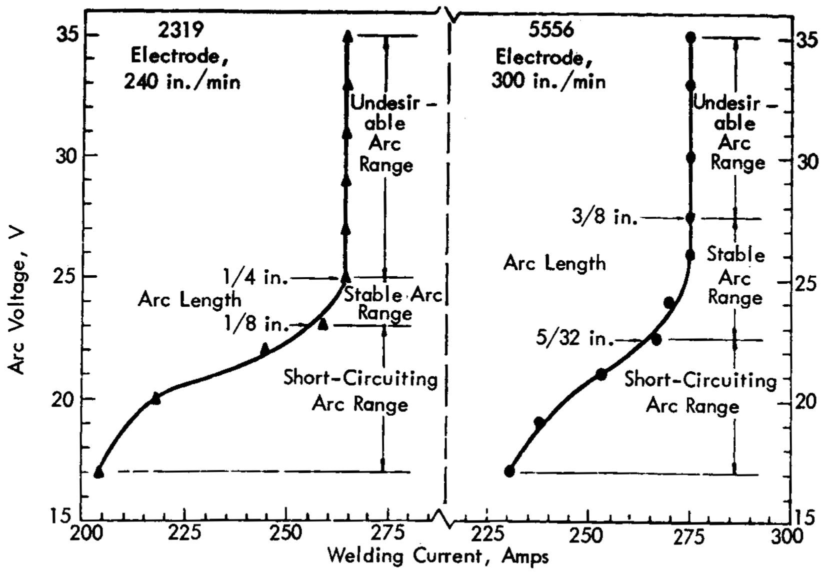

FIGURE 29.—Arc stability for 1/16-inch-diameter 2319 and 5556 electrodes (ref. 33).

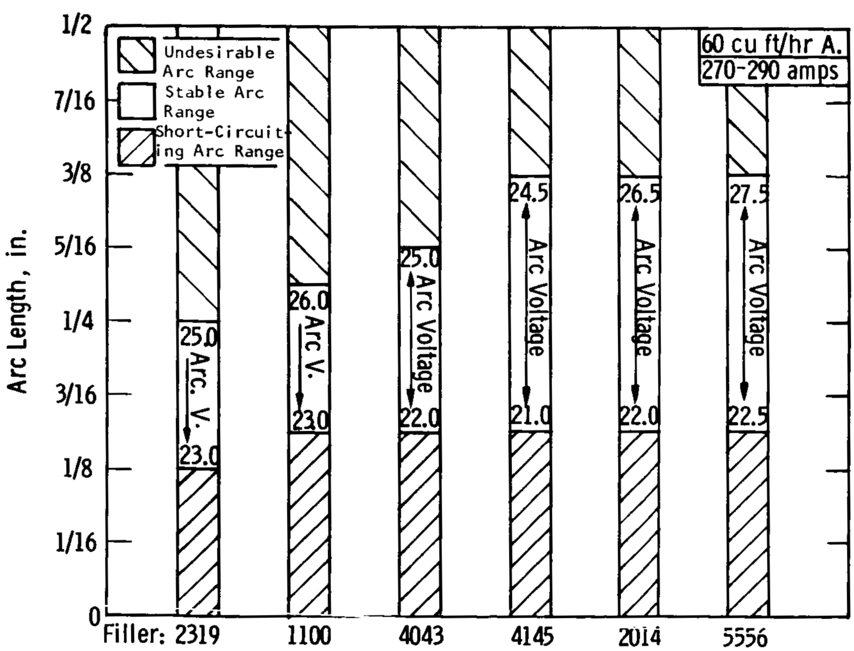

FIGURE 30.—Arc stability for 1/16-inch-diameter 2319, 1100, 4043, 4145, 2014, and 5556 aluminum alloy electrodes (ref. 33).

6. Solution heat treating 2319 electrode reduced $CuAl_2$ particles in the wire microstructures but did not significantly improve arc stability.
7. A 65 percent helium–35 percent argon shielding gas mixture increased M788 and M789 melt-off rates and reduced weld spatter with no apparent decrease in arc stability.
8. Eliminating zirconium or vanadium to reduce segregation in 2319 type electrode dangerously increased susceptibility to weld cracking.

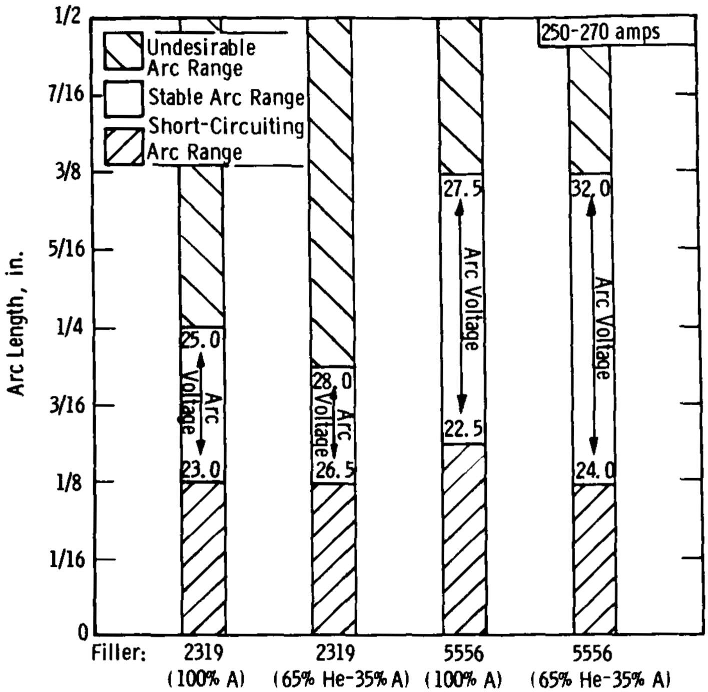

FIGURE 31.—Arc stability for 1/16-inch-diameter 2319 and 5556 electrodes with 100 percent argon and 65 percent helium-35 percent argon shielding gases (ref. 33).

Some of the details are shown graphically in figures 27 to 31.

A word of caution is mandatory at this point regarding the dangers inherent with fumes generated during welding when certain elements such as cadmium or zinc are present.

> Cadmium can become toxic if heated high enough to allow the formation of cadmium oxide fumes. Severe respiratory ailment, and even death, may result if concentrations in excess of the allowable threshold limit of 0.1 mg

CdO/m^3 are breathed for prolonged periods of time. Two samples were collected at 280 amps current with no room or local exhaust ventilation in order to represent the worst possible welding conditions encountered. These samples had cadmium oxide concentrations of 4.4 and 6.9 mg/m^3, respectively. These values were 44 to 69 times the allowable threshold limit of 0.1 mg CdO/m^3, indicating that rigid ventilation procedures need to be observed for safe welding with this electrode. Because of this hazard, and the fact that zinc additions were as effective as cadmium for arc stability, it was decided to discontinue any further testing with the cadmium-containing filler.

Zinc is not a toxic metal, but noxious metal fume fever can result if zinc or magnesium fumes are inhaled in amounts exceeding the threshold limit of 15.0 mg/m^3. Chills, fever, and nausea usually occur within 4 to 8 hours after exposure and disappear almost invariably within 24 hours. Normal exhaust procedures should provide adequate protection for electrodes with zinc or magnesium (ref. 33).

Aluminum Fastening

Because of the weight savings that could be realized, there was a natural interest in the possibilities of using titanium alloy fasteners. When considered for aluminum alloys, the possibility of galvanic corrosion must be carefully examined. Table 22 illustrates the wide difference between titanium and aluminum. A study by Nelson and Williamson (ref. 34) of the Marshall Space Flight Center indicates that fasteners of Ti-6Al-4V can be used to connect aluminum components without significant sacrifice of the integrity of the connection in a normal atmospheric environment if special installation procedures are followed to control galvanic attack. These procedures are as follows:

1. Extreme care must be taken during fastener installation to prevent damage to the protective coating of the components. Minimum protection for the aluminum components should consist of a conversion coating (MIL–O–5541) and one coat of zinc chromate primer (MIL–P–8585).
2. Fasteners must be dipped in zinc chromate primer and installed wet.
3. After installation, fasteners and adjacent area must be touched up with zinc chromate primer. This would include any bare areas, such as broken collars or pins, that occur during installation.

Titanium fasteners should not be used with aluminum components in any areas where the above procedures cannot be used, unless the environment is extremely mild and can be closely controlled.

239–345 O—67——7

TABLE 22.—*Galvanic Series for Some Metals and Alloys*

[Ref. 34]

Corroded End (Anodic or Least Noble)

Magnesium
Magnesium alloys
Zinc
Aluminum

ALUMINUM ALLOYS

Cadmium
Carbon steel
Cast iron
Stainless-steel type 410(active)
Stainless-steel type 430(active)
Ni-Resist
Stainless-steel type 304(active)
Stainless-steel type 316(active)
Hastelloy C(active)
Lead
Nickel(active)
Inconel(active)
Hastelloy B(active)
Brasses
Copper
Bronzes
Monel
Nickel(passive)
Inconel(passive)
Stainless-steel type 410(passive)
Stainless-steel type 430(passive)
Stainelss-steel type 304(passive)
Stainless-steel type 316(passive)

TITANIUM

Hastelloy B(passive)
Hastelloy C(passive)
Silver
Graphite
Gold
Platinum

Protected End (Cathodic or Most Noble)

TITANIUM

Weldability of titanium alloys was only briefly studied (refs. 25, 36), probably because melting and rolling facilities for titanium-alloy production were not available at the time the NASA program was started. A simple evaluation was made of high-strength sheet having a yield strength greater than 150 000 psi. Six materials, all 0.040 inch thick, were TIG welded with cold-wire feed and the resultant welds were tested at room temperature to determine bend ductility, tensile strength, and chemical composition. Toughness evaluations were not made. These alloys might be of interest for aerospace components, but no new or novel techniques were reported in the period covered by this survey.

High-strength, all-beta alloys were studied to determine tensile properties and fracture toughness of as-deposited TIG welds made on B–120 VCA titanium alloy mill-annealed or cold-rolled-and-aged sheet, having a thickness between 0.120 and 0.140 inch. Properties were not influenced by changes in the welding practice within the range investigated. Included in the investigation were the effects of changing the number of weld passes, using different filler wire materials, and using different fixturing materials and techniques. High-voltage electron beam welding offers no significant improvement in toughness over TIG welding. Welds with less porosity and more uniform penetration are produced by multipass welding with copper fixturing than by techniques using single-pass and steel fixturing.

> A cyclic testing technique was developed during this program (ref. 36). It effectively evaluates and predicts the performance of B–120 VCA titanium-alloy TIG weldments under simulated operating conditions.
>
> The critical partial crack lengths for as-TIG welded cyclic test specimens can be interpreted in terms of the Irwin equation for the stress intensity factor (K) around the edge of partial cracks to yield a plane strain fracture toughness value of 328 in-lbs/in ^{2}.
>
> Residual welding stresses decrease the apparent fracture toughness of B–120 VCA titanium alloy weld metal and therefore can cause premature failure of weldments containing small defects. The toughness of the weld metal, therefore, may be 4.5 times greater than previously reported (529 rather than 119 in-lbs/in ^{2}), since the values obtained previously were subject to the effect of residual stresses.
>
> The residual tensile stress distributions in as-deposited B–120 VCA titanium alloy TIG weldments can be altered to place the weld in residual compression by a hot rolling process. The process reduces the weld thickness about 10 percent and produces slight internal remelting, but does not significantly influence the mechanical properties of the weldment. The process produces welds which, in many instances, have more ductile-appearing fracture surfaces, and also improves the weld soundness by eliminating porosity. Hot-rolled welds behave satisfactorily during hydrostatic loading and full scale components fabricated using this technique all burst above the design minimum burst pressure (720 psig) with failure origins outside of the welds.

Detail test data for measured residual stresses, incidence of porosity upon tensile stress at first-crack initiation, and critical crack lengths as related to failure stresses are shown in figures 32 to 36. The gas analyses of the electron beam welds evaluated ranged from 0.013 to

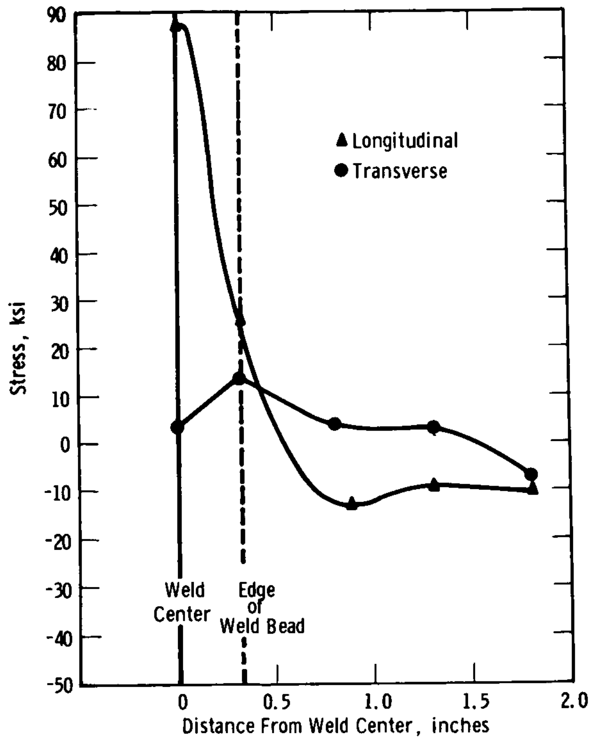

FIGURE 32.—Residual stress gradient across as-deposited B–120 VCA titanium-alloy TIG weldment (ref. 36).

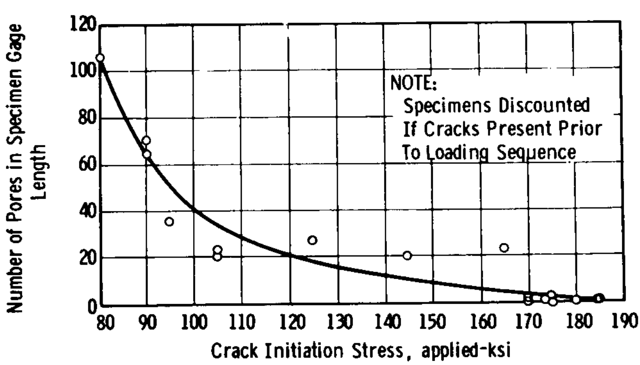

FIGURE 33.—Relationship between incidence of porosity and stress level to produce first crack initiation in TIG-welded B–120 VCA titanium cyclic-test specimens (ref. 36).

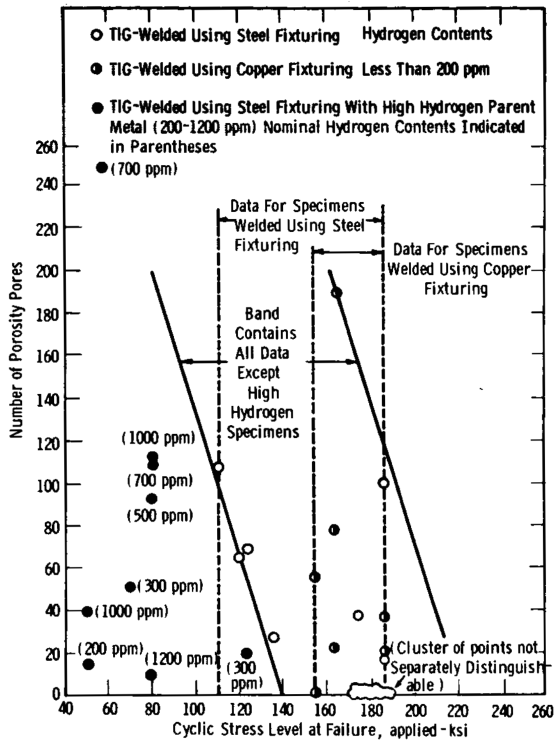

FIGURE 34.—Influence of incidence of porosity on cyclic-test failure stress in B–120 VCA titanium-alloy TIG welds (ref. 36).

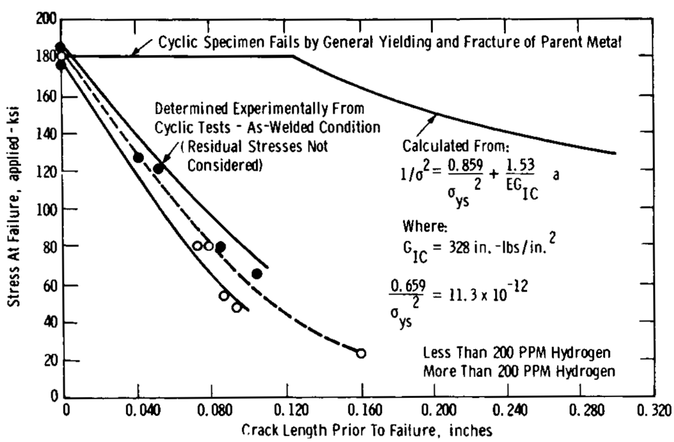

FIGURE 35.—Relation between critical crack length of partial cracks and failure stress in TIG-welder B–120 VCA titanium-alloy in cyclic specimens (ref. 36).

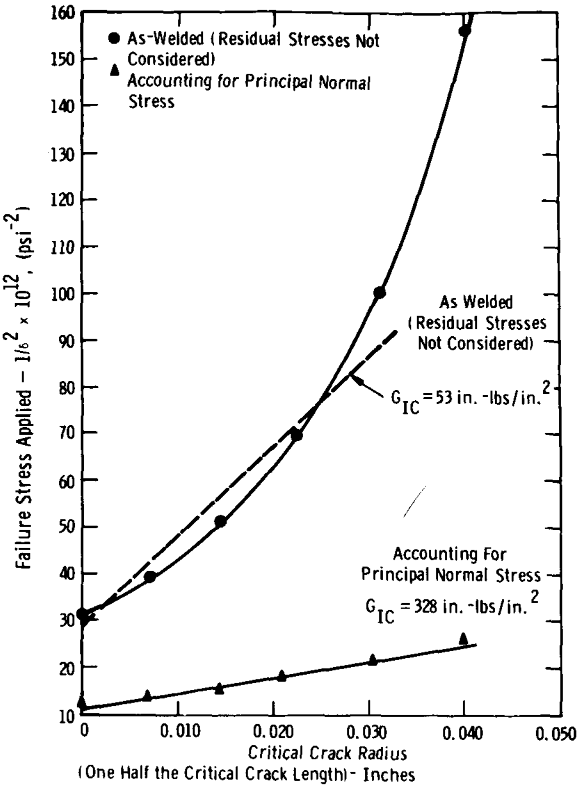

FIGURE 36.—Relation between critical crack radius for partial cracks and failure stress in B-120 VCA titanium-alloy cyclic specimens (ref. 36).

0.14 percent H_2 and from 0.102 to 0.126 percent O_2. The beta alloy studied had the nominal composition: Ti plus 13 percent V, 11 percent Cr, and 3 percent Al.

Titanium alloys are of interest to the electrical industry as heat shields, as components of supporting nuclear equipment, and to the deep submergence programs.

BERYLLIUM

Satisfactory bonds for window assemblies between 0.001-inch-thick beryllium and AISI 310 austenitic steel were achieved by ultrasonic welding with an aluminum foil insert 0.001-inch thick (ref. 37). Vacuum-tight joints were made but the need for high quality beryllium for such application is noted. Figure 37 shows acceptable and unacceptable bonds.

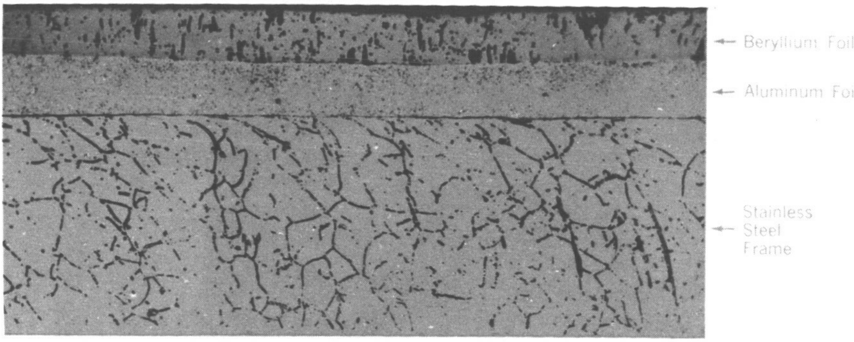

(a) Within the land, × 500

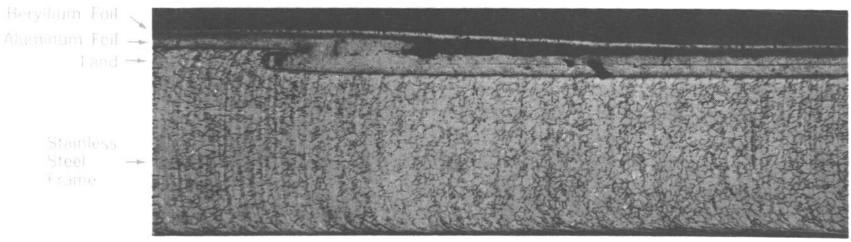

(b) Edge of land, × 100

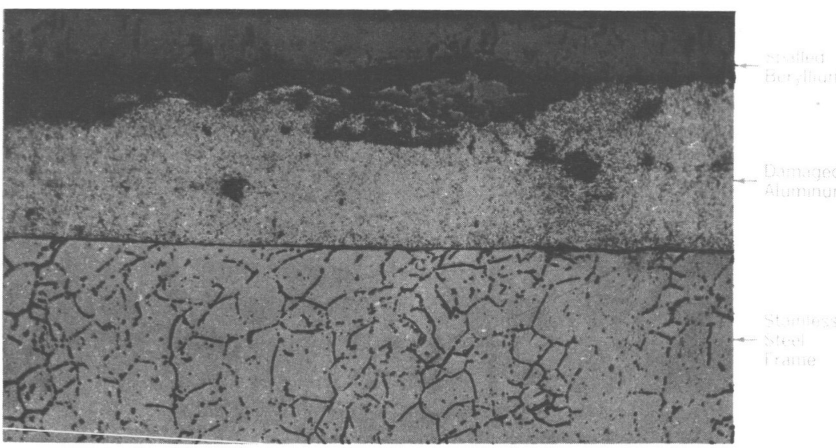

(c) Beyond weld, × 500, showing foil damage

FIGURE 37.—Photomicrographs of ultrasonic welds between beryllium and austenitic steel, using aluminum foil as intermediate layer (ref. 37). (Steel electrolytically etched in 10 percent oxalic acid and beryllium etched in 10 percent HF with 90 percent ethanol.)

PRECEDING PAGE BLANK NOT FILMED.

CHAPTER 6

Refractory Metals and Vanadium

VANADIUM

Although vanadium is not classified as a refractory metal, it is included in this section because it seems to fit best here considering the nature of the information, and because of the many similarities between vanadium and the refractory metals regarding their characteristics and application potentials. Royster, Manning, and Dysleski (ref. 38) at the Langley Research Center reported, in 1965, investigation of the physical properties and weldability of two vanadium-bearing alloys—one a vanadium base with approximately 75 percent vanadium and the other a columbium base with 39 percent vanadium. Vanadium-base alloys, because of their strength-to-weight ratio, are of interest as potential structural materials for aerospace application in the 1800 to 2400° F range. However, since vanadium forms an oxide (V_2O_5) that melts at 1250° F, this fact must be considered in relation to applications in oxidizing atmospheres at elevated temperatures.

This investigation included determination of tensile properties at room temperature and 1800 to 2400° F, evaluation of oxidation characteristics of silicide-coated and uncoated material, and studies of joining by TIG and EB welding. The two alloys studied were of the following nominal chemical composition:

(1) 74.9 percent V+20 percent Cb+4 percent Ti+1 percent Zr+0.1 percent C, hereafter referred to as V–20Cb

(2) 60 percent Cb+39 percent V+1 percent Zr, hereafter called V–60Cb

The silicide coatings used for oxidation protection were—

(1) A pure silicide;

(2) A modified silicide containing Cr, Ti, C, and Ta; and

(3) A modified silicide containing Cr, Fe, and B.

The parameters for welding both the V–20Cb and the V–60Cb alloy were determined through experimentation on small specimens. Table 23 contains the details for both TIG and EB welding. Bend-test specimens, used to evaluate the welds, were tested with the weld normal to the contact radius of the ram so that the characteristics of the weld and the heat-affected zone were explored. Results are given in table 23. Good welds could be made in both alloys without causing

TABLE 23.—*Parameters for the Butt Welding of Vanadium Alloys*

[Ref. 38]

(a) *Tungsten Inert Gas*

Machine type	ac, dc inert arc and metal arc welder
Backup gas	Argon
Flow rate	6 cu ft/hr
Torch type	Heliarc
Torch size	M 50A
Electrode	3/32 thoriated tungsten
Shielding gas	Argon
Flow rate	20 cu ft/hr
Travel speed	35 (low speed) in./min
Polarity	Direct current, straight polarity
Current	120 A

(b) *Electron beam*

Accelerating potential	120 kV
Beam current	2.8 mA
Welding speed	20, 30, and 40 in./min
Beam deflection	0
Vacuum	10^{-4} mm Hg

(c) *Bend Test Data for Welded Uncoated V–Cb Sheet*

Material	Type of weld	Weld speed, in./min	Ultimate load, lb	Bend angle at ultimate load, deg	Load at failure, lb	Bend angle at failure, deg
V–60Cb	Tungsten inert gas		660	20	[a]	[a]
V–20Cb	Tungsten insert gas		407	22	273	40
V–20Cb	Electron beam	40	420	22.5	[a]	[a]
V–20Cb	Electron beam	30	420	22.5	[a]	[a]
V–20Cb	Electron beam	20	420	22.5	[a]	[a]

[a] Specimen did not fail.

embrittlement using usual TIG or EB welding techniques. The alloys exhibited good bend ductility; however, the vanadium base alloy (V–20Cb) did show some slight cracking. Analysis of bend angle versus load indicates the V–20Cb alloy to be only about two-thirds as strong as the V–60Cb alloy.

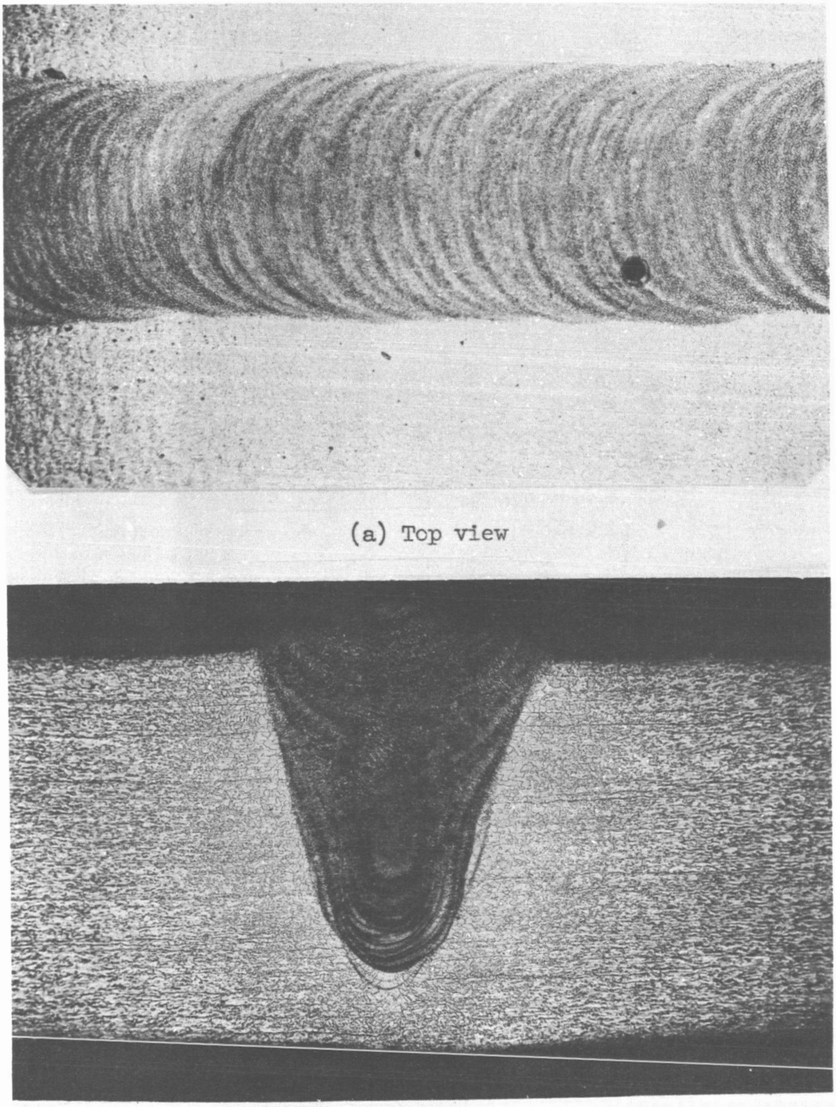

(a) Top view

(b) Edge view

FIGURE 38.—Photomicrographs showing the top and edge view of V–60b material after electron beam welding at 30 in./min.

The following were among the conclusions reached as a result of this work (ref. 38):

(1) The coated vanadium-base and the coated columbium-base alloys appear to have promise as structural materials in the 1800 to 2400° F range.

(2) Material loss to oxidation for the uncoated alloys is rapid at elevated temperatures and protective coatings against oxidation are required.

(3) There appears to be a need for a diffusion barrier between the silicide coatings and the vanadium-base alloy substrate if the alloy is to be used in thin sheets.

(4) Fabrication studies indicated that machining and forming operations can be performed with relative ease on the V–20Cb alloy, but machining difficulties are encountered with the V–60Cb alloy. Both alloys can be tungsten inert gas and electron beam welded without much difficulty (fig. 38).

COLUMBIUM

A study involving in-vacuum electron beam welds and in-chamber tungsten arc welds on the following alloys is reported by Lessman and Stoner (refs. 39–43).

Alloys Studied in Welding Experiments

Designation	*Compositions*	*Designation*	*Compositions*
AS–55	Cb+5W+1Zr+0.2Y+0.06C	Cb–752	Cb+10W+2.5Zr
		D–43	Cb+10W+1Zr+0.1C
B–66	Cb+5Mo+5V+1Zr	FS–85	Cb+27Ta+10W+1Zr
C–129Y	Cb+10W+10Hf+Y	SCB–291	Cb+10W+10Ta

Detailed compositions are given in table 24. At the time of this writing, this investigation was not complete, but some partial results were reported. Evaluations were made using bend-test transition temperatures for the base metal, TIG welds, and EB welds. Results are presented in figure 39. Bend test values for 3/8-inch-thick plate are being made—best values available at room temperature over the range of 3t to 16t bend radius are:

Results from Bend Tests in Welding Experiments

Alloy designation	Bend-test values, deg	
	Longitudinal	Transverse
B–66	4	4
C–129Y	132	27
Cb–752	29	45
D–43	39	47
FS–85	125	145
SCb–291	160	132

TABLE 24.—*Chemistry of As-Received Refractory Materials*
[Ref. 43]

Alloy	Form	Heat	Certified analysis (average)												Check chemistry, ppm		
			Weight percent									ppm					
			Zr	Hf	Mo	V	Y	Re	W	Ta	Cb	C	O	N	C	O_2	N_2
AS-55	Sheet	430-7	1.07				0.02-0.3		4.74		Bal.	306	190-600	155	440	750	200
B-66	Plate	DX-609	1.00		5.17	4.89					Bal.	95	110	63	37	120	70
	Sheet	DX-609	1.00		5.17	4.89					Bal.	95	110	63	44	150	30
	Wire	DX-569	1.10		5.23	5.61					Bal.	17	70	64	130	140	90
		DX-603	.92		4.55	4.85					Bal.	40	82	75	130	190	60
C-129Y	Plate	6.6-57033		10.25					10.8		Bal.	65	160	15	58	200	30
		610-57204		10.10					10.85		Bal.	80	50	58			
	Sheet	46-70617		9.5			0.105		9.8	0.135	Bal.	85	105	50	36	102	60
	Wire	6.6-57033		10.25					10.8		Bal.	65	160	15	52	120	50
Cb-752	Plate	52165	2.70						9.8		Bal.	50	76	10	16	84	70
	Sheet	52208	2.90						9.9		Bal.	40	143	102	21	180	80
	Wire	52183	2.90						9.6		Bal.	30	60	120	51	120	90
D-43	Plate	43-398-13	.97						10.3		Bal.	835	63	32	930	64	20
	Sheet	43-398-13	1.00						9.9		Bal.	1,046	200	32	1,100	180	10
	Wire	43-372-1	.88						9.7		Bal.	810	52	33		85	60
FS-85	Plate	85D-740	.94						10.6	28.1	Bal.	20	90	60			
	Sheet	85D-739	.95						10.43	27.61	Bal.	40	40	52	12	98	50
	Wire	85D-695	.97						10.2	28.0	Bal.	20	40	30	34	73	40
SCb-291	Plate	2255							10.0	9.83	Bal.	20	110	40	22	101	20
	Sheet	1991							9.9	9.6	Bal.	12	65	76	17	110	50
	Wire	1825							10.1	9.2	Bal.	10	67	70	12	130	50
Ta-10W	Plate	60B-758							9.90	Bal.		50	40	20	5	10	10
	Sheet	60B-758							9.90	Bal.		50	40	20	12	66	100
	Wire	60B-609															
T-111	Plate	2691		1.7					7.05	Bal.		18.5	10	26	27	34	10
	Sheet	6-65042-Ta		2.0					8.8	Bal.		80	50	35			
	Wire	DX-571		2.01					8.12	Bal.		10	20	10	17	23	20
T-222	Plate	5.510-65041		2.55					9.2	Bal.		115	50	20	100	29	10
	Sheet	5.510-65041		2.55					9.2	Bal.		115	50	20	100	29	10
	Wire																
W-Re	Sheet	3.5-75002						25.6	Bal.			40	50	35	8	8	10
W	Sheet	KC-1350							Bal.						6	10	10
		KC-1353							Bal.						9	15	1

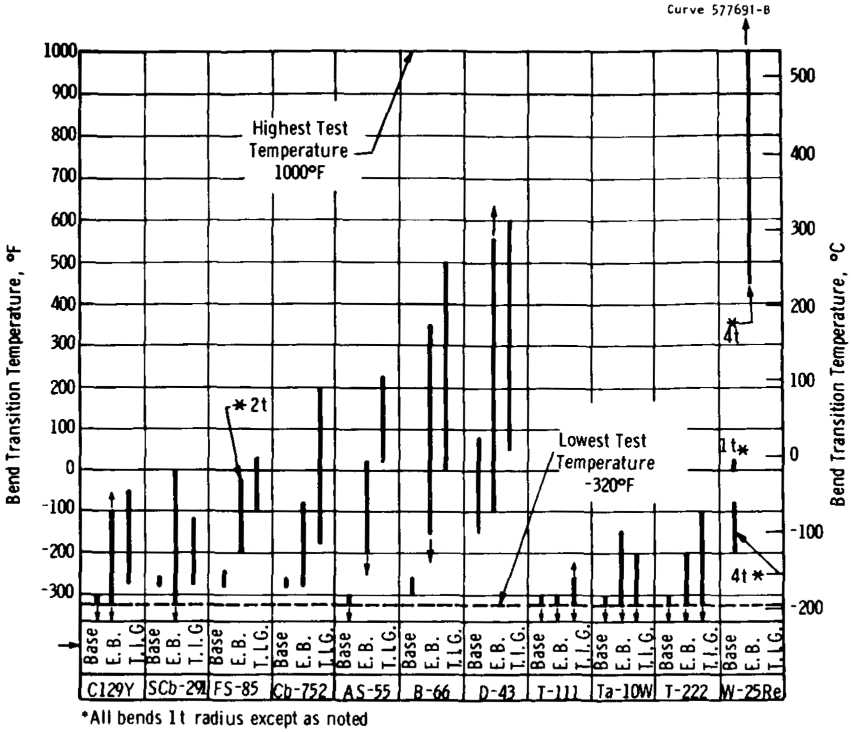

FIGURE 39.—Transition temperature ranges for unwelded sheet, electron beam, and TIG welds in refractory metals (ref. 43).

The range of temperatures encompassing the transition temperatures are often rather broad, as indicated in figure 39. In general, welding with either the electron-beam or tungsten-arc processes was damaging; that is, the transition temperature of the welded joints was higher than the unwelded base metal.

TANTALUM

Three tantalum-base alloys (table 24) were investigated along with the columbium alloys just discussed (refs. 39–43). These alloys were:

Designation	*Composition*
T–111	Ta+8W+2Hf
T–222	Ta+9.6W+2.4Hf+0.01C
Ta–10W	Ta+10W

The transition temperatures for the 0.035-inch sheet were significantly lower for the tantalum alloys than those obtained for the columbium alloys (fig. 39). While welding caused some damage, the transition temperature was raised slightly above that of the base metal; the highest limit observed was −100° F. This relatively excellent performance of the welded tantalum alloys is compatible with the

good performance of unalloyed tantalum, anomalous superiority that is not explainable on the basis of crystal lattice structure.

The one reported value for bend tests in 3/8-inch welded Ta+10W plate at room temperature was for 141° deformation both longitudinally and transversely without cracking.

All welds were porosity free, except that the tungsten arc welds in T–222 commonly contained porosity for speeds less than 30 inches per minute.

TUNGSTEN

As part of the same investigation (Lessman and Stoner) covering columbium and tantalum alloys, evaluation of tungsten and tungsten-25 percent rhenium alloy was begun (table 24) (ref. 43). Some difficulties were experienced during electron beam welding of sheet material of the tungsten-25 percent rhenium alloy with excessive cambering and opening of the joint. Welds were brittle at temperatures below +450° F and often at temperatures as high as 1000° F (fig. 39). Residual stresses were sufficiently high to cause self-rupture of the welds in some instances, but this phenomenon could be eliminated by early stress-relief annealing.

PRECEDING PAGE BLANK NOT FILMED.

CHAPTER 7

Dissimilar Metals Joining and Sealing

Joining dissimilar metals by various processes is a technology applicable to—and often necessary in—the manufacture of new products (ref. 44). For many applications, a combination of metals is needed. Consequently, the problem of dissimilar metals joining arises frequently. Combining steel for strength with aluminum for thermal conductivity or of stainless steel for corrosion resistance with copper for electrical conductivity are examples which come quickly to mind.

Not only must the application design requirements be considered but the dissimilar-metals couple must be examined in the light of the process to be used and the characteristics of the junction after the joint is made. Characteristics of the base metals must be examined with regard to such properties as thermal expansion and thermal conductivity. Dissimilar characteristics can complicate the joining problem or in some cases make application of a particular joining method impossible.

The characteristics of any dissimilar-metals union are a function of the alloy system formed and the effect of the joining process on the extent of the interchange of atoms between the two metals. Often dissimilar metal bonds are brittle, but the degree can be influenced by the joining technique. In processes using filler metals, the role of such metals in the resultant joint must be evaluated.

When brittle compounds are formed, the quantity and extent of their effect on the union are strongly influenced by the amount of metallic intermixing that occurs. Welding in general produces more likelihood of extensive brittle compound formation than brazing, and diffusion bonding usually produces the least. In general, however, regardless of the process, if the two dissimilar metals form brittle intermetallic compounds in their alloy system, then the higher the temperature and the longer the time of exposure to temperature during joining, the greater will tend to be the brittleness of the resultant joint.

Table 25 lists procedures found suitable for joining certain dissimilar metal combinations.

239-345 O—67——8

TABLE 25.—*Some Dissimilar Metal Couples and Bonding Processes*

[Ref. 44]

Union	*Procedure*
Aluminum to stainless steel	Dip braze after tin coating the stainless steel
Aluminum to stainless steel	Soldering after nickel plating the aluminum
Aluminum to stainless steel	Diffusion bonding after interface coating application
Aluminum to stainless steel	Dip braze after Ag plating stainless steel
Aluminum to beryllium	Direct dip braze
Stainless steel to beryllium	Vacuum braze
Stainless steel to molybdenum	Vacuum braze
Stainless steel to low-alloy steel	Percussion-stud welding
Titanium to aluminum	Tungsten-arc inert-gas shielded brazing with aluminum brazing alloy
Titanium to aluminum	Soldering after plating Ni on Ti and Al
Titanium to stainless steel	Resistance-welding-machine braze
Tungsten to titanium	Tungsten-arc inert-gas brazing with aluminum brazing alloy
Tungsten to copper	Tungsten-arc inert-gas brazing with aluminum brazing alloy
Tungsten to stainless steel	Tungsten-arc inert-gas brazing with aluminum brazing alloy
Tungsten to aluminum	Tungsten-arc inert-gas brazing with aluminum brazing alloy
Tungsten to molybdenum	Electron-beam welding
Molybdenum to columbium	Electron-beam welding
Molybdenum to stainless steel	Electron-beam welding
Nickel wire to copper wire	Capacitor discharge resistance microwelder
Copper to nickel	Diffusion bonding after tin soldering
Columbium to stainless steel	Inert-gas braze

Electron beam welding is a useful method of joining dissimilar metals. Advantages of electron beam welding are—

(1) Welding is done in vacuum with minimum external contamination of weld;

(2) Welds are deep penetrating, resulting in narrow welds and narrow heat-affected zones (HAZ);

(3) Precise control of welding variables is possible; and

(4) The process can be used with thin or thick materials.

One comparison of the difference in the weld-zone characteristics between electron-beam-welded and TIG-welded 0.095-inch-thick titanium is given in the following (ref. 44):

Weld process	Width of weld, in.	Width of HAZ, in.	Grain size of weld, in.
TIG	0.375–0.438	0.140–0.180	0.035
EB	0.060	0.002	0.010–0.025

Of interest in this comparison—and similar results are obtainable on other materials—is the smaller weld zone, narrower heat-affected zone, and smaller weld metal grain size in the case of electron beam welding.

Ultrasonic welding can also be useful in joining dissimilar and similar metal couples, but this technique is generally limited to thin materials, at least in one of the members. Essentially, ultrasonic welding is the combination of intimate contact and friction, the friction being generated by the vibratory energy. Adhesion or welding is accomplished without the addition of welding current. Workpieces or metals to be joined are clamped together under moderately low static force and then ultrasonic energy is transmitted into them for a brief time. A metallurgical bond is accomplished without arc or sputter and with a minimum of alloying being developed. Consequently the tendency toward brittleness is minimized. Some dissimilar (and similar) metal combination satisfactorily welded ultrasonically are shown in table 26.

At the Lewis Research Center, a boltless joining and sealing method was conceived for use in cryogenic research (ref. 45). The basic concept is shown in figure 40. It features an annular reentrant cavity which is filled to an appropriate level with a low melting bismuth, lead, tin, antimony alloy, selected because it expands on cooling. Thus, it can perform both holding and sealing functions. Because of the nature of the joint design, similar or dissimilar metals combinations can be accommodated.

At Lewis, the attachment was used to fasten and seal pressure vessels at the seam between a cylinder and head. The initial design was intended for high-pressure service over a range of temperatures from 70 to −452° F. The seal has proven quite reliable in cryogenic applications at pressures up to 2000 psi.

Significant features of this type of joint construction are—

(1) Ease of assembly and disassembly by simply heating the joint above the melting point of the alloy which does not form a wetted bond.

(2) Reusability of the individual components.

TABLE 26.—*Some Dissimilar Metals Combinations Welded by Ultrasonics*

[Ref. 44]

Combination	Aluminum	Copper	Germanium	Gold	Kovar	Molybdenum	Nickel	Platinum	Silicon	Steel	Zirconium
Zirconium	X	X				X				X	X
Steel	X	X				X	X	X		X	
Silicon	X			X							
Platinum	X	X		X	X		X	X			
Nickel	X	X		X	X	X	X				
Molybdenum	X					X					
Kovar	X	X		X	X						
Gold	X	X	X	X							
Germanium	X										
Copper	X	X									
Aluminum	X										

The presence of blanks does not necessarily mean that such a combination is impossible or impractical. In most cases the combination has not been attempted or studied.

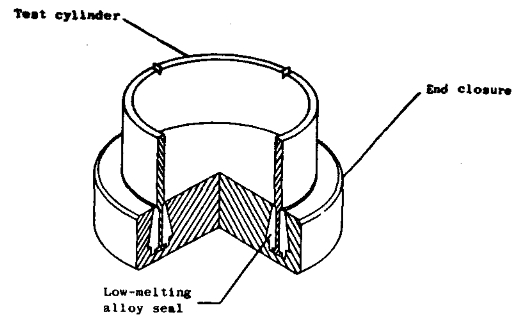

Figure 40.—Original NASA design of boltless joining and sealing method (ref. 45).

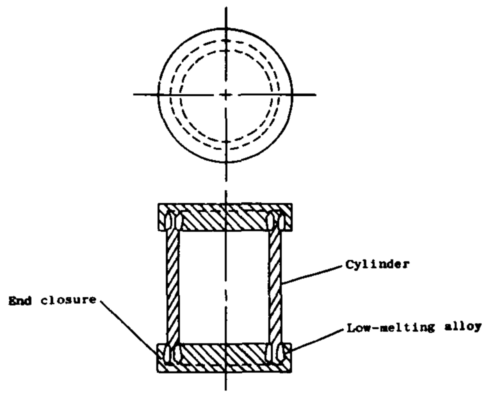

Figure 41.—Boltless attachment in vessel application (ref. 45).

(3) Effectiveness of the presure seal.
(4) Minimum induced stress in the cylinder component.
(5) The ability to connect dissimilar metals.

The boltless attachment and pressure seal concept has proved to be of such great value in research at Lewis that it appears that the concept and variations based on it could have major value to the industrial community as well (ref. 45).

A somewhat similar general method of joining meals has been used industrially for such applications as mounting of rule-die blades in the boxboard industry, and holding complex punch-and-die assemblies in the metals stamping and forming industry.

An obvious application of the new concept is in the manufacture and testing of tanks. Less obvious, however, is expansion of the concept to achieve a broad family of positioning, joining, and sealing applications based on this "formed cavity and third material" concept.

The initial concept with the low-melting-point metal in the joint boundary area limits application to room temperature and below. If the principle is expanded to include filler alloys with higher melting points, or the use of epoxy resins or liquid elastomers like polyurethane, the application possibilities are extended considerably. The following are examples of how the idea might be developed.

Pressure vessels for handling gases and liquids at cryogenic temperatures are a continuing problem. In the adaptation in figure 41, the boltless attachment in used in fabricating a vessel which might have improved reliability and increased ease of assembly.

Figure 42 is a schematic drawing of a concentric or jacketed pipe system that allows joining of pipes in locations where access for brazing, soldering, or welding might be difficult. Access to the inner pipe for direct heating would not be necessary, and if, for example, epoxy cements were used, there would be no need to apply heat. The ability to break and remake the joints easily would be impaired when epoxy cements are used.

Another application possibility is the joining of similar or dissimilar metal couples in seams for structural or containment applications. There is a need for convenient methods of forming seams which are both structurally sound and liquid or vapor tight. Figure 43 shows two possible applications of this joining technique. The joint in figure 43(*a*) is designed for completion of the seam between sheets of relatively thin structural material. The matrix material, which could be a thermosetting plastic, would be injected after location of the parts relative to each other and would form both a permanent fastening and a vapor seal. The joint in figure 43(*b*) has a configuration more closely related to that shown in the original concept. It could be used for fastening relatively heavy members and could be considered for use in load-bearing structures.

In general, when materials are to be evaluated in irradiation experiments, the materials are encapsulated to control the environment and to eliminate hazards associated with uncontrolled particulate and gaseous material. Both encapsulation and the opening of capsules after irradiation are expensive and time-consuming tasks. Figure 44 shows how the fastening and sealing concept could be adapted for use in a capsule. The capsule could take the form of a cup with a female groove in the lip. The groove could be filled to an appropriate level with matrix material which could be heated by induction or other appropriate means while the lid was placed in position. Subsequent to irradiation and by remote handling at the hot cell, the capsule could be brought to an elevated temperature which would permit simple lifting and removal of the lid. This concept would be appropriate for use in cold-wall capsules.

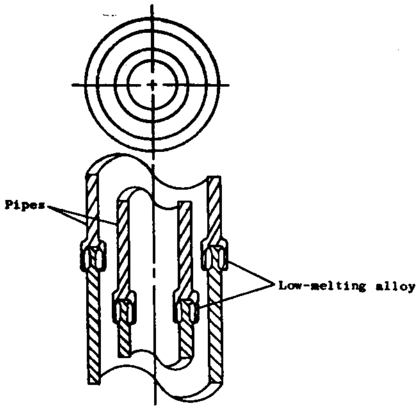

FIGURE 42.—Boltless joining used in concentric pipe assembly (ref. 45).

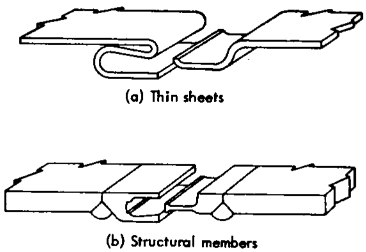

FIGURE 43.—Boltless application in seams (ref. 45).

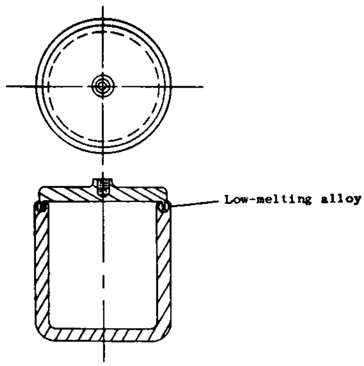

FIGURE 44.—Boltless method applied to encapsulation (ref. 45).

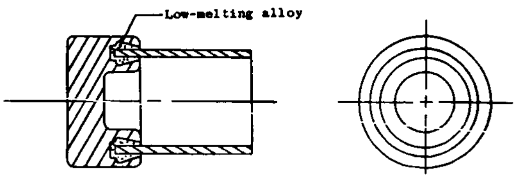

FIGURE 45.—Chucking method for precision work using boltless application (ref. 45).

Use of the basic concept at Lewis was directed toward holding a thin-walled cylinder with minimal induced extraneous stresses. This use suggests an area of further application in the metalworking industries. In many cases, it is important that a part be turned or ground to small wall thicknesses with no error induced by clamping forces, vibration, or thermal effects. Figure 45 shows the concept utilized as a holding fixture for precision cylindrical grinding. Two such devices could be used for grinding between centers.

Figure 46 shows a fastener designed to permit leveling or alinement of joints. The shaping in uniform convolutions permits the insertion of the pin, leg, dowel, or other member to any desired depth during the last operation of assembly. One merit is that the system can be freed and adjustments in the amount of projection can be made conveniently. A different design would be required if such a joint were subject to tension or torsion.

In many applications of the basic design, the introduction of an intermediate matrix material is quite difficult, if not impossible. Figure 47 shows a pipe joint before and after it is "made." In this design, the thermoplastic pipe is heated by the metallic receiver, and longitudinal force is applied until both cavities flow full of pipe material. Under some circumstances this technique might be successfully adapted to joining metallic pipe or tubing; for example, heating the pipe or tubing by induction and then driving the hot end into the coupling to cause deformation of the pipe or tubing and developing a joint.

Research on adhesion between metallic solids was sponsored by NASA to identify underlying mechanisms and interaction processes involved when two atomically clean metallic surfaces are brought together (refs. 46–49). NASA's interest, of course, is related to problems of seizure or unwanted bonding of materials in the space environment. Adhesion between metal surfaces is related to friction, cold welding, sintering, grain boundary strength, and fatigue. Consequently, research into adhesion should benefit the metals-joining field.

Studies of the adhesion, or lack of it, between similar- or dissimilar-metal surfaces under atmospheric conditions, vacuum, and high vacuum should produce information relating to the bonding of metals by pressure or diffusion techniques. Studies have shown that some couples tend to adhere, while others show no tendency to interact:

Adhesion Tendencies

Adhesion	*No adhesion*
Iron-aluminum	Copper-molybdenum
Silver-copper	Silver-molybdenum
Copper-nickel	Silver-iron
Nickel-molybdenum	Silver-nickel

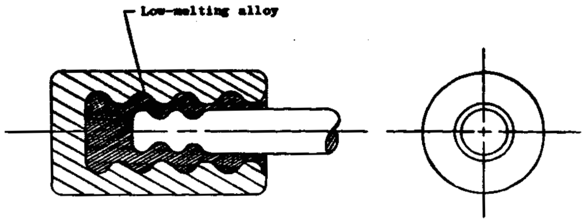

FIGURE 46.—Alinement mechanism using boltless method (ref. 45).

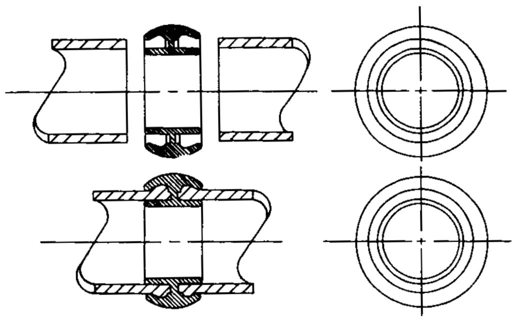

FIGURE 47.—Pipe connection using boltless method (ref. 45).

Material combinations which do not adhere under conditions of very clean surfaces and ultravacuum (to 10^{-10} torr) can be expected to be more difficult to join by diffusion or pressure than those which do adhere.

It is possible that techniques will come from such studies for joining similar or dissimilar metals involving minimum pressure and heat to avoid brittle intermetallic layers produced by diffusion or eliminate entirely the damaging effect of heat on the base metals.

PRECEDING PAGE BLANK NOT FILMED.

CHAPTER 8

Electronic Component Interconnections

Packaging of electronic components into high-density modules and assemblies led to exploitation of resistance welding of component connections and interconnections in NASA applications (refs. 50, 51). Fundamentals, determination of optimum parameters, equipment, interconnection and component lead materials, weld inspection, and process control were treated in detail (ref. 50).

Since pressure, time, and energy are the controllable variables for producing a weld, proper application of these variables is of paramount importance. An isostrength diagram should be prepared to determine which settings of the three variables will result in the strongest, most consistent weld. The isostrength diagram is a graphical representation expressing the strength of the weld as a function of energy and pressure. When completed, the diagram shows which parameters are most suitable for producing optimum welds with specific materials.

On the isostrength diagram (fig. 48), pressure is plotted on the ordinate and energy on the abscissa. At each set of coordinates within the plot, the strength of the weld produced at these coordinates is recorded. The plot may be completed by selecting increments of energy and pressure and then producing welds at each coordinate point. This is a lengthy procedure, however, and a statistical approach has been developed which produces the same results in a much shorter period.

The statistical approach involves selecting an arbitrary starting point. Several welds are made at this initial setting and pull tested. The average breaking strength of this group of welds is then recorded at the appropriate coordinate point on the isostrength diagram. Four additional points are selected at definite increments of pressure and energy in such a manner that the four points fall around the initial point. A number of welds are made at each of these points, pull tested, and the average break strength recorded at the respective coordinate points. The point which displays the highest break strength is the direction in which future tests proceed. An arbitrary point selected in the direction indicated by the preceding test and the aforementioned procedure are used to determine the direction in which to continue testing. The strongest constant strength before spitting occurs is outlined. Center coordinates of this region become the machine settings for production welds.

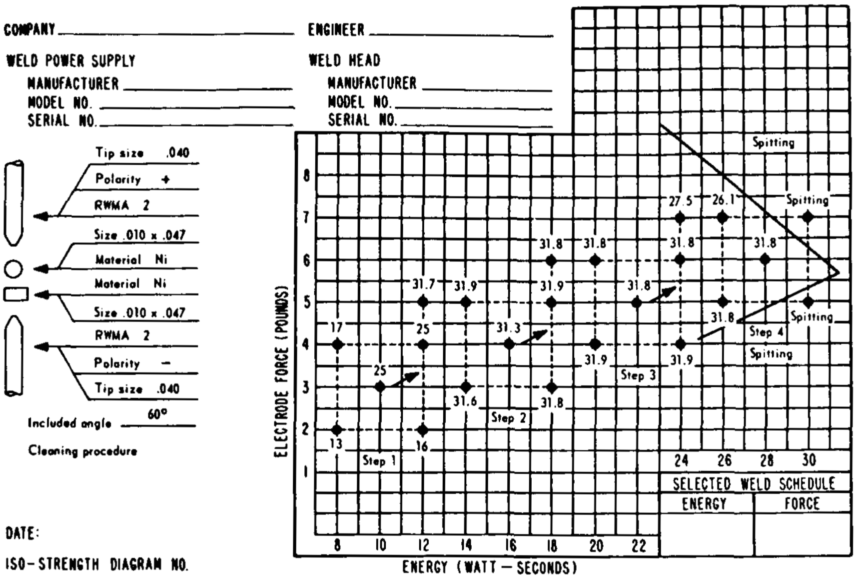

(a) Preparing the isostrength diagram

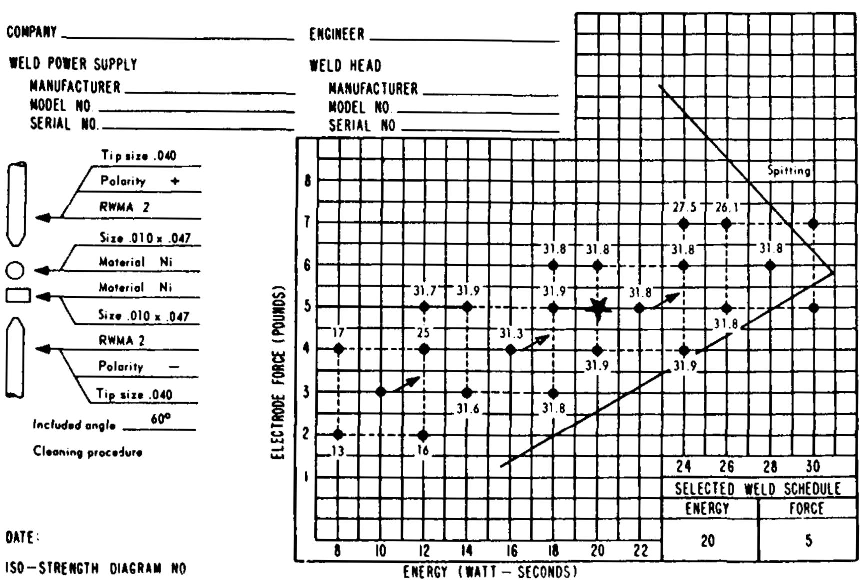

(b) The finished isostrength diagram

FIGURE 48.—Procedures for reporting isostrength diagrams (ref. 50).

For example, the following procedure might be used to determine the best machine settings for welding two 0.010-inch by 0.047-inch nickel ribbons together:

(1) **Record the materials, electrode types, date, and such in the appropriate places on the isostrength diagram (fig. 48(*a*)).**
(2) Select any arbitrary point as a starting position. In this case, the initial point is 3 pounds' pressure and 10 watt-seconds of energy. Five welds are made at this point, pull tested, and the average strength calculated. The average strength (25 pounds) is then recorded. (See step 1, fig. 48(*a*).)
(3) Select four points around the initial point to determine in which direction to proceed. Increments of 1 pound are selected for pressure, and increments of 2 watt-seconds are chosen for energy. The points to investigate then become (8,4), (12,4), (8,2), and (12,2). At each of these points, five welds are produced, pull tested, and the break strength averaged. One additional point is investigated at (12,5). This completes step 1, and all that remains is to determine which point to use as a starting value for step 2. (See fig. 48(*a*).)
(4) From the values obtained in step 1, it is evident that increased values of pressure and energy are necessary to produce the strongest weld. The starting value of step 2, then, is selected as (16,4). Peripheral points are selected as in step 1 and the entire procedure repeated.

In this example, four steps are necessary before the isostrength diagram is complete (fig. 48(*b*)). All that remains to be done is to select the area that produces consistently strong welds. The center coordinates of this area become the settings used for production work.

The area selected should now be verified for repeatability. This is accomplished by taking a larger number of samples and performing a metallurgical examination of some and pull tests on the rest.

Selection of increments for varying the pressure and energy settings for isostrength tests may be made in any convenient units. Those selected for the preceding example were 1 pound of pressure and 2 watt-seconds of energy, but more critical materials may dictate that smaller increments be used, such as 0.5 pound of pressure and 1 watt-second of energy.

When welding dissimilar materials, or materials of unequal thickness, the heat unbalance caused by the different conductivities of the weld materials can be offset by the proper choice of electrode materials. Generally, electrodes having high electrical resistance, such as molybdenum or tungsten, are required for welding materials of high conduc-

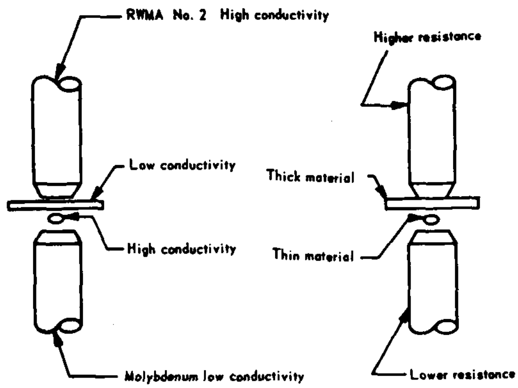

FIGURE 49.—Creating heat balance (ref. 50).

tivity. Conversely, electrodes having low resistance (RWMA No. 2 [1]) are required for materials having low conductivity (fig. 49). This electrode/material relationship helps to maintain the proper heat balance at the weld interface. Another method for obtaining heat balance is to decrease the face area of the electrode which contacts the higher conductivity material. This will increase the current density through the material.

Selection of an electrode of proper composition solves only half the problem. The electrode design must also be considered as it will depend upon the geometry of the materials to be welded, accessibility of the materials, flexibility of the leads, and the weld schedule requirements.

The vertically opposed electrode (fig. 50(*a*)) is preferred because the force exerted on the materials is one of pure compression which reduces wear on the tip and the weld head. In addition, straight-shank, flat-tip electrodes are easier to fabricate and maintain. However, in most cases, the straight electrode cannot be used because of accessibility problems. When such a problem arises, the offset configuration is used (fig. 50(*b*)). Two requirements must be fulfilled when using the offset electrode design: sufficient cross-sectional area is needed for proper current flow, and the electrode must be mechanically strong enough to transmit the required pressure.

Another problem encountered when welding dissimilar metals is that of polarity sensitivity. Adverse effects to welds occur when the improper electrode polarity is used. In welding certain dissimilar combinations, a definite decrease in weld strength is noticeable if the correct polarity is not observed.

[1] Resistance Welding Manufacturers Association.

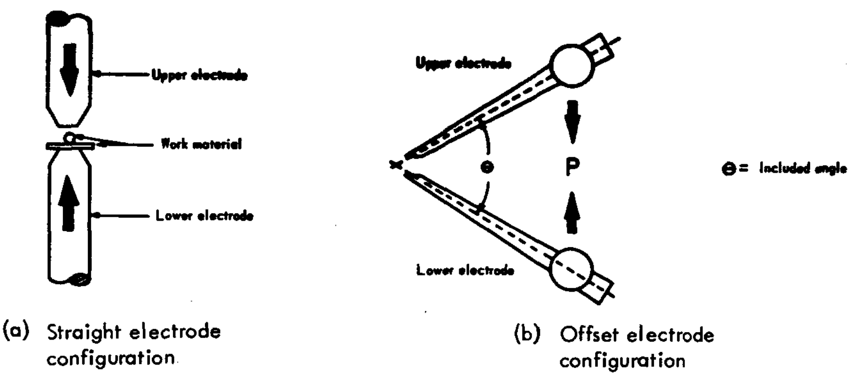

FIGURE 50.—Electrode configurations (ref. 50).

Materials which have been determined to be polarity sensitive when welded to a nickel ribbon are copper and Kovar. In most cases, a reduction in pull strength of greater than 50 percent is noticeable. There are undoubtedly other combinations which exhibit this phenomenon. Table 27 is a comparison of pull strengths for normal and reversed polarities of nickel ribbon (0.010 x 0.047 inch) welded to goldplated Kovar (0.017-inch diameter).

TABLE 27.—*Effect of Reversed Polarity on Weld Strengths at 4 Pounds Pressure*

[Ref. 50]

Energy, W-sec	Pull strength	
	Normal polarity (nickel (−), Kovar (+))	Reversed polarity (nickel (+), Kovar (−))
7.5	19.0	6.5
7.5	19.7	8.0
7.5	18.8	7.8
7.5	20.3	7.6
7.5	19.5	7.1
7.5	19.0	8.3
7.5	19.0	8.8
7.5	19.6	7.9
7.5	18.9	7.1
7.5	18.3	7.7
Average	19.2	7.7

Properties of materials which have the greatest bearing on weldability (resistance welding) are: electrical resistivity, thermal conductivity, and melting point. An equation relating these properties to a weldability index is cited by R.D. Enquist [2] as follows:

$$W=\frac{R}{FK_t}\times 100$$

where

W=Weldability index
R=Resistivity (ohm-centimeters)
F=Melting point (degrees Celsius)
K_t=Thermal conductivity

The equation is empirical and as such does not yield valid results in all instances. Weldability indices for various materials are shown in table 28. Results are fairly consistent with practical experience gained by experimentation. Note that the weldability index for copper is lowest in the table, indicating it is most difficult to weld.

Materials used for interconnection and component leads can be divided into four basic categories, as follows:

(1) Pure or semipure metals;
(2) Alloys;
(3) Plated metals; and
(4) Clad metals

Some of the more common materials in these categories are given in table 29. Materials are plated or clad to improve their ability to resist corrosion or to obtain unique characteristics. In general, clad materials, such as copper-clad steel, are avoided. A notable exception to this is the use of Dumet. Since the weldability of the material can be directly related to the cladding material or the base material, depending on the thickness of the cladding, variations cause differences in the requirements of the weld system parameters of pressure and energy.

Weld sequencing is another important processing variable which must be specifically defined to provide for orderly and efficient weld programing to minimize defective welds and missed welds. In general, weld sequencing should proceed from one end of a run to the other, making all intermediate welds in order, as illustrated in figure 51(*a*). Another acceptable sequence is shown in figure 51(*b*). If a properly planned sequence is not followed, excess interconnect ribbon may result (fig. 51(*c*)).

---

[2] Enquist, R. D., "Metallurgy of Welding" presented at Welded Electronic Packaging Association Symposium, Palo Alto, Calif., Aug. 21, 1961.

TABLE 28.—*Weldability Indices of Materials*

[Ref. 50]

Category	Metal	Resistivity, ohm-cm	Melting point, °C	Thermal conductivity, K_t [a]	Weldability index
Ferrous metals	Iron	9.71	1539	0.18	3.51
	Cobalt	6.24	1495	.165	2.46
	Nickel	6.48	1455	.22	2.15
Light metals	Aluminum	2.655	660	.53	.76
	Magnesium	4.46	650	.38	1.80
Conductive and noble metals	Copper	1.673	1083	.94	.16
	Silver	1.59	960	1.0	.17
	Gold	2.19	1063	.71	.29
	Platinum	9.83	1773	.17	3.26
	Palladium	10.8	1554	.17	4.10
Refractory	Molybdenum	5.17	2625	.35	.56
	Tungsten	5.5	3410	.48	.34
	Tantalum	12.4	2996	.13	3.19

[a] Calorie centimeters/second/square centimeter/degree C (taken from "Metallurgy of Electronic Welding," by R. D. Enquist).

239-345 O—67—— 9

TABLE 29.—*Materials Used for Electronic Welding*

[Ref. 50]

Category	Commercial name	Basic composition, percent	Plating	Clad	Used for—
Pure and semipure	Nickel "A" [a]	99 nickel			Interconnecting material and component leads.
	Copper	Copper	Solder or tin dipped		Component leads.
Alloys	Kovar (Rodar) [a]	17 Co, 29 Ni, 53 Fe	Usually gold		Transistor and diode leads.
	Alloy 90	12 Ni, balance Cu			Interconnect material.
	Alloy 180	22 Ni, balance Cu			Interconnect material.
Clads	Dumet [a]	42 Ni, 58 Fe	Usually gold	Copper sheath	Component leads.
	Copperweld	Steel core		Copper	Interconnect material.
	Nickel-clad copper	Copper core		Nickel	Interconnect material.

[a] Standardized materials.

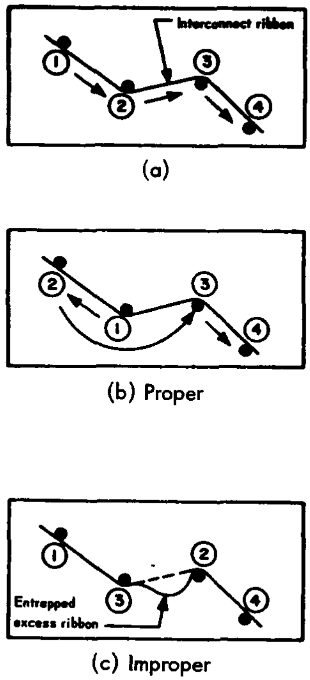

FIGURE 51.—Weld sequences (ref. 50).

Although this information is intended primarily for guidance in high-density packaging of electronic components, the equipment and techniques employed are adaptable to welding of round wire to round wire, strip or foil to round wire, strip or foil to strip or foil, flat wire to flat wire, and other combinations that arise. This resistance welding equipment can also be modified to serve as an energy source for brazing small components, wires, and foils.

PRECEDING PAGE BLANK NOT FILMED.

CHAPTER 9

Fracture Testing

Pressurized devices must have a designed-in and built-in safety factor against catastrophic rupture. This is true of rocket cases, and of welded transformer cases, heat exchangers, and pressure vessels as used in the electrical industry. The face-centered-cubic metals, such as the aluminum alloys (ref. 29), have excellent resistance to fracture propagation, particularly at subambient temperatures. The advent of the high-strength Maraging and H–11 steels as possible materials for rocket motor cases prompted an investigation into their fracture toughness (K_{I_c}), particularly in the welded and welded and aged conditions, as required to produce maximum strength. For this purpose, welded plate metals having yield strengths of 248 000 psi, and more, were evaluated (ref. 52). Weld metal strengths were not provided, but welds were made from wires and in plates shown below.

Compositions of Test Plates and Wires

Element	Composition, weight percent					
	Plate heat No.		Weld wire	Weld centers		
	X14636	X53013		MIG	Short arc	TIG
C	0.03	0.02	0.02	0.02	0.02	0.02
Mn	.06	.02	.03	.03	.03	.03
P	.005	.006	.004	.003	.002	.004
S	.010	.009	.005	.005	.005	.005
Si	.010	.04	.02	.04	.03	.02
Cu	-------	.12	-------	-------	-------	-------
Ni	18.37	17.59	18.24	18.0	18.2	18.0
Cr	-------	-------	-------	-------	-------	-------
Mo	4.70	4.80	4.62	4.60	4.60	4.60
Co	8.49	8.06	7.90	8.28	7.79	7.67
Ti	.42	.49	.45	.43	.43	.43
Al	.13	.07	.09	.10	.09	.11
H_2	-------	-------	.00015	-------	-------	-------
O_2	-------	-------	.0014	-------	-------	-------
N_2	-------	-------	.0025	-------	-------	-------

The ductility of the unwelded plate metals in the aged condition was low; the tensile elongation being from 4.0 to 4.6 percent in 2 inches, and the area reduction from 30 to 33 percent.

Test specimens, notch locations, and failure locations are shown in figures 52, 53, and 54. The K_{I_c} values obtained are shown below.

Fracture Toughness From Bend Tests

(1) U.S. Steel Corp. Plate, 0.16 inch thick, 280 ksi yield strength

	K_{I_c} (ksi$\sqrt{\text{in}}$)
3-inch-wide center notch	77.0
Single edge notch	78.4
Calculation	84.4
By Bueckner formula	82.5

(2) Plate from second source, air melted, ¾ inch thick, 0.2 percent yield strength, >248 ksi

	K_{I_c} (ksi$\sqrt{\text{in}}$)
Compliance bend tests	79.5
Calculated	81.3
Single edge notch	81.5
Plate 1, bend bar, perpendicular	67.4
Plate 2, bend bar, parallel	68.1
Plate 2, edge notch tear, perpendicular	71.3
Plate 1, edge notch tear, parallel	73.5

	K_{I_c} (ksi)				
	Weld center	Fusion zone	HAZ	Dark band	Plate
TIG welds:					
Plate 2, bar perpendicular to rolling direction	69.6	82.1	74.7	66.9	77.0
Plate 1, bar parallel to rolling direction	83.8	100.0	94.6	96.6	84.3
MIG welds:					
Plate 6, bar perpendicular to rolling direction	74.3	------	93.6	------	77.0
Plate 5, bar parallel to rolling direction	77.7	------	91.3	------	84.3
Short-arc welds:					
Plate 7, bar perpendicular to rolling direction	56.9	------	90.1	------	77.0
Plate 11, bar parallel to rolling direction	72.8	------	106.8	------	84.3

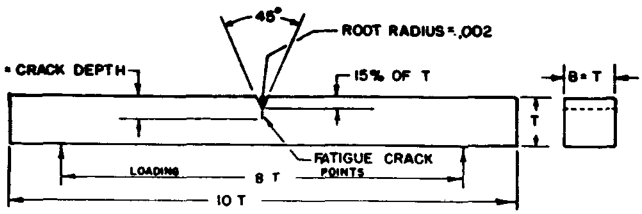

FIGURE 52.—Notched bar specimens for G_{Ic} values (ref. 52).

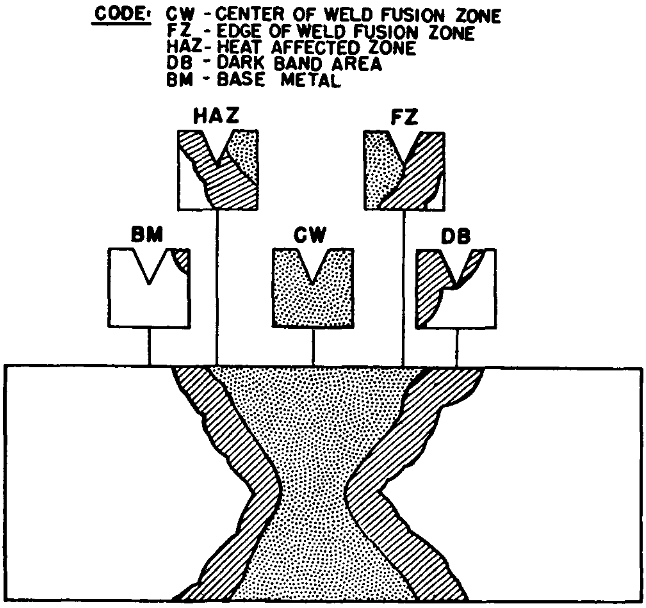

FIGURE 53.—Locations of fatigue crack tipped notches (ref. 52).

K_{I_c} values from the bend tests agreed with those from edge notched tear tests. Rolling direction on K_{I_c} for both heats of the 250 grade steel was highly significant. The average K_{I_c} values for TIG welds in bars cut parallel with the rolling direction were higher by significant amounts than for bars cut perpendicular to the rolling direction. This was true for all four cited notch positions in the weld. The margins of superiority were magnified over that in the base plate. The greatest average K_{I_c} was found in the heat-affected zone for short-arc welds. For the 250-ksi yield strength steel, the directionality effect in the base plate was reflected in the welds. The TIG welds were more consistent and generally better than for the other two types of welds investigated. Superiority of K_{I_c} for shallow (versus deeper) notches

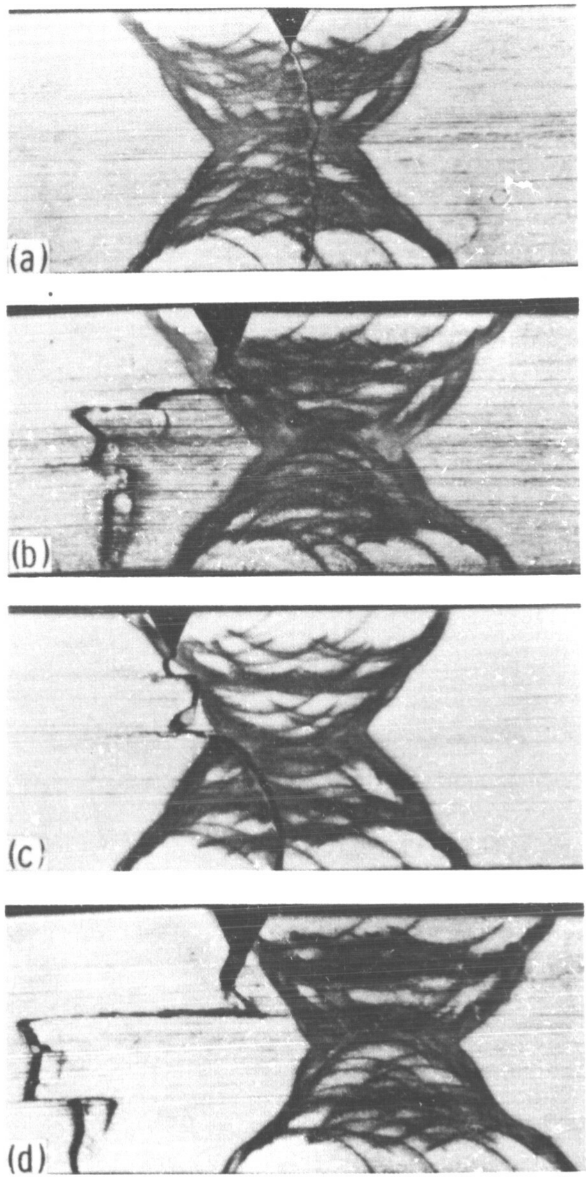

FIGURE 54.—Cross sections of typical bend specimens after K_{Ic} tests of TIG welds in 18 percent Ni maraging steel (250 000 psi, 0.2 percent yield strength). (Sections transverse to plate rolling direction. Notch roots tipped with fatigue cracks.) (ref. 52.) (a) Notch in center of weld (b) Notch root at edge of weld fusion zones (c) Notch root within heat-affected zone (d) Notch root at juncture of heat-affected zone and base metal.

in base plate could be explained on the basis of finer grain size and fewer carbide precipitates. Wide differences in K_{I_c} between different bars, but in the center of the welds at equal depths, were correlated with microstructure. Coarse-grained weld deposits with dendrites alined mainly along the fracture path showed less toughness than fine dendrites randomly oriented. The center-of-weld toughness was less than at any other location.

PRECEDING PAGE BLANK NOT FILMED.

CHAPTER 10

Summary

The authors have reviewed publicly available, unclassified documents about metals joining relating to NASA-sponsored projects and programs. These documents were selected from the NASA data bank by means of a rather extensive keyword list. The purpose of this review was to identify inventions, innovations, and advancements and bring them to the attention of the industrial community so that nonaerospace applications might benefit more quickly and on a broad base from the space program.

The NASA-sponsored work available for this review did not represent an overall planned R&D program to advance metals-joining knowledge. Rather, what has been presented in this review resulted essentially from encounters with day-to-day joining problems and the need for solutions to achieve space goals. There was interest in improved application and control of MIG and TIG welding processes, and efforts were made to automate welding procedures, such as vertical welding, to obtain more consistent results, free from operator variables. The use of fiber optics coupled with closed-circuit television for close monitoring of welding should be useful in automated installations.

Work involving electron beam and laser welding was reported by several authors; however, laser-welding technology is in its infancy and only pulsed laser operations is possible at present. Certainly progress in laser technology leading to continuous laser operation will be of major interest to metals-joining technologists. Electron beam welding offers potential to make welds with a depth-to-width ratio up to 20 : 1, thus minimizing the need to create large grooves which must then be laboriously filled a pass at a time. Also, with electron beam, focused spots on the order of 0.01 inch in diameter are possible, opening a degree of control for some applications not available with arc processes. Unfortunately, the electron beam to date has of necessity been used in vacuum chambers and this seriously hampers exploitation of this process. Industrial programs are currently underway to develop "air" electron beam welding so that the vacuum chamber limitations can be avoided. Certainly the capabilities of the electron beam process to accommodate thick material (~2 inches), dissimilar metals, and

combinations of wide disparity in thickness are worth reemphasis here.

A major emphasis was found on welding and the weldability of aluminum alloys. A program was undertaken to develop improved strength, readily weldable aluminum alloys in plate thickness. Such efforts are natural in view of NASA interest in high strength-to-weight ratio alloys. Although the program was of significant scope and thorough, the advent of improved strength, weldable aluminum alloys was not forthcoming. This program resulted, however, in a comprehensive survey of existing aluminum-alloy systems—both commercial and experimental—and the text of the literature survey phase is a very worthwhile, concise summary of aluminum-alloy metallurgy and related weldability.

Studies of the effect of environmental gas pressure on welding of aluminum were made by the British Welding Research Association under NASA sponsorship on an Al-Mg alloy similar to 5456. Successful welds were made at argon pressures from 1 to 30 psia with the gas metal-arc process. The effect of variations in ambient pressure was significant in that drop detachment frequency increased with pressure, the current drawn for a given filler metal feed rate increased with increasing pressure, and the arc voltage drawn for a fixed arc length increased with pressure. At pressures below 5 psia, the arc became diffuse and energy input to the base metal was rapidly dissipated. Welding speeds must then be correspondingly reduced.

Refractory metal alloys in the columbium, tantalum, and tungsten families were the subject of an investigation to evaluate weldability and elevated temperature stability. Most of the information available related to columbium-base alloys; however, this program, as of the latest document reviewed, was just beginning to develop interesting data. Evaluations to date were based on determination of ductile to brittle transition temperature by means of bend tests.

It is common today to find applications requiring joining of dissimilar metals and certainly it would be expected to find this problem among the joining problems encountered by those manufacturing space program hardware. The characteristics of such dissimilar metals joints are directly related to the alloy system formed by the particular combination of metals involved, the joining process used and its effect on the extent of alloying in the dissimilar-metal couple, and significant disparity between properties of the metals being joined. A variety of methods were found suitable for dissimilar-metals joining, including soldering, brazing, dip brazing, electron beam welding, and ultrasonic welding.

Another area of activity worth noting in the NASA activities was the effort expended in preparation of two rather definitive specifications; one on soldering (MSFC-PROC-158B) and one relating to aluminum welding (M-ME-MPROC-700.1). In addition, NASA document NASA SP-5011 covering welding of electronic assemblies is worthy of study by anyone interested in exploiting this technological area.

PRECEDING PAGE BLANK NOT FILMED.

References

SOURCES: Unclassified NASA and NASA-sponsored publications may be consulted at the following Federal regional technical report centers: University of California, Berkeley; University of Colorado Libraries, Boulder; Library of Congress; Georgia Institute of Technology, Atlanta; The John Crerar Library, Chicago; MIT, Cambridge, Mass.; Linda Hall Library, Kansas City, Mo.; The Columbia University, New York, N.Y.; Carnegie Library of Pittsburgh; Southern Methodist University, Dallas; and the University of Washington Library, Seattle.

Such publications also are sent to public libraries in Anchorage, Baltimore, Birmingham, Boston, Bridgeport, Brooklyn, Buffalo, Charlotte, N.C., Cincinnati, Cleveland, Dayton, Detroit, Denver, Fort Worth, Hartford, Kansas City, Mo., Little Rock, Los Angeles, Miami, Memphis, Milwaukee, New Orleans, Oakland, Oklahoma City, Phoenix, Pittsburgh, Rochester, San Diego, San Francisco, San Antonio, St. Louis, St. Paul, Seattle, Toledo, Trenton, and Wilmington.

Some NASA publications are available for purchase from the Clearinghouse for Federal Scientific and Technical Information Center, Springfield, Va. 22151; others from the Superintendent of Documents, U.S. Government Printing Office, Washington, D.C. 20402.

1. GLACKIN, J. J.; AND GOWEN, E. F., JR.: Evaluation of Fasteners and Fastener Materials for Space Vehicles. Annual Report, SPS Laboratories, Standard Pressed Steel Co., Jenkintown, Pa., Dec. 31, 1964, N65–22848.
2. MONTY, B. E.: The NASA Soldering Program. Trans. American Society for Quality Control, 1964, pp. 91–95, A64–23650.
3. ANON.: Procedure for Soldering of Electrical Connections (with) High Reliability. NASA TM X–54760 (MSFC–PROC–158B), NASA Marshall Space Flight Center, Huntsville, Ala., Feb. 15, 1963, N64–33034; and Quality Requirements for Hand Soldering of Electrical Connections. Dec. 1964, NPC 200–4.
4. SINCLAIR, J. H.; AND GYORGAK, C. A.: Effect of Two Braze Coatings, Processing Variables and Heat Treatments on 1200° F Stress-Rupture Strength of L–605, A–286, and Inconel 700 Sheet. NASA TN D–1880, Lewis Research Center, Cleveland, Ohio, Nov. 1963, N64–10334.
5. FREIS, F. M.: Integrated Welding Controls, Wire Feed, and Travel Speed. Armour Research Foundation, Illinois Institute of Technology, Chicago, June 1, 1963, N64–17572.
6. ANON.: Economy Automation for Welding of Space Vehicles. NASA SP–5009. Selected Welding Techniques, Part II. Marshall Space Flight Center, July 1964, pp. 32–34, N64–32642.
7. *Ibid.*, pp. 1–2.
8. LAMBASE, J. M.: Determination of TIG Welding Control Parameters and Requirements for the Automation of Out-of-Position Welding. North American Aviation, Inc., Los Angeles, Calif., Nov. 1962, N64–27874.

9. LAMBASE, J. M.: Determination of TIG Welding Control Parameters and Requirements for the Automation of Out-of-Position Welding. North American Aviation, Inc., Los Angeles, Calif., Nov. 1963, N65-16832.
10. RUDY, J. F.; ET AL.: Development of Weave Bead Techniques for Multi-Pass Vertical MIG Welding of Aluminum Alloys. Illinois Institute of Technology Research Institute, Chicago, NASA CR-55902, IITRI-B243-13, Final Report, Aug. 6, 1963, N64-17693.
11. GROVE, E. L.; RAZIUNAS, V.; LOSEKE, W. A.; AND DAVIS, B. K.: Spectrographic Monitoring of Inert-Gas Shields for Atmospheric Contaminants. Welding Journal, Research Suppl., June 1964, pp. 282-s-288-s, A64-20668.
12. WALL, W. A.; AND SWAIM, L. K.: Analysis of Closed Circuit Television and Fiber Optics for Remote Visual Control of TIG Welding. Marshall Space Flight Center, Huntsville, Ala., NASA TM X-53131, Sept. 17, 1964, N65-12018.
13. ANON.: Fiber Optics. Selected Welding Techniques, Part II. Marshall Space Center, Huntsville, Ala., NASA SP-5009, July 1964, p. 24. N64-32642.
14. *Ibid.*, Special Welding Nozzle Configuration. pp. 21-23.
15. *Ibid.*, Development of Improved Weld Filler Wire. pp. 19-20.
16. ANON.: Selected Welding Techniques. Marshall Space Flight Center, Huntsville, Ala., NASA SP-501, Apr. 1963, pp. 1-22, N63-15862.
17. ANON.: Upset Metal Edges for Increased Weld Joint Strength. Selected Welding Techniques, Part II. Marshall Space Flight Center, Huntsville, Ala., NASA SP-5009, July 1964, pp. 8-10, N64-32642.
18. TULISIAK, G.: Electron Beam Application to Welding Space Propulsion Components. NASA Lewis Research Center, Cleveland, Ohio, Proceedings of the Electron Beam Symposium, Sixth Annual Meeting, J.R. Morley, ed., Alloyd General Corp., Medford, Mass., Apr. 1964, pp. 98-111, A64-17286.
19. ANON.: Electron Beam Welding and Gas Metal-Arc Welding vs. Electron Beam Welding. Selected Welding Techniques, Part II. Marshall Space Flight Center, Huntsville, Ala., NASA SP-5009, July 1964, pp. 14-18, N64-32642.
20. SCHWINGHAMER, R. J.: Laser Welding. Marshall Space Flight Center, Huntsville, Ala., NASA TM X-53285, June 23, 1965, N65-28961.
21. GRISAFFE, S. J.; AND SPITZIG, W. A.: Observations on Metallurgical Bonding Between Plasma Sprayed Tungsten and Hot Tungsten Substrates. Lewis Research Center, Cleveland, Ohio. Trans. Quarterly, American Society for Metals, vol. 56, no. 3, Sept. 1963, pp. 618-628, A63-24016; and GRISAFFE; AND SPITZIG: Preliminary Investigation of Particle-Substrate Bonding of Plasma-Sprayed Materials. Sept. 1963, NASA TN D-1705.
22. SPITZIG, W. A.; AND GRISAFFE, S. J.: Metallurgical Bonding of Plasma Sprayed Tungsten on Hot Molybdenum Substrates. Lewis Research Center, Cleveland, Ohio, NASA TN D-2510, Nov. 1964, N65-10636.
23. SPITZIG, W. A.; AND GRISAFFE, S. J.: Analysis of Bonding Mechanism Between Plasma-Sprayed Tungsten and a Stainless Steel Substrate. Lewis Research Center, Cleveland, Ohio, NASA TN D-2461, Sept. 1964, N64-29336.
24. ANON.: Development of the All-Welded Common Bulkhead. Douglas Aircraft Co., Inc., Santa Monica, Calif., Jan. 1965, N65-26406.
25. ANON.: Development of the All-Welded Common Bulkhead. Douglas Aircraft Co., Inc., Santa Monica, Calif., Nov. 1964, N65-22167.
26. BRENNECKE, M. W.: Electron Beam Welding Heavy Gage Aluminum Alloy 2219. Welding Journal, Research Suppl., vol. 4, no. 1, Jan. 1965, pp. 27-s-39-s, A65-15986.

27. SALTER, G. R.: The Effect of Pressure on the Gas Metal-Arc Welding of Aluminum Alloys. BWRA Welding Journal, Research Suppl., vol. 44, no. 3, Mar. 1965, pp. 107–s–115–s, A65–21239.

28. FRICKE, W. G., JR.; HANEY, E. G.; ANDERSON, W. A.; AND HUNSICKER, H. Y.: Weldable High Strength Aluminum Alloys, Phase I, Literature Survey. Alcoa Research Laboratories, New Kensington, Pa., Aug. 20, 1963, N64–13067.

29. WESTERLUND, R. W.: Development of a High Strength Aluminum Alloy, Readily Weldable in Plate Thicknesses, and Suitable for Application at −423°F. Progress Report No. 13, Alcoa Research Laboratories, New Kensington, Pa., Aug. 19, 1964, N64–28846.

30. BAYSINGER, F. R.: Investigation of Welding and Fabricability of Kaiser Experimental Alloy MR39A. Kaiser Aluminum and Chemical Corp., Spokane, Wash., May 21, 1964, N65–21777.

31. LENAMOND, N. G.; MCDONALD, J.; AND SPEIRS, K. K.: Development of Welding Techniques and Filler Metals for High Strength Aluminum Alloys. Progress Report 33, Southwest Research Inst., San Antonio, Tex., Apr. 15, 1964, N64–29705.

32. STEEN, M. V.: Aluminum Alloy 2319 Weld Wire Investigation. Lockheed Missiles and Space Co., Sunnyvale, Calif., June 16, 1964, N64–209687.

33. DUDAS, J. H.: Arc Stability and Melting Characteristic of Welding Wire for Use with 2219 Aluminum Alloy Plate. Alcoa Research Laboratories, New Kensington, Pa., Nov. 30, 1963, N65–21779.

34. NELSON, E. E.; AND WILLIAMSON, J. G.: Corrosion Problems Associated with the Use of Titanium Fasteners to Connect Aluminum Components. Marshall Space Flight Center, Huntsville, Ala., MTP–P and VE–M–63–13, Sept. 30, 1963, N64–11381.

35. BROTHERS, A. J.; HARTENS, H. E.; AND WOOD, H. L.: Properties of Welded High-Strength Titanium Alloy Sheet. Jet Propulsion Lab., Calif. Inst. Tech., Proceedings of Amer. Soc. for Testing and Materials, vol. 63, 1963, pp. 646–656, N64–25506.

36. GODFREY, L.; AND MAKOWSKI, G.: Final Report on Research and Development of Titanium Rocket Motor Case, Vol. III, Development of Welding Practice. Pratt and Whitney Aircraft, E. Hartford, Conn., Oct. 31, 1963, N64–20910.

37. MUNFORD, J. A.; CANTOR, B. R.; AND PILTCH, A.: Ultrasonic Welding of a Beryllium Window Assembly. Goddard Space Flight Center, Greenbelt, Md., NASA TM X–935, Jan. 1964, N64–12956.

38. ROYSTER, D. M.; MANNING, C. R., JR.; AND DYSLESKI, C. A.: Mechanical Properties, Oxidization Characteristics, and Weldability of Two Uncoated and Coated Vanadium-Base Alloys. Langley Research Center, Hampton, Va., NASA TN D–2616, Feb. 1965, N65–16749.

39. LESSMANN, G. G.; AND STONER, D. R.: Determination of the Weldability and Elevated Temperature Stability of Refractory Metal Alloys. Second Quarterly Report, Westinghouse Electric Corp., Astronuclear Laboratories, Sept. 21–Dec. 21, 1963, N64–20725.

40. *Ibid.*, Third Quarterly Report, Dec. 21, 1963–Mar. 21, 1964, N64–25764.

41. *Ibid.*, Fourth Quarterly Report, Mar. 21–June 21, 1964, N64–31455.

42. *Ibid.*, Fifth Quarterly Report, June 21–Sept. 20, 1964, N65–14394.

43. *Ibid.*, Sixth Quarterly Report, Sept. 21–Dec. 1964, N65–20885.

44. Gatsek, L. F.: Bonding and Welding of Dissimilar Metals. North American Aviation, Inc. Transforming and Using Space-Research Knowledge. NASA–UCLA Symposium and Workshop, Los Angeles, Calif., NASA SP–5018, June 2, 1964, N65–18528.
45. Anon.: A Technique for Joining and Sealing Dissimilar Materials. Lewis Research Center, Cleveland, Ohio, NASA SP–5016, June 1965.
46. Keller, D. V., Jr.: Adhesion Between Atomically Clean Metallic Surfaces. Syracuse University Research Institute, N.Y., July 1962, N64–10372.
47. Keller, D. V., Jr.: Adhesion Between Atomically Clean Surfaces. Syracuse University Research Institute, N.Y., NASA TN D–2228, Feb. 1964, N64–14730.
48. Keller, D. V.; Franklin, W. M., Jr.; and Hauser, D.: Adhesion Between Atomically Pure Metallic Surfaces, Part III. Syracuse University Research Institute, N.Y., July 1964, N64–29217.
49. Ham, J. L.: Investigation of Adhesion and Cohesion of Metals in Ultrahigh Vacuum, Final Report. National Research Corp., Cambridge, Mass., Nov. 27, 1963, N64–12032.
50. Anon.: Welding for Electronic Assemblies. Technology Handbook, Marshall Space Flight Center, Huntsville, Ala., NASA SP–5011, Nov. 1964, N65–13535.
51. Lyons, J. C.; and Dargo, D. R.: Welded Electronic Module Fabrication. Goddard Space Flight Center, Greenbelt, Md., NASA TN D–2321, June 1964, N64–23235.
52. Kies, J. A.; Smith, H. L.; Romine, H. E.; and Bernstein, H.: Fracture Testing of Weldments. Naval Research Lab., Washington, D.C., NASA CR–140, Dec. 1964, N65–12449.

Nominal Composition of Aluminum Alloys

Alloy	Si	Cu	Mn	Mg	Cr	Zn	Ti	V	Zr	Cd	Sn	Fe
M788		6.4	0.3			0.25	0.13	0.10	0.11			
M789		6.4	.3			1.0	.13	.10	.11			
M791			.21	2.22	0.13	6.20			.10			0.16
M793			.21	1.64	.13	6.51			.10			.18
M822			.34	2.25		5.91	.10		.14			.17
M825		6.3	.3				.06	.10	.12	0.15	0.05	
1100	(99.0 percent aluminum minimum)											
D1495				3.0		4.5						
D1707				3.0		7.3						
2014	0.8	4.4	0.8	.4								
2024		4.5	.6	1.5								
2219		6.3	.3				0.06	0.10	0.18			
2319		6.3	.3				.15	.10	.18			

4043	5. 0											
4145	10. 0	4. 0										
4543	6. 0			. 25								
X5039				3. 9		3. 0						
5052	[a] . 45			2. 5	0. 25							
5083			. 8	4. 45	. 10							
5086			. 45	4. 0	. 10							
5183			. 8	4. 75	. 15							
5456	[a] . 40		. 8	5. 2	. 10							
5554	[a] . 40		. 8	2. 7	. 10		. 10					
5556	[a] . 40		. 8	5. 2	. 10		. 10					
6061	. 6	. 25		1. 0	. 25							
X7002		. 8	. 18	2. 5	. 20	3. 5						
X7003			. 30	1. 3	. 15	4. 8						
X7005			. 45	1. 4	. 15	4. 6	. 04		. 15			
X7006	[a] . 35			1. 75		4. 3						
X7038			. 5	3. 5		4. 5						
7039			. 25	2. 8	. 20	4. 0						
7075		1. 6		2. 5	. 30	5. 6						
7079		. 6	. 20	3. 3	. 20	4. 3						
7178		2. 0		2. 7	. 30	6. 8						
7277		1. 25		2. 0	. 25	4. 0						

[a] Silicon + iron.

U.S. GOVERNMENT PRINTING OFFICE: 1967 O—239-345

"The aeronautical and space activities of the United States shall be conducted so as to contribute . . . to the expansion of human knowledge of phenomena in the atmosphere and space. The Administration shall provide for the widest practicable and appropriate dissemination of information concerning its activities and the results thereof."

—NATIONAL AERONAUTICS AND SPACE ACT OF 1958

NASA TECHNOLOGY UTILIZATION PUBLICATIONS

These describe science or technology derived from NASA's activities that may be of particular interest in commercial and other non-aerospace applications. Publications include:

TECH BRIEFS: Single-page descriptions of individual innovations, devices, methods, or concepts.

TECHNOLOGY SURVEYS: Selected surveys of NASA contributions to entire areas of technology.

OTHER TU PUBLICATIONS: These include handbooks, reports, notes, conference proceedings, special studies, and selected bibliographies.

Details on the availability of these publications may be obtained from:

National Aeronautics and Space Administration
Code UT
Washington, D.C. 20546

Technology Utilization publications are part of NASA's formal series of scientific and technical publications. Others include Technical Reports, Technical Notes, Technical Memorandums, Contractor Reports, Technical Translations, and Special Publications.

Details on their availability may be obtained from:

National Aeronautics and Space Administration
Code US
Washington, D.C. 20546

NATIONAL AERONAUTICS AND SPACE ADMINISTRATION
Washington, D.C. 20546